C.P. No. 1185

C.P. No. 1185

PROCUREMENT EXECUTIVE, MINISTRY OF DEFENCE

AERONAUTICAL RESEARCH COUNCIL

CURRENT PAPERS

Cumulative Damage in Fatigue with Particular Reference to the Effects of Residual Stresses

by

P. R. Edwards

Structures Dept., R.A.E., Farnborough

LONDON: HER MAJESTY'S STATIONERY OFFICE

1971

PRICE £1·75 NET

U.D.C. 539.431 : 539.319 : 669.715 : 621.886.4

C.P. No.1185

November 1969*

CUMULATIVE DAMAGE IN FATIGUE WITH PARTICULAR REFERENCE TO THE EFFECTS OF RESIDUAL STRESSES

by

P. R. Edwards

SUMMARY

In this Report factors affecting the accuracy of Miner's Rule are discussed. An investigation is also described of the cumulative damage behaviour of DTD 5014 aluminium alloy lug specimens using random loading. It is concluded that the deviations from Miner's Rule observed in the investigation can be ascribed mainly to the action of residual stresses associated with yielding at the point of fatigue initiation. An attempt is made to quantify this effect.

---

* Replaces RAE Technical Report 69237 - ARC 32168

CONTENTS

CONTENTS (Contd.)

Conversions: 1 ksi = 1000 lb(f) in^{-2} = 6.894 MNm^{-2} = 0.685 Hb .

SYMBOLS

CA	suffix - refers to constant amplitude loading
D	fatigue damage
E	modulus of elasticity
$E(\sigma)$	$\left[\frac{\text{Number of crossings of stress } \sigma \text{ by variable amplitude waveform}}{\text{Number of crossings of mean stress by variable amplitude waveform}}\right]$
h	parameter which governs the overall stress amplitude of an exponential loading spectrum[23]
K_p	stress concentration factor under conditions of yielding at the stress concentration
K_t	stress concentration factor under elastic strain conditions
K_t'	stress concentration factor ($d\sigma_{max}/d\sigma_{net}$) under elastic conditions, after yield at the stress concentration
ℓ	crack length
m	parameter which governs the overall stress amplitude of an exponential loading spectrum[23]
$M = \frac{\sigma_y}{K_t \sigma_{af\ell}}$	a parameter which governs partly the sensitivity of materials to residual stresses
n	number of stress cycles
n_1 , n_q	number of stress cycles at stress levels σ_1 , σ_q
n_o	number of crossings of the mean stress by variable amplitude waveform
n_p	number of peaks in variable amplitude waveform
n_b	number of cycles under block programmed loading conditions
N	number of cycles to failure
N_1 , N_q	number of cycles to failure at stress levels σ_{a1} , σ_{aq}
N_ℓ	number of cycles to crack length ℓ
p_1 , p_2	proportion of total number of cycles at stress levels 1, 2 in a block programme
$p_m(\sigma)$	probability of occurrence of stress maxima of amplitude Note that $\int_0^\infty p_m(\sigma)\, d\sigma = 1$
s	suffix - refers to spectrum loading
S_p	pre-stress ratio
X_1	an exponent which varies with alternating stress level σ_{ai}

SYMBOLS (Contd.)

σ, σ_1, σ_2	stress
σ_a, σ_{a1}, σ_{a2}	alternating stress amplitude
σ'_a	fatigue strength adjusted for residual stress change
$\sigma_{af\ell}$	σ_a at 10^8 cycles to failure
σ_m	net mean stress
$\sigma_{\ell m}$	local mean stress
$\sigma_{\ell mr}$	local mean stress [illegible] random loading
σ_R	residual stress
σ_p	maximum (peak) load applied during variable amplitude cycling sequence
σ_r, σ_{r1}, σ_{r2}	rms alternating stresses
σ_y	yield stress
σ_u	U.T.S.
ε	strain
ε_y	yield strain
ε_R	residual strain
λ	stress corresponding to a 5 ft/sec gust on the Royal Aeronautical Society spectrum

1 INTRODUCTION

At the design stage of engineering structures it is necessary to obtain a first estimate of fatigue endurance for any fatigue sensitive components. In many cases, such as loading in motor vehicle suspensions over uneven road surfaces and loading in aircraft structures due to atmospheric turbulence, service loadings are variable amplitude in nature, and so it is necessary to employ one of the published cumulative damage rules [1-21]. Despite the multiplicity of rules available, the original Palmgren Miner Cumulative Damage Hypothesis, (Miner's Rule[10,21]) is still generally in use in industry for this purpose[22]. There are several reasons for this. Firstly, it is simple to use and is often regarded as giving a conservative (safe) prediction, although this is not necessarily correct. Secondly, standard S-N curves are commonly available and most of the practical alternative methods of life prediction require additional data which in many cases would be expensive to obtain, and finally none of the subsequent rules has yet been proved sufficiently reliable to outweigh the probable increased complication of their use.

It is primarily the aim of this Report to investigate the limitations of Miner's Rule in order that designers may have a better appreciation of the circumstances in which the rule is unsafe, or safe, and to suggest and investigate possible modifications to the rule in order to improve accuracy.

Many cases in which the rule does not give a good prediction of the fatigue life of aluminium alloys can be explained by the influence of residual stresses acting at the point of fatigue initiation. Such stresses can be generated by local yielding at stress concentrations under the highest loads applied or may be already present due to manufacturing processes. In section 3 of this Report the influence of residual stresses on cumulative damage behaviour is discussed. In Appendices A - F other reasons for inaccurate prediction are also discussed, including variation of relative damage rate with stress, cycles below the fatigue limit, effect on life of the particular load at which a component fails, and the effects of fretting.

On the basis of the foregoing discussion a general approach to cumulative damage is suggested in section 4, based on a simplified method of accounting for the effects of residual stresses.

Finally, section 5 describes an investigation of the cumulative damage behaviour of aluminium alloy lug specimens in order to explore the validity of the concepts developed above. The investigation covered the determination of

fatigue life under constant amplitude and two types of variable amplitude loading each at three mean stress levels. Measurements were made of residual static strength at different stages in the fatigue life under the various types of loading action. By this means the relative rates of accumulation of fatigue damage under constant and variable amplitude loading were determined.

The results of the investigation broadly confirmed the concepts developed in section 4.

2 MINER'S RULE AND METHODS OF ASSESSING ITS VALIDITY

2.1 Statement of the Rule

The Rule states that if any component is subjected to a variable amplitude loading sequence containing stress amplitudes σ_{aq} (q = 1, 2, 3 ...p) then the fraction of the total life used up by any single stress cycle at stress amplitude σ_{aq} is given by $1/N_q$, where N_q is the number of cycles to failure of the component under stress amplitude σ_{aq} alone.

Therefore the total fraction of the fatigue life used up by a variable amplitude waveform is $\sum_{q=1}^{q=p} \frac{n_q}{N_q}$ where n_q is the number of cycles of stress amplitude σ_{aq} contained in the variable amplitude waveform. Therefore the Rule predicts failure when $\sum_{q=1}^{q=p} \frac{n_q}{N_q} = 1$.

Although as originally stated[10] Miner's Rule was intended to apply to life to the 'first crack' there is no fundamental reason why it cannot be applied to life up to any state of damage. However, the accuracy of prediction in so doing may well depend on the damage state considered.

2.2 Methods of verification

Many investigations have been carried out to determine the applicability of the Rule under a number of loading conditions. Tests involved in this work have been of two main types. First is the 'step' test, where testing commences under constant amplitude loading at one alternating stress level and the level is changed after a fixed number of cycles to a second stress level. Subsequent level changes may be made, the levels all increasing or all decreasing consecutively. Testing is continued to failure at a predetermined final level. The second type of test is the mixed spectrum test*, which

*In this Report 'spectrum' refers to a spectrum of amplitudes and not of frequencies as in 'power spectrum'.

approximates more closely to service loading condition. In such a test loads may be applied in repeated programmes, with each programme consisting of n_1 cycles at level σ_{a1}, n_2 at level σ_{a2} etc., (block programme loading). A further refinement of the mixed spectrum test is the random test in which cycles are applied having amplitudes called up at random with a predetermined probability of occurrence of each amplitude. There are a number of variations on the two types of test.

The performance of Miner's Rule is generally judged by the cumulative cycle ratio, $\sum_{q=1}^{q=p} \frac{n_q}{N_q}$ at failure, usually shortened to $\sum \frac{n}{N}$. This is equal to the ratio $\frac{\text{achieved life}}{\text{predicted life using Miner's Rule}}$ for random tests, and for programmed tests where the number of programmes to failure is large. $\sum \frac{n}{N}$ is not equal to this ratio for step tests except when $\sum \frac{n}{N} = 1$. (See Appendix G.)

3 THE EFFECT OF GEOMETRIC RESIDUAL STRESSES ON CUMULATIVE DAMAGE BEHAVIOUR

It is apparent from a study of the literature that Miner's Rule can give highly inaccurate estimates of fatigue life under variable amplitude loading. For instance, values of $\sum \frac{n}{N}$ varying from 0.01 [23] to 8 [24] have been reported. Geometric residual stresses can explain much of the variation in $\sum \frac{n}{N}$, and are discussed in this section. [Other factors are discussed in the appendices, namely variation of relative damage rate with stress and associated changes in fatigue mechanism (Appendix A), effect of the load at which a component fails (Appendix B) effect of low level stress cycles (Appendix C), effect of strain hardening (Appendix D), effect of fretting (Appendix E) and crack propagation considerations (Appendix F).]

3.1 *Geometric residual stresses* generated in notched specimens at a positive mean stress*

Geometric residual stresses are generally held to be responsible for certain aspects of the behaviour of notched aluminium alloy specimens. For such specimens under a variety of loading actions $\sum \frac{n}{N}$ has been shown to increase with increase in mean stress [25] and commonly exceeds unity at positive mean stresses [16,24-30]. The reasons why this does not necessarily apply to

*In this Report the term 'geometric residual stress' is used to describe relatively large-scale residual stresses. These may be due to manufacturing processes or local yielding at stress concentrations associated with the geometry of the structural element concerned. The term is used to differentiate these stresses from microscopic stresses corresponding to strain hardening, and from residual stresses at the tip of a crack.

other materials and, in particular to many components in medium and low strength steels are explained in section 3.3. The behaviour mentioned above of notched aluminium alloy specimens can be explained as follows, simplified to apply strictly only to a uniaxial stress state at the notch root.

Consider a notched specimen having a stress concentration factor K_t, and made of a material having a stress-strain curve as shown in Fig.1. The application of a net mean stress σ_m will give rise to a stress $\sigma_1 = K_t \sigma_m$ at the notch root. Assume that an alternating stress σ_a is applied of such a value that $(\sigma_m + \sigma_a) K_t$ is less than σ_y. In this case the material at the root of the notch will cycle between $\sigma_2 = (\sigma_m + \sigma_a) K_t$ and $\sigma_3 = (\sigma_m - \sigma_a) K_t$. The local mean stress $\sigma_{\ell m}$ will of course be σ_1. If σ_a is larger so that $(\sigma_m + \sigma_a) K_t > \sigma_y$, then the maximum stress at the root of the notch under cyclic loading will be given by $\sigma_4 = (\sigma_m + \sigma_a) K_p$, where K_p is the stress concentration factor under conditions of yielding at the notch root. This is not a simple value to calculate since K_p is itself a function of the plastic strain. However, an approximate value for σ_4 can be obtained by assuming that ε_4 is equal to the elastic strain, i.e.

$$\varepsilon_4 = K_t \frac{(\sigma_m + \sigma_a)}{E} \quad . \tag{2}$$

The corresponding value of σ_4 can then be obtained from the stress/strain curve. The error involved in using the elastic strain value will depend upon the stress concentration factor, the slope of the post-yield stress/strain curve and upon the elastic strain ε_4. For fatigue life prediction in aluminium alloys it should be sufficiently accurate to assume that equation (2) holds, provided the maximum strain at the notch root does not exceed 2%.

After σ_4 is reached (on the first quarter cycle of the net alternating stress amplitude σ_a) the material at the root of the notch will cycle purely elastically between σ_4 and σ_5 where

$$\sigma_5 = \sigma_4 - 2K_t' \sigma_a$$

where K_t' is the new elastic stress concentration factor for the notch after the geometric distortion which accompanied the initial plastic strain. For maximum strain values at the notch root of 2%, the error in assuming $K_t = K_t'$ is negligible. Therefore

$$\sigma_5 = \sigma_4 - 2K_t \sigma_a$$

so that the new local mean stress $\sigma_{\ell m}$ is

$$\sigma_6 = \sigma_4 - K_t \sigma_a \quad . \tag{3}$$

If the alternating stress is made larger the maximum local stress will increase to say σ_7, but the local mean stress σ_8 will be larger than $\sigma_7 - K_t \sigma_a$ due to local compressive yielding between A and B* . Cycling at this level will therefore involve plastic yielding on every cycle unless the hysteresis loop ABC is ultimately closed by a cyclic strain hardening process.

Fig.2 shows the calculated variation in local mean stress with alternating stress level under constant amplitude loading for the lug specimens used in the investigation reported in section 5 of this Report. It has been assumed that the stress concentration acts as a pure strain concentration, i.e. equation (2) holds, and no allowance has been made for the effects of compressive yielding. Fig.3 shows the variation in $\sigma_{\ell m}$ (Ref.32) measured on a large notched specimen of L65 with a stress concentration factor of 2.27 and demonstrates how local compressive yielding can affect the results. The stress history at the notch root was determined by a method used in Ref.33.

If a well-mixed random loading sequence which is symmetrical about the mean is applied to such a specimen, it can be seen that the local mean stress will be governed by the value of the highest alternating stress applied σ_p so that

$$\sigma_{\ell mr} = \sigma_4 - \sigma_p K_t \tag{4}$$

where σ_4 is now the maximum local stress corresponding to the peak stress σ_p. Equation (4) will be modified if local compressive yielding occurs giving a larger value of $\sigma_{\ell m}$ as in Fig.3 for values of σ_a greater than 8.8 ksi rms. Under random loading, therefore, due to the presence of a compressive residual

---

*After initial plastic tensile yielding, local compressive yielding will occur at stresses much more 'tensile' than the initial compressive yield point. Similarly, the yield point in tension is lowered by any prior plastic straining in compression. This phenomenon is known as the Bauschinger Effect (Ref.31).

stress, $\sigma_{\ell mr}$ will be lower than (or equal to) the local mean stresses which existed under the constant amplitude loading actions used to obtain the part of any S-N curve which were needed in turn to predict the life under random loading. This results in less damage per cycle in the random loading case than is predicted from the constant amplitude data. Hence Miner's Rule tends to be conservative for notched specimens under symmetrical loading at positive mean stress levels. At zero mean stress $\sigma_{\ell m}$ will be zero under both random and sinusoidal loading so no corresponding effect on $\sum \frac{n}{N}$ is to be expected.

Methods of life prediction based on accounting for such effects of residual stresses have been published[16,17,18].

It was explained above how residual stresses increase $\sum \frac{n}{N}$ for notched aluminium alloy specimens at a positive mean stress; it was assumed that the load spectrum was symmetrical and well-mixed, so that the effects of tensile and compressive yielding cancelled out and $\sigma_{\ell m}$ remained effectively constant throughout the life. In practice this does not happen since a finite number of cycles must usually elapse before the highest load in the spectrum is applied and the residual stress state is fully developed. Also in practice the loading may not be symmetrical, so that the largest tensile and compressive loads may not occur close together and may be of different magnitudes (e.g. largest tensile loads due to aircraft maneouvre and largest negative loads due to air-ground-air cycles). In this case when yielding occurs under the compressive loads, any subsequent low amplitude fatigue cycles have their associated damage amplified by the raised local mean stress, and vice-versa for those following large tensile loads. Provided the variation in $\sigma_{\ell m}$ is known the effect on fatigue life can, in principle be assessed as in section 4.6.

3.2 Residual stresses already present in components

The state of stress of specimens before testing commences is of considerable importance. Geometric residual stresses can be introduced by many manufacturing processes (e.g. turning, grinding, milling, rolling) or introduced deliberately with the object of improving fatigue performance, by coining, shot peening, or by subjecting a notched component to a single unidirectional load[23,34-38]. The effect of such stresses on Miner's Rule can be illustrated as follows:

Assume a number of notched specimens are preloaded before testing to the highest value of load (static + dynamic) expected to be encountered under an intended symmetrical variable amplitude loading pattern, thus introducing

geometric residual stresses. These specimens are then taken as 'new' specimens to be tested under variable and constant amplitude loading at a positive mean stress to determine the applicability of Miner's Rule. In the absence of local compressive yielding, tensile local yielding will not occur under either type of loading and so the value of $\sigma_{\ell m}$ will be the same for both constant amplitude and variable amplitude loading actions. Hence $\sum \frac{n}{N}$ will be less than for specimens which have not been preloaded because, in the case of the preloaded specimens, the beneficial effect of the residual stresses applies under constant amplitude as well as under variable amplitude loading. An as illustration, reduced values of $\sum \frac{n}{N}$ have been shown for preloaded lug specimens under programmed loading[39] compared with values for specimens which were not preloaded.

Similarly, if tests on specimens which have been subjected to a tensile preload are carried out at zero mean stress, compressive yielding may occur under the highest cyclic loads. This will increase the value of $\sigma_{\ell m}$ with increase in alternating stress (i.e. opposite effect to that shown in Fig.2) and so produce a reduction in $\sum \frac{n}{N}$. A series of such tests have been carried out on 7075-T6 aluminium alloy notched specimens in rotating bending[23]. The specimens were first axially preloaded to values given by the pre-stress ratio:

$$S_p = \frac{\text{nominal elastic maximum stress at notch root}}{\sigma_u} .$$

After the pre-stressing, constant amplitude and random loading spectrum tests were performed at different overall stress levels, the applied random spectrum having an exponential distribution of load amplitudes. In Fig.4, the data obtained has been replotted to show the variation in $\sum \frac{n}{N}$ with alternating stress at different pre-stress ratios and it can be seen that positive pre-stress ratios giving compressive residual stresses result in low values of $\sum \frac{n}{N}$ and vice versa.

In this section it has been shown that geometric residual stresses can be of extreme importance in cumulative damage of aluminium alloy specimens, since they can cause large variations in $\sum \frac{n}{N}$. All the examples quoted have involved notched aluminium alloy specimens since residual stresses can easily be induced by local yielding at the notch root. However, it is clear that since machining operations can induce residual stresses into the surface of plain specimens, such variations in $\sum \frac{n}{N}$ can apply to all classes of specimen.

3.3 Conditions for effectiveness of residual stresses

For residual stresses to be effective in altering the fatigue life two conditions must be fulfilled. First, the stresses must be reasonably stable under cyclic loading below the yield point. If such stresses are relaxed by low amplitude cycling, then local mean stresses in notched specimens will tend to reduce progressively under fatigue loading, regardless of the loading action. In this case, any changes in the magnitude of $\sigma_{\ell m}$ which do occur, as described in the last section, due to local yielding may well be insignificant if the rate of decay of $\sigma_{\ell m}$ is large enough. Secondly, the yield point of the material must be considerably above $K_t \sigma_a$ at the lowest value of σ_a which produces significant fatigue damage $\sigma_{af\ell}$. If $K_t \sigma_{af\ell} > \sigma_{yp}$ then the local mean stress in a notched specimen will always be relatively close to zero under symmetrical loading greater than the fatigue limit stress $\sigma_{af\ell}$, regardless of the value of the net mean stress. In this case residual stresses cannot be sustained under cyclic loading of any significant amplitude because the first cycle after the introduction of such stresses will relax them by local yielding. The parameter governing whether or not this occurs is therefore the ratio

$$\frac{\sigma_y}{K_t \sigma_{af\ell}} = M \text{ , i.e. residual stresses will not be effective unless } M > 1 \text{ .}$$

This has been shown to be the case in Ref.38. Tests were carried out on notched specimens of 61S aluminium alloy in both the precipitation hardened and the soft condition. It was found that preloading with a single unidirectional load changed the life of the heat treated specimens but not those in the soft condition. Measurements using X-ray diffraction showed that in the latter case the residual stresses were close to zero after the first few cycles, but this did not apply in the former case. For the latter case M was close to unity.

Fig.5 shows the results of an investigation[40] in which residual stresses were introduced into square-sectioned bars of mild steel and aluminium alloy by overstraining in bending. Stress cycles of the amplitude shown were then applied to the specimens. The residual stresses at various numbers of cycles were determined by cutting the bar and measuring the residual strains by means of strain gauges. The results show a sharp initial fall in residual stress over 10^5 cycles for the mild steel specimens, and a subsequent gradual drop in value even at ±4 ton/in^2 (±9 ksi) which was far below the fatigue limit. The aluminium alloy specimens showed no appreciable fall in residual stress up to 10^7 cycles at any stress amplitude below the fatigue limit. Fig.6 shows the

effect of the residual stresses on the fatigue life of the bars, demonstrating a much greater effect for aluminium alloy than for mild steel as would be expected from the stress measurements.

When M is close to one, calculations of residual stresses are complicated by the action of the Bauschinger Effect since the yield stress is likely to be exceeded frequently in both directions and its actual values therefore (tensile or compressive) depend at any moment on the previous strain history. In order to demonstrate this it was decided, at R.A.E., to subject a plain steel specimen to a strain history similar to that experienced by the material on the initially compressed surfaces of the flat bars of Ref.40. For that material M was equal to about 1.05. Fig.7 shows the measured behaviour of the specimen under the strain history resulting from initial overstraining in compression ABC, followed by elasto-plastic unloading CD to a residual stress state of 16.5 ksi at D , i.e. an initial residual stress value somewhat less than half the yield stress, as in the investigation of Ref.40. The application of one stress cycle DEGHG of approximately ±7.5 ksi (±250 $\mu\varepsilon$) reduced the residual stress value to σ_G = 10.7 ksi by yielding along DE . The figure also shows the behaviour of the material during subsequent strain cycles of ±500, 750, 1000 and 1250 $\mu\varepsilon$ giving further large changes in residual stress state. Fig.7 is not strictly comparable with the strain history used in Ref.40 since due to the Bauschinger Effect the drop in σ_R on the first cycle is highly dependent on the magnitude of the initial plastic strain BC , and this value is not clear from that work. The mechanism by which large drops in σ_R can occur is however demonstrated, together with the reversed plastic cycling which occurs at only moderate loads. The subsequent (see Fig.5) progressive drop in residual stress after the first stress cycle was probably due to the corresponding lowering of the yield point (cyclic strain softening) which occurs for mild steel under fatigue cycling[41,42] (see Appendix D). For the aluminium alloy specimens described in Ref.40, M was equal to about 2.4.

Many low and medium strength steel components are therefore not greatly affected by residual stresses due to the low yield point of such steels compared with the fatigue limit stress and the tendency for residual stresses to be relaxed under low-level cyclic loading. This lack of sensitivity to residual stresses has been further demonstrated[43-45] in tests on medium strength steel notched specimens, which have been shown to be affected relatively little by mean stress or the application of single unidirectional high loads. However as was stated in section 3.1 the arguments in section 3

strictly only apply to a uniaxial stress state at the point of fatigue initiation. In cases where complex stress systems exist (e.g. in welded structures) a more widely applicable criterion for yield should be used such as maximum octahedral shear stress. In such circumstances residual stresses may be important in steel structures.

3.4 Percentage of life affected by geometric residual stresses

Once a crack begins to propagate through a geometric residual stress field it is not a simple matter to predict behaviour. In particular the size of the specimen is likely to be an important factor. This can be seen by considering the case of a fatigue crack propagating from an edge notch in an infinite sheet (Fig.8a) subjected to fatigue loading at a positive mean stress, the loading being high enough to cause local yielding, giving rise to a residual stress σ_R. If the notch is extremely large the fatigue crack will, throughout the fatigue life, be effectively the same as an edge crack (Fig.8b) in an infinite sheet in which the general alternating stress is $K_t \sigma_a$ (provided σ_a is not high enough to give rise to alternating plasticity) and the mean stress is given by $(K_t \sigma_m - \sigma_R)$. Since mean stress has an effect on crack propagation rate of aluminium alloys[46] the value of σ_R will affect the rate of fatigue damage during crack propagation. It should be borne in mind that frequently σ_R may be large enough to give compressive stresses at the notch root over parts of the loading waveform and this may be expected to further reduce the crack propagation rate[47].

It can be concluded then that geometric residual stresses may affect the fatigue damage growth rate to some extent throughout the fatigue life, where initiation is from a very large notch, i.e. where in the uncracked specimen the elastic stress value does not change significantly over the depth d in Fig.8. For smaller notches of the same K_t value, cracks will propagate through regions of significantly diminishing residual stress and hence such stresses are likely to be most effective in the early stages of fatigue life. For very small sized specimens where the stress field at the crack tip quickly becomes comparable in size with the geometric residual stress field the effect of residual stresses is likely to be small since the residual stress field will be dispersed early in the life.

It follows therefore that where $\sum \frac{n}{N}$ is increased by a geometric residual stress field, in general, in the absence of any other effects $\sum \frac{n}{N}$ should be greatest for damage states reached early in the life. This assumes of course that $\sum \frac{n}{N}$ for crack propagation is unity in the absence of residual

stresses. The results quoted in Appendix F suggest, in fact, that for crack propagation tests in the absence of geometric residual stresses $\sum \frac{n}{N}$ may be expected to be close to unity for Gaussian random loading in aluminium alloy specimens but greater than unity for gust loading spectra where the ratio of peak stress to rms stress is greater.

4 AN APPROACH TO CUMULATIVE DAMAGE

In this section a general approach to cumulative damage is described which it is hoped contains the elements of a practical method of life prediction. A first attempt at devising such a method is also described.

The method assumes that for notched and plain specimens the value of $\sum \frac{n}{N}$ is known in the absence of yielding at the point of fatigue initiation during the fatigue life. The method then in principle accounts, where necessary for the effects of geometric residual stresses introduced by local yielding under the loading action. Specific cases are covered, namely that of notched aluminium alloy specimens at a positive mean stress under a symmetrical loading action, that of a residual stress initially present in the specimen due to manufacture, and finally the case of air-ground-air cycles. It should, however, be emphasised that prediction for any kind of loading action can be dealt with in a similar manner. The principle of the method is that Miner's Rule must be applied to the actual stress history at the point of fatigue initiation. This history may not be a simple function of the net stress history as discussed in section 3.

Before the actual method is described, however, the question of consistency of Miner's Rule in the absence of geometric residual stresses is discussed (section 4.1). This is, of course, fundamental to the accurate working of the method. Data is reviewed, for which, if the specimens used were free of manufacturing stresses, geometric residual stresses would not be formed subsequently. It is suggested, however, that the wide variation in values of $\sum \frac{n}{N}$ under similar loading actions could be substantially due to stresses induced in manufacture, since in no case were any stress measurements made prior to testing.

4.1 Consistency in test results

One of the great difficulties confronting any investigator when examining cumulative damage behaviour is the apparent lack of consistency of many of the results in the literature. However it is often difficult to find two sets of data which are directly comparable and it is practically impossible to isolate many factors giving different values of $\sum \frac{n}{N}$ from the work of different

investigators. In Table 1 a collection of data is shown all obtained under Gaussian random loading. All the tests are either on plain specimens, or on notched specimens at zero mean stress. This choice is to isolate any geometric residual stress effects, assuming all of the specimens were initially stress-free. No clad specimens have been included since such specimens have been shown to exhibit cumulative damage behaviour different from those in the bare material (Appendix A). Finally to eliminate load sequence effects no programmed tests have been included. The lack of consistency of the aluminium alloy results[48-54] is quite remarkable for example at 10^6 cycles $\sum \frac{n}{N}$ values range from 1.7 to 0.04. Possible reasons for the differences include:-

(a) Bending or direct stress conditions

The two lowest values of $\sum \frac{n}{N}$ for aluminium alloy were for direct stress conditions[50,53] although not for the steel specimens. If this trend for aluminium alloy specimens is significant, size would also be a factor since very large specimens in bending approach stress conditions over the area of action of fatigue identical to that of specimens under direct stress.

(b) Different waveform irregularities

The effect of waveform irregularity on fatigue life has been investigated by a number of workers[51,53,55]. No general pattern seems to have emerged, even on whether life as measured by numbers of zero crossings increases or decreases with irregularity factor. Tentatively it can be stated that between values of $\frac{n_o}{n_p}$ of 1.0 and 0.8, life is unlikely to vary by more than a factor of 1.5. An examination of Table 1 shows therefore that waveform irregularity is unlikely to be a major factor in accounting for the variation observed.

(c) Different truncation values

The effect of truncation level $\frac{\sigma_p}{\sigma_r}$ on $\sum \frac{n}{N}$ has been investigated[58] for mild steel specimens. Little variation was shown in $\sum \frac{n}{N}$ for truncation levels varying between 3.5 and 5.5. Although truncation level was not measured in every investigation quoted in Table 1, in every case where it was measured[50,52,56,57] it equalled or exceeded 3.5 times the rms level. Hence difference in truncation level between different investigators is unlikely to be the main cause of the variation in values of $\sum \frac{n}{N}$, assuming no difference in behaviour in this respect between steels and aluminium alloys.

Other possible reasons for inconsistency include surface finish, size of specimen and state of heat treatment of the material. If, however, any of these factors are of importance, it is not at present clear by which mechanism $\sum \frac{n}{N}$ is being affected.

One other phenomenon which shows promise of being largely responsible for test result inconsistency is the effect of residual stresses due to manufacture. In section 3.2 it was shown how such stresses can be the cause of large variations in $\sum \frac{n}{N}$ in aluminium alloy specimens (see Fig.9) and can give rise to values of $\sum \frac{n}{N}$ greater than unity. It was also shown that mild and medium strength steel specimens are generally unaffected in this way. Although only three investigations[56-58] on such steels are quoted in Table 1, and there are differences in bandwidth and stress concentration factor, $\sum \frac{n}{N}$ values are remarkably consistent. Therefore, while it is impossible to say with certainty whether or not manufacturing stresses are responsible for the variation in results of different investigations on aluminium alloy specimens, the evidence quoted here is consistent with this hypothesis. If this is so, the results of such investigations on aluminium alloys are of little use without any initial measurement of the state of stress of specimens before testing. A number of methods are available to do this, and a bibliography of papers on this subject is given in Ref.59.

4.2 Method of approach

On the basis of the factors discussed in the previous sections of this Report, the following approach to cumulative damage is suggested.

In particular sectors of engineering, certain conditions are likely to be common to large numbers of components, i.e. type of material, general loading action, the occurrence or otherwise of fretting and the maximum load as a percentage of ultimate. Other conditions exist which will vary more from component to component, i.e. rms alternating stress, initial state of stress, mean stress, and stress concentration factor. At present common practice is to design components from previous experience, using Miner's Rule where necessary.

As always in fatigue it is difficult to generalise, but test results show that for non-welded components in medium and low strength steels $\sum \frac{n}{N}$ is rarely greater than unity or less than 0.3 [43,56-58]. This is despite the possible beneficial effects of coaxing (Appendix C) and strain hardening

(Appendix D). The circumstances under which beneficial effects have been found to predominate are stated in Appendix C. For such steel components too, mean stresses do not greatly affect either absolute life or $\sum \frac{n}{N}$ for the reasons already stated[44]. Also stress concentrations do not greatly affect $\sum \frac{n}{N}$ for these materials. Hence it can be concluded that for non welded components in low and medium strength steels present design practice is adequate in principle, but it should be emphasised that it is advisable when using the Rule to assume a value of $\sum \frac{n}{N}$ of about 0.5. This is put forward as an average obtained in practice and not as a 'safe' value - the life so estimated will generally be divided by a safety factor to cover scatter, corrosion, and other effects. In cases where a large proportion of stress cycles are below the fatigue limit a lower value of $\sum \frac{n}{N}$ should be assumed.

For components made of aluminium alloy it is necessary to account for the effects of geometric residual stresses in addition to making some general assumption about the values of $\sum \frac{n}{N}$ to be obtained for initially stress-free specimens in the absence of subsequent local yielding. It has not yet been proved that $\sum \frac{n}{N}$ is relatively consistent for different aluminium alloys under such conditions. However, it has been shown in section 4.1 that this is at least a possibility. Once such values of $\sum \frac{n}{N}$ have been established for particular load spectra under the above conditions, residual stress effects can be accounted for by the method described in the next section or a development thereof. Geometric residual stresses are affected by conditions which were stated earlier in this section to vary considerably from component to component, e.g. initial stress state, mean stress and stress concentration factor, which means that life prediction needs to be considerably more involved for aluminium alloy components than for those in medium and lower strength steels.

4.3 Method of life prediction

Methods of life prediction which account for the effects of geometric residual stresses have been published[16-18]. All such methods are similar in principle. The method described here is based on the work in Refs.38 and 60, in which the behaviour of notched aluminium alloy specimens under constant amplitude loading after a unidirectional preload or change in net mean stress, was explained by the change in local mean stress and the use of the Goodman diagram.

In section 3.1 it was shown that the local mean stress at the root of a stress concentration in an aluminium alloy component under loading at a constant amplitude σ_a and a positive mean stress σ_m is given by equations (2) and (3),

in the absence of local compressive yielding. Where local compressive yielding occurs, $\sigma_{\ell m}$ is greater than the values given by equations (2) and (3) (see Fig.1). Under random loading, therefore, the local mean stress $\sigma_{\ell mr}$ is given by the highest stress in the applied load spectrum σ_p (i.e. equations (2) and (4)). Consider an alternating stress amplitude σ_a within the random loading spectrum. Under loading at this amplitude, the local mean stress $\sigma_{\ell m}$ is given by σ_6 in equations (2) and (3). Hence if the life under random loading is to be predicted from data obtained at stresses σ_a then such data should be adjusted for a change in local mean stress $\sigma_{\ell m}$ to $\sigma_{\ell mr}$. Data can be adjusted by means of the Goodman relationship[61]. Let σ'_a be the adjusted fatigue strength corresponding to σ_a : therefore

$$\sigma'_a = \sigma_a \left(\frac{\sigma_u - \sigma_{\ell mr}}{\sigma_u - \sigma_{\ell m}} \right) \quad . \tag{4}$$

The adjustment to any set of values of σ_a is clearly different for each value of maximum stress σ_p, so that for every value of maximum stress there is a different fictitious S-N curve to which Miner's Rule should be applied in order to obtain an estimate of the random fatigue life. Fig.9 shows such a set of curves obtained from the investigation described later in this Report. Each of the fictitious S-N curves cuts the experimentally obtained curve at the maximum stress in the spectrum for which that curve is valid, i.e. curve A can be used to predict fatigue life under any load spectrum in which the maximum stress is $6\sqrt{2}$ ksi (the factor of $\sqrt{2}$ appears since all stresses are rms on this diagram). Finally it may be necessary to introduce a further modification to the predicted life to account for the factors which tend to make Miner's Rule overestimate the life of plain specimens. For simplicity this was not done when applying the rule in section 6.5.

4.4 Allowance for the presence of stresses due to manufacture

In order to account for stresses already present in a specimen it is strictly necessary to know the value of the residual stress σ_R and of the accompanying residual strain ε_R at the point of fatigue initiation. Fig.10 shows the stress/strain curve for a material under consideration. Point A represents the state of stess at the point of fatigue initiation before testing commences. On initial loading, therefore, the stress/strain relationship will follow the line AB. As to what will happen in the region of B, this is not clear and will be governed by the state of strain hardening of the material. For simplicity it will be assumed here that loading will follow the

line ABC . The calculation of predicted life proceeds exactly as in the previous section except that curve ABC is used instead of curve DBC . If the post yield σ/ε curve is fairly flat, as in the figure, there is little error involved in assuming ε_R to be zero, since the strain is only of importance insofar as it enables the stress at the maximum load in the spectrum and the corresponding $\sigma_{\ell m}$ to be calculated. In Fig.10 the error in $\sigma_{\ell m}$ in making this assumption would be the difference between σ_1 and σ_2 .

In cases where, due to a particular combination of residual stress and mean stress, compressive yielding occurs at a lower amplitude than tensile yielding, the procedure is the same as previously, except that the compressive stress/strain curve must be used, and $\sigma_{\ell m}$ will increase with alternating stress amplitude from a negative value (cf. Fig.3).

4.5 Accuracy of the method

Accuracy in using the method will depend on a number of factors:-

(a) The effectiveness of residual stresses probably depends on size as discussed in section 3.

(b) The shape of the mean stress/alternating stress diagram is an important factor in the method. In section 4.3 it was proposed to use the Goodman line, which gives a straight line of constant fatigue strength for the relationship between mean and alternating stress. Other relationships may give a better result[61]. In particular, there is evidence that fretting can affect the relationship[62].

(c) The reliability of any prediction depends to a large extent on the accuracy with which $\sigma_{\ell m}$ is calculated. As was shown in section 3 and Fig.1, for high peak loads the action of the Bauschinger Effect is to change the value of $\sigma_{\ell m}$ from that given by equations (2) and (3). As a general rule[31] the Effect becomes of significance approximately when the local stress changes sign after yielding in one direction, e.g. after tensile yielding some compressive yielding will occur as soon as the stress becomes negative. Figs.42 - 44 show predicted and achieved fatigue lives under random loading conditions in the programme described later in this Report. In this case the Bauschinger Effect may be expected to be significant at stresses above approximately 2.5 ksi rms. Its effect will be to reduce the values of predicted lives above this stress level.

(d) The prediction strictly only applies to the parts of the fatigue life fully affected by residual stresses and so should tend to overestimate their effect. Work is needed to determine the percentage of fatigue life so affected.

4.6 Developments of the method

In the foregoing sections it was assumed that the basic fatigue information used to calculate variable amplitude fatigue lives was in every case data obtained under constant amplitude conditions, i.e. the S-N curve. Methods of life prediction have been devised for components subjected to symmetrical load spectra [8,63,64] in which data obtained under a standard form of variable amplitude loading were used in the place of the S-N curve.

These methods, similar to each other in principle, can be summarised as follows.

It is possible in many cases to obtain the same load amplitude distribution as that found in service by applying stationary random loading with a Gaussian distribution of amplitude in sequential 'blocks' of different root mean square values, for different lengths of time. Thus the load spectrum can be synthesised by a number of stationary random components. In Ref.8 a method of so synthesising service load spectra was described, and an aircraft gust loading spectrum was synthesised by only three random rms levels, say σ_{r1} for p_1 of the time, σ_{r2} for p_2 of the time etc. Thus the fatigue damage caused by each of these three components can be assessed and the life predicted accordingly. Life prediction for service loading proceeds as if Miner's Rule was being applied to a block programme containing three constant amplitude levels, except that N_1 is now the fatigue life under stationary random loading at stress level σ_{r1} and so on, so that life under service spectrum loading

$$N_s = \frac{1}{\frac{p_1}{N_1} + \frac{p_2}{N_2} + \frac{p_3}{N_3} + \ldots} \quad . \tag{5}$$

Clearly it is possible to develop the method of section 4 to use variable amplitude data. In principle, representative values of $\sigma_{\ell mr}$ are calculated for a range of values of random rms stress from consideration of the peak stress at these levels, so enabling a diagram similar to Fig.2 to be drawn, except that the alternating rms stresses refer to stationary random loading. Next the σ-N curve (random loading S-N curve) is adjusted for the values

of $\sigma_{\ell mr}$ which apply under service spectrum loading, so that a set of fictitious σ-N curves is constructed similar to the set of fictitious S-N curves in Fig.9. Each fictitious σ-N curve can be used to predict fatigue life under any spectrum loading which contains the particular value of σ_p, the maximum load in the spectrum that applies to that curve. For the prediction, equation (5) is used with N_1, N_2 etc. being the lives on the fictitious σ-N curve corresponding to σ_{r1} and σ_{r2}. The advantages of this method are as follows.

(a) The basic data would be conditioned to some extent for the effects of different relative damage rates, variation with stress of residual static strength at failure and for cycles below the fatigue limit.

(b) The values of $\sigma_{\ell mr}$ for the basic data would be closer to those existing under the service loading action. Corrections for geometric residual stress would then be smaller and as a consequence more accurate.

(c) Stresses, initially present in the specimens used to obtain the basic data, would in many cases be relaxed under the variable amplitude loading and would therefore not affect the prediction.

An alternative approach would be to use, in obtaining basic constant amplitude S-N data, specimens which had been initially loaded to a value approximating to the highest load expected in the service load spectrum. This would again ensure that values of $\sigma_{\ell m}$ were more representative for the basic data. A standard preload value could be used for design data, and adjustment for the correct value of $\sigma_{\ell m}$ could be made. Note (b) above would then apply.

The inclusion of air-ground-air cycles in block programmes has been shown to result in a large reduction in life. This reduction which was greater than predicted by Miner's Rule was attributed to the action of geometric residual stresses[65]. Allowance for air-ground-air cycles can be made by extending the method of section 4. The damage associated with such cycles can be calculated using Miner's Rule applied to the material at the point of fatigue initiation. The calculated damage due to cycles immediately after such cycles will then in general have to be modified, since any local compressive yielding due to the air-ground-air cycle (yielding will be accentuated by the Bauschinger Effect) will increase $\sigma_{\ell mr}$ and hence also the subsequent damage rate. This situation will continue, with $\sigma_{\ell mr}$ progressively reduced by local yielding under each succeeding higher positive load after the air-ground-air cycle, until the highest positive load in the spectrum or the next air-ground-air cycle is

applied. This is shown diagrammatically in Fig.11. The upper diagram represents the net stress history on an aircraft component during an air-ground-air cycle. The lower diagram shows the corresponding variation of $\sigma_{\ell mr}$ at a stress concentration on the component. The accelerated fatigue damage rate due to the raised level of $\sigma_{\ell mr}$ between A and B can be accounted for as in section 4.3.

5 CUMULATIVE DAMAGE PROGRAMME

Much work is required to investigate fully the validity of the approach to cumulative damage and develop the method outlined in section 4. The programme described in this section was initiated in order to make a start on such an assessment by determining the cumulative damage behaviour of aluminium alloy specimens with fretting, under a wide range of symmetrical stressing conditions. Tests were carried out at three mean stress levels, 10, 16 and 25 ksi, under three types of loading, that is sinusoidal constant amplitude and two shapes of variable amplitude load spectrum. The variable amplitude loading action used was in all cases narrow-band Gaussian random loading, giving a load pattern in the form of a randomly modulated sine wave, Fig.12a, at a frequency of 112 Hz, and having a Rayleigh distribution of peaks (Fig.12b). This loading action under 'stationary' conditions, i.e. constant long term rms level, was the first of the random loading conditions used. The second random loading condition was obtained using the technique of random programming[8] to apply to the specimen a stress spectrum based on the gust spectrum contained in the Royal Aeronautical Society data sheets[66] (nearly exponential peak distribution). Random programming consists of the sequential application to the specimen of 'blocks' of random loading at different rms levels for different lengths of time (see sections 4.5 and 5.2).

In order to better understand the manner in which fatigue damage accumulated under the various types of loading, 'partial damage' tests were conducted in addition to those carried out to total failure, i.e. specimens were fatigued for a given percentage of the expected life to failure, and were broken statically to determine the state of fatigue damage. In this work fatigue damage was defined by the fall-off in residual static strength.

5.1 *Fatigue machine and associated equipment*

A 20 ton Avery Schenck resonant fatigue machine was used (Figs.13 and 14). This machine has been modified[8] to perform fatigue tests under either stationary random, random programmed or constant amplitude conditions.

Broadly the modifications consisted of replacing the standard inertial excitation unit with an electro-dynamic shaker which could be used to apply either random or constant amplitude excitation to the machine.

Monitoring of the dynamic load was achieved by the use of semiconductor strain gauges mounted on the dynamometer ring of the machine. The output of a full bridge of these gauges was sufficient to drive a random noise voltmeter directly (see Fig.14). This instrument has a dc output corresponding to meter deflection, and was in turn used to supply a dc trace recorder, enabling a continuous monitor to be made of the alternating stress level. For constant amplitude tests the random noise voltmeter was used with a time constant setting of 0.3 second, so that any relatively rapid fluctuations in the alternating load were detected. For random loading, on the other hand, a setting of 30 seconds was used so that the monitor showed only an integrated long-term value of root mean square stress. The rms level under all loading conditions was controlled by changing the input amplitude voltage level to the machine when limit switches were actuated on the trace recorder. This method of control was satisfactory in the case of random loading, but required some skill in the case of constant amplitude tests when setting the excitation frequency at the beginning of the test. If the frequency was not set correctly, large changes in amplitude would occur when the specimen started to crack and the control rate was not always fast enough to compensate. Therefore, in a few cases, specimen tests were rejected because of overloading. For this reason a controller, which alters the machine amplitude by changing the excitation frequency, is at present being assessed, and should simplify testing.

Resonant fatigue machines, in general, take the form of lightly damped single degree of freedom mechanical systems, having a constant amplitude force input at a frequency close to the machine resonance. If a 'white noise' (constant power spectral density) force input is substituted, the machine filters out all frequencies relative to a narrow band centred on the resonant frequency. It can be shown[67] that if the amplitude distribution of the white noise excitation is approximately Gaussian and the response of the machine is linear, then the loading waveform of the machine is a randomly modulated sine wave with a Gaussian amplitude distribution a Rayleigh distribution of peaks (Fig.12b), i.e. a narrow-band random process. In practice, the idealised white noise input is usually replaced (as in Fig.14) with noise filtered by a band pass filter centred on the resonant frequency of the machine. The object of this is to

reduce the required power output of the main drive amplifier and to avoid exciting unwanted machine resonances. This last point was of particular importance in this investigation since the mechanical resonant system of the machine in Fig.13 took the form of a beam, and so was a multi-degree of freedom system. In order to increase the operating frequency of the machine, all tests were carried out with the beam excited in its first overtone mode at 112 Hz, rather than in its fundamental mode at about half this frequency.

For random programmed tests the programmer altered the root mean square value of the input signal to the machine in steps by switching the random signal through each of three attenuators in repeated order.

Analysis of the random load pattern was accomplished by supplying the output from the strain gauges to an instrument which can count the number of times each of ten independently preset voltage levels is crossed in a positive-going direction. This is a more accurate method of measuring the shape of the load spectrum than the previously used[8] method of monitoring the envelope of the random loading waveform. Typical measured load spectra are shown in Figs.15 and 16.

5.2 Load spectrum for random programmed tests

As in Ref.8, the load spectrum chosen for the random programmed tests was that implied by the gust spectrum in the Royal Aeronautical Society data sheets[66]. For the purpose of this investigation, a new synthesis was prepared (Fig.17) to give a spectrum with a smaller relative number of counts at the lower stress levels than that used previously. In this way the length of time to failure was reduced for the random programmed tests. Fig.17 also shows a comparison between the synthesis used in this programme and that used previously. In Figs.16 and 17 σ/λ is a non-dimensional amplitude parameter, where σ is the actual stress and λ is that value of stress corresponding to a 5 ft/sec gust on the Royal Aeronautical Society spectrum. The method of synthesis of the spectrum from three random components is described in Ref.8. Table 19 gives details of the programmed spectra used in the fatigue tests.

5.3 Specimen and material

Chemical composition and tensile test results for the DTD 5014 aluminium alloy are given in Table 2, and a typical measured stress/strain curve for the material is given in Fig.18. All the specimen material came from the same melt.

Specimen and pin dimensions are given in Fig.19. As can be seen, the specimen is in the form of a double-ended lug. Failure in fatigue for such specimens occurs at the points shown, where a stress concentration factor of 2.96 is close to an area of fretting. Sample specimens were tested to determine approximately the state of macroscopic residual stress at the point of fatigue initiation. Strain gauges having a 2 mm gauge length were first attached to the specimen as shown in Fig.19. After the gauge had been connected to a strain gauge bridge, the bridge was balanced, a jeweller's sawcut was made, as shown, to relax any longitudinal residual stresses at the gauge to zero, and the bridge rebalanced so as to measure the change in strain. This residual strain value was used to calculate the longitudinal residual stress.

5.4 *Test procedure*

Fatigue tests were carried out by applying fluctuating tension at 112 Hz, and all specimens were assembled without grease or anti-fretting compound between the pins and the holes. For selected random and random programmed tests the distribution of levels crossed (spectrum shape) was measured. Typical results of these analyses are shown in Figs.15 and 16*. These in general confirm the measurements taken during the previous investigation, demonstrating that at the higher random stress levels the amplitude distribution tended to truncate so that few peak alternating stresses were obtained greater than σ_m, provided

$$\frac{\sigma_m}{\sigma_{rms}} \leqslant 3.$$

Not unexpectedly, it was found that the stress spectrum truncated more sharply on the compressive side than on the tensile side. Fig.20 shows the estimated truncation levels at all the stress levels tested.

The results of the tests under the three types of loading are shown in Tables 3 - 11 and Figs.21 - 29. In all cases the stress value plotted is the root mean square stress. Partial damage tests were conducted for constant amplitude and stationary random loading by breaking statically specimens which had been fatigued to various percentages of the expected endurance. The failing load was recorded in these tests and the change in residual strength from the uncracked state was regarded as a measure of the fatigue damage. The results of the partial damage tests are given in Tables 12 - 17 and Figs.30 - 32 and were

*In the text, and diagrams, the mean and alternating rms stresses are shown, for example as 10/3.5 which represents 10 ksi mean stress with 3.5 ksi rms alternating stress.

used to construct S-N and σ-N (stationary random) curves which applied to different measured states of fatigue damage, i.e. 95, 90, 80, 70 and 60 per cent of the uncracked static strength (see Figs.21, 22, 24, 25, 27 and 28). Partial damage tests were not carried out under programmed random loading. It is hoped to do this at a later date.

Lives under stationary random loading to different states of fatigue damage were predicted using Miner's Rule by means of the corresponding curves obtained under constant amplitude conditions. Also the rule of section 4 of this Report was used to predict life, assuming initial compressive residual stresses of 0, 10 and 20 ksi (see Figs.33 - 35). $\sum \frac{n}{N}$ values using Miner's Rule are given in Figs.36 - 38. For the purpose of the prediction no allowance was made for the Bauschinger effect - it was assumed that equations (1) and (2) hold where they give positive values of $\sigma_{\ell m}$. Where negative values were given by the equations $\sigma_{\ell m}$ was taken to be zero, i.e. the assumption was made that the compressive yield point remains the same after tensile yielding. The effect on Miner's Rule of the static strength at failure was also estimated (see Table 18 and section 6.3). For random programmed tests, lives to failure were predicted using Miner's Rule, the rule of section 4 and the rule of Ref.8, which is described in section 4.6 (see Figs.23, 26 and 29). In all cases where Miner's Rule was used the truncation levels of the random waveforms were taken into account.

5.5 Accuracy and consistency of test results

Certain inconsistencies were found during testing. Specimens were machined in two batches, and most of the first batch was used up before the start of the partial damage tests. These tests are labelled 'first test series' in Figs.21 - 29. Therefore the partial damage tests were carried out almost entirely using the second batch of specimens. Subsequently, further tests were carried out to check lives to failure. The results of these tests are labelled 'second series of tests' in Figs.21-29. In general the second series of tests confirm the first. There are, however, two exceptions, both under random loading. First, at 10/1 ksi the second test series differed from the first by a factor of about 2:1 on life. Secondly, at 25 ksi mean there was a similar difference at stresses above alternating stresses of 4 ksi. In no other case was a significant difference found. Only at 25/4 ksi was the difference significant in the partial damage tests, and here the conclusions of the work were not affected.

In Figs.21, 22, 24, 25, 27 and 28 the S-N and σ-N curves and $\sum \frac{n}{N}$ values for the intermediate states of fatigue damage are clearly not as accurate as the curves for final failure, since they were constructed from a knowledge of the S-N and σ-N curves to final failure together with data from partial damage tests at only two or three stress levels. It is, however, believed that the overall trends shown in these curves are reliable. All the constant amplitude S-N curves at the various states of damage are shown as having approximately the same fatigue limit. This is because none of the unbroken fatigue test specimens, which were all subsequently broken statically, showed any more than 5% drop in static strength compared with the average uncracked strength.

6 DISCUSSION OF EXPERIMENTAL RESULTS

Typical broken specimens are shown in Figs.39 and 40. It was found that failure always occurred from an area of fretting close to the point of maximum stress concentration.

The results show that in this investigation $\sum \frac{n}{N}$ was generally greater than unity under random and random programmed conditions (see Figs.23, 26, 29 and 33 - 35), in line with a number of other investigations into cumulative damage of aluminium alloy specimens with stress concentrations at a positive mean stress (see section 3.4). Exceptions to this were found at the alternating stresses below 10/2 ksi random loading. Under random loading conditions at 10 ksi mean stress, $\sum \frac{n}{N}$ was found to increase with rms stress at all states of damage up to 3.5 ksi alternating stress, the highest value tested (Fig.36). At 16 and 25 ksi mean stress $\sum \frac{n}{N}$ increased up to a maximum value at about 2.5 ksi (Figs.37 and 38) and thereafter decreased. Also under the stationary random loading $\sum \frac{n}{N}$ values were generally greater for initiation than for the total life to failure, and were higher for random programmed tests than for stationary random loading.

The various aspects of the performance of Miner's Rule referred to above are discussed in more detail in the following sections. The results should be considered in the light of the fact that the part of the investigation in which strain gauges were used to determine the initial stress state showed evidence of initial compressive residual hoop stresses around the hole varying between 4 and 15 ksi. Accordingly, life predictions based on 0, 10 and 20 ksi initial compressive stresses are included in Figs.23, 26, 29 and 33 - 35. It should be noted that only about fifteen strain gauge readings were taken in establishing the actual residual stresses; it was felt that owing to variations in readings from specimen to specimen a more comprehensive investigation was desirable. The results of this investigation will be published later.

6.1 Rate of accumulation of fatigue damage

In Appendix A the effect on cumulative damage of variation in relative damage rate with stress, is discussed at some length since it has received a great deal of attention in the past. It was concluded that for spectrum loading the effect was not large. However, the shapes of 'damage against percentage life' curves can be of some value in deducing the relative magnitudes of other conditions effecting cumulative damage.

Comparison of the results of the partial damage tests with those of Ref.68 shows a marked difference. Whereas with the notched and plain specimens of 2024-T3 aluminium alloy used in that investigation macroscopic cracks were not recorded until relatively late in the life, in this case, under constant amplitude loading at least at the lower stresses, large cracks were present very early in the life (Fig.39). This difference was almost certainly due to the action of fretting and demonstrated how crack initiation time can be reduced in its presence.

The partial damage tests under constant amplitude loading also showed that at all three mean stress levels the reduction in residual static strength early in the life occurred relatively faster at low than at higher stress levels. This is an effect opposite to that which has been found for plain specimens (Appendix A)and there are three likely explanations for this. One explanation is again the action of fretting. Fretting lowers the fatigue limit and so at stresses below the unfretted fatigue limit will reduce the fatigue life from virtually infinity to a finite value. Hence on a percentage life basis, fretting is more effective at reducing fatigue initiation time at low than at high stresses. Therefore fretting may reverse the trend of initial relative fatigue damage rate with stress. Geometric residual stresses also provide an explanation for the reversal in trend. In a notched specimen under constant amplitude loading, at a positive mean stress, such residual stresses reduce the local mean stress as the alternating stress is increased. As a result of this, the rate of *fatigue damage initiation should not increase with stress in a notched specimen* as fast as in a plain specimen. Thirdly, the fact that specimens which are fatigued at high stress levels will fail at the lowest state of damage (Appendix B), tends to cause the observed trend in damage accumulation. If, to take an extreme case, a specimen were cycled such that the maximum stress in the cycle was 99% of the ultimate, then very little fall in residual strength would be detectable during the life. Hence at the lower stress levels the residual strength against percentage life curve must show a greater drop, at least in the later stages of the life.

There is some evidence from the partial damage tests to support fretting as having some effect on the shape of the residual strength curves. From Fig.2 it can be seen that for initially stress-free specimens at 10 ksi mean, under constant amplitude loading, the local mean stress was unaffected by alternating stresses up to 4 ksi rms. (Initial compressive residual stresses would increase the unaffected stress range.) Fig.30, however, shows that, early in the life, damage still accumulated faster at 2 ksi than at 4 ksi. Hence since residual stresses were not effective, fretting was a likely cause of the particular variation of damage rate with stress measured here.

As for the effect of damage state at failure, Fig.41 shows the results at 25 ksi mean, replotted to represent failure under all alternating stresses at the state of damage corresponding to failure at 1.5 ksi rms. As can be seen, by comparison with Fig.40, the general trends of the damage against percentage life curves were not affected by the changed failure criterion, and would clearly also not be affected at the other mean stress levels. Damage state at failure was therefore not important in this case.

Relative damage rates under random loading showed trends different to those under constant amplitude loading. This is discussed in section 6.2.

6.2 Evidence for the presence of geometric residual stresses

Under random loading, the residual strength against cycles curves show that at 16 and 25 ksi mean, at the lower stress levels, damage did not accumulate nearly as fast early in the life as it did under constant amplitude loading at similar lives (see Figs.31 and 32). Different behaviour was shown with 10 ksi mean stress where at 1.5 ksi rms the trend was similar to that found under constant amplitude loading (Fig.30) and $\sum \frac{n}{N}$ was less than unity. This was the only random loading case in which the maximum static plus dynamic loads were not high enough to cause yielding at the root of the stress concentration. This different behaviour strongly suggests that the initial, relatively reduced, rate of damage accumulation under random loading at the higher mean stresses was associated with geometric residual stresses. It can be deduced that residual stresses increased the initiation time relative to the crack propagation time at the lower random stress levels at 16 and 25 ksi mean, to produce the trend in damage/percentage life shown. This is further demonstrated in Figs.36 - 38 in which $\sum \frac{n}{N}$ is shown to have been larger up to damage states reached early in the life, than for final failure except at 10/1.5 ksi, i.e. $\sum \frac{n}{N}$ was greatest for the initiation.

In another respect the shapes of the σ-N curves at 25 and 16 ksi mean stress are consistent with the effects of geometric residual stresses (Figs.34 and 35). At the approximate stress above which the Bauschinger Effect (section 3.1) was operative the σ-N curves straighten or even bend slightly towards the low life direction rather than maintain a concave shape as predicted by Miner's Rule. This produced a decrease in $\sum \frac{n}{N}$ (Figs.37 and 38). The predictions of fatigue life based on consideration of residual stresses as in section 4 show a similar reflex shape for the predicted σ-N curves with the point of inflection at a higher stress than that found in practice. Allowance for the Bauschinger Effect should lower the point of inflection and so reduce this discrepancy between the experimental and predicted results.

Finally, as in Ref.8, for the random programmed tests at all mean stress levels $\sum \frac{n}{N}$ to failure was consistently greater than under stationary random conditions. This general trend is also predicted by the method of section 4. However, recent work has shown that $\sum \frac{n}{N}$ values greater than 1 can be obtained for crack propagation under a gust load spectrum[69]. It is therefore possible that parts of the increases in $\sum \frac{n}{N}$ in the programmed random cases were in the later stages of life.

6.3 Residual static strength

The partial damage tests were used to obtain an estimate of the effect on Miner's Rule of residual static strength at failure by means of the construction of S-N curves representing life to various values of static strength. Fig.42 shows S-N curves, at the three mean stress values, representing life to a static strength value given by the highest load in the random spectrum, at the rms levels shown. Therefore, for example, if the life to failure at 25/6 ksi random is required using Miner's Rule but allowing for the effect of residual static strength, then the Rule should be applied to the left-hand curve instead of that to final failure at 25 ksi mean. Table 18 shows the modification due to this phenomenon required for the calculated lives. The largest effect can be seen to have occurred at a mean stress of 25 ksi, at which the highest static plus dynamic loads were applied. The conclusions reached in Appendix B (that the effect on the achieved life of a bolted joint would only be large if loads approaching the uncracked static strength of the specimen were to be applied during the fatigue life) clearly also applies in this case. One point however needs clarification. Although the effect has been expressed, in this case, as a percentage change in life, in principle the effect of this phenomenon is to

shorten the life by a given number of cycles rather than by a given percentage since the rate of fall off of residual strength is a function of crack growth rate and does not depend on initiation time. Therefore, if the total achieved life is shortened by an unfavourable interaction in the initiation stage, the effect of residual strength at failure will be proportionally greater. In the case of this investigation the effect, as a percentage of the achieved life, was generally less than shown in Table 18, since $\sum \frac{n}{N}$ in most cases was greater than one.

6.4 Performance of modified Miner's Rule[8]

The results of the tests carried out under programmed random loading (Figs.26 and 29) indicate that at the higher mean stresses the modified rule (described in Ref.8 and section 4.6) applied to random data gave a significantly better prediction than Miner's Rule based on constant amplitude data. At 10 ksi mean stress (Fig.23), however, Miner's Rule was marginally superior. In all cases $\sum \frac{n}{N}$ was greater than unity. The generally superior performance of the modified rule can be explained by the conditioning argument of section 4.6. The question as to whether constant amplitude, preloaded constant amplitude or Gaussian random loading data (see section 4.6) is the most efficient for use in life prediction can only be settled by further experimental work.

6.5 Performance of rule of section 4

Consider first the results of random tests at 10 ksi mean (Fig.33). The interesting characteristic here is the near vertical portion of the σ-N curve. As can be seen, the sharp upward trend in the curve was predicted by the rule assuming zero initial compressive residual stresses, but its severity was underestimated. Also, although the rule gave a good prediction for final failure, this was probably coincidental. In considering this apparently good prediction *it should be noted that the plot of* $\sum \frac{n}{N}$ *against stage in life* (Fig.36) clearly indicates that the longer than expected life is due to the fact that there is a very high value of $\sum \frac{n}{N}$ early in the life and not a constant value all the way through. This initial value was underestimated by the rule (see predicted results for 95% static strength - Fig.33), and the good agreement for the final failure case was only obtained by assuming the full residual stress effect, i.e. constant $\sum \frac{n}{N}$ over the whole life. When an initial compressive residual stress was assumed of 10 ksi or greater, the prediction became practically identical with that of Miner's Rule.

It is therefore doubtful whether all of the increase in $\sum \frac{n}{N}$ was due to geometric residual stresses in the case above. However, as discussed below, under programmed random loading at 10 ksi mean, and under both types of loading at the other mean stresses the results were consistent with geometric residual stresses being the most important factor causing deviations from Miner's Rule.

At 16 ksi mean stress, if the assumed initial residual stress were to be zero, residual stresses should have some effect on the predicted life over the entire stress range. This is because the mean stress on its own is sufficient to bring the stress at the stress concentration close to yield. Under this mean stress there is a large difference in predicted life when using the rule of section 4, depending upon the assumed state of initial stress (Fig.11). In one respect the results are similar to those of 10 ksi, in that Miner's Rule gave a reasonable prediction up to a given stress, in this case about 1.5 ksi, and above this stress the life was longer than predicted. Again the behaviour is explained qualitatively by the new rule, the point of deviation from Miner's Rule being governed by the assumed initial residual stress (Fig.34). However, in this case the new rule greatly over-predicted the deviation even at the damage state representing 95% static strength. As was discussed in section 6.2, the presence of a point of inflection in the σ-N curve was predicted by the rule of section 4 and allowance for the Bauschinger Effect should lower the predicted point of inflection closer to that actually achieved.

At a mean stress of 25 ksi considerable local yielding occurred under the application of the mean load on its own. Therefore the predictions using the new rule were practically the same, for the three values assumed of initial residual stress (see Fig.35). This factor also means that yielding will have occurred under any loading cycle, however small the amplitude, provided it has not at any time been preceded by any cycle of a larger amplitude. For this reason residual stress effects were at a maximum down to the lowest stress levels. The performance of the rule at this mean stress level is essentially similar to that at 16 ksi mean with zero assumed initial residual stress.

Under programmed random loading (Figs.23, 26 and 29) the new rule over-estimated the life in every case for lives to final failure. This is to be expected in view of the performance of the rule under stationary random loading, and because the rule assumed initiation conditions throughout the life; as discussed in section 3.3 residual stresses may be expected to be more effective early in the life.

Despite the limitations of the rule in terms of accuracy of life prediction, the results of the experiments are encouraging in that the main characteristics of the cumulative damage behaviour of the specimens bore out the general approach to cumulative damage outlined in section 4, i.e.

(1) Miner's Rule was unconservative under loading conditions which did not cause local yielding.

(2) Where $\sum \frac{n}{N}$ was greater than unity the improvement was associated with the earlier stages of the fatigue process.

(3) $\sum \frac{n}{N}$ increased with increase in mean stress. The rule predicted that the optimum effect is reached for initially stress-free specimens approximately when the mean stress alone just causes yielding at the notch root. For mean stresses above this value the magnitude of $\sigma_{\ell m}$ at a particular value of alternating stress is almost independent of mean stress, and so little further improvement in $\sum \frac{n}{N}$ should occur. The results of the investigation were consisistent with this.

(4) $\sum \frac{n}{N}$ increased with alternating stress, reaching a maximum in the approximate region in which the Bauschinger Effect became operative.

(5) $\sum \frac{n}{N}$ was greatest for the loading condition (programmed random) with the highest $\frac{\text{peak stress}}{\text{rms stress}}$ ratio.

6.6 Scatter

In tests on plain specimens of aluminium alloy[50,70] and high strength steel[71] it has been found that scatter at the longer fatigue lives is significantly less under random than under constant amplitude loading. In the present investigation, although not enough specimens were tested to obtain accurate scatter factors it is clear that in general there was no significant reduction under random loading. Scatter was generally low under constant amplitude loading in these tests, as is usual for this type of specimen[72], where fretting shortens the initiation time. This is to be expected because scatter is normally attributed to the crack initiation phase rather than crack propagation[73], an hypothesis which has been confirmed by crack growth measurements over the entire life of notched and unnotched aluminium alloy specimens[68]. It therefore follows that any improvement in scatter under random compared with constant amplitude loading will be much less where fretting is present, since initiation is a much smaller percentage of the fatigue life under fretting conditions.

6.7 Further practical considerations

It was noted earlier that the results show a variation in damage against percentage life different in the random case from that found under constant amplitude loading. This fact has practical implications in two directions.

First, in any structural component there will be an acceptable value to which the residual strength may drop before the component is considered unsafe. From the designer's point of view, then, it is preferable that fatigue lives should be expressed in terms of life to a given residual strength rather than to life to total failure, although fatigue data is commonly in the form of the latter. Figs.36 to 38 show that $\sum \frac{n}{N}$ values are not necessarily the same for the two cases. It is reasonable to deduce that where residual stresses give values of $\sum \frac{n}{N}$ of less than one for final failure (e.g. low mean stress and large occasional compressive loads in a notched specimen) $\sum \frac{n}{N}$ for initiation may be very low - this will lead to a comparatively early fall off in residual strength. This leads to the second consideration, that when tests are carried out on an aluminium alloy component to determine the variation of residual strength with life, a representative service loading action must be applied if misleading results are to be avoided.

7 SUGGESTIONS FOR FURTHER WORK

It is suggested that the work described in this Report be extended in the following ways:-

(a) The strain gauge investigation to determine the initial state of residual stress of the specimens at the point of fatigue initiation may be extended.

(b) Partial damage tests may be extended to cover programmed random loading.

(c) An investigation may be conducted using the techniques described in Ref.33 to determine the magnitude of the Bauschinger Effect. The results can then be used to modify the life predictions using the rule of section 4.

(d) The random data may be used to predict the programmed random lives as suggested in section 4.4.

(e) Lives may be calculated applying the rule of section 4 to a selected percentage of the life. For the rest of the life $\sum \frac{n}{N}$ will be assumed to be 1.

(f) It is hoped that the work may also be extended later to obtain 'pre-loaded constant amplitude data' so that this can be evaluated for use in life prediction, as suggested in section 4.4.

(g) Further programmes are envisaged at present to repeat the work described in this Report on specimens in different materials and of different configurations, i.e. notch without fretting, and clamped joint.

(h) Some improvement in the accuracy of life prediction may be achieved by the use of a more representative mean stress/alternating stress than the Goodman diagram (section 4.5). Work is at present being carried out at R.A.E. on clamped joints, in which failure occurs from an area of fretting in the absence on a geometric stress concentration[72], which will shed some light on this.

8 CONCLUSIONS

Factors affecting the performance of Miner's Rule have been reviewed.

8.1 For aluminium alloys, geometric residual stresses strongly affect cumulative damage behaviour and can cause Miner's Rule to either overestimate or underestimate fatigue life. These stresses may be present in specimens due to manufacturing processes and may also be produced by local yielding at points of fatigue initiation under high loads in either direction. A commonly encountered case where $\sum \frac{n}{N}$ is affected by residual stresses is that of initially stress-free notched aluminium alloy components; under a symmetrical loading action at a positive mean stress Miner's Rule usually underestimates fatigue life for such specimens.

Another case arises when residual stresses are introduced unintentionally during manufacture of components or deliberately to improve fatigue performance. For components where such initial compressive stresses are present $\sum \frac{n}{N}$ may be expected to be low. Where such a tensile stress is present, $\sum \frac{n}{N}$ may be expected to be high.

8.2 An investigation into cumulative fatigue damage was carried out using aluminium alloy lug specimens. The results of this work strongly indicated that geometric residual stresses were the most significant cause of deviations in $\sum \frac{n}{N}$ from unity. Although a simple rule to account for these stresses did not give good quantitative predictions, the qualitative agreement was good and it is believed that a practical and reasonably accurate rule can be developed along the same lines.

8.3 Fretting, by causing crack propagation to occupy a greater proportion of the fatigue life, can affect the magnitude of the relative contributions from residual stresses and other factors which are of importance in cumulative damage.

8.4 Residual stresses do not greatly affect the behaviour of medium and low strength steels in many cases, mainly because the material properties are such that the local mean stress is reduced close to zero on the first cycle of any significant amplitude.

8.5 For aluminium alloy lug specimens the variation of residual static strength throughout the fatigue life was found to depend greatly on loading action and stress level. For this reason, when tests are carried out on an aluminium alloy component to determine the variation of residual static strength with life, a representative service loading action must be applied if misleading results are to be avoided.

Appendix A

VARIATION IN RELATIVE DAMAGE RATE WITH STRESS

Fatigue damage D can be defined as a variable, beginning at zero at the start of the fatigue life of a component and reaching unity at failure. The shape of the 'damage against percentage life' curve can then be taken arbitrarily to be some convenient shape (e.g. a straight line) at any chosen alternating stress level and stressing condition, e.g. waveform, mean stress. Under different stressing conditions, and in particular at different stress levels under constant amplitude loading, the shape of the damage against percentage life curves may well be different.

It has been proved[74] that if

(a) the relative rate of damage accumulation under constant amplitude loading $\left(\frac{dD}{d\,\frac{n}{N}}\right)$ varies with stress at fixed values of $\frac{n}{N}$, the percentage fatigue life consumed, (i.e. there are different shapes of damage against percentage life curves at different stresses) and:

(b) the damage rate under spectrum loading is a simple average of $\left(\frac{dD}{dn}\right)_{CA}$ (i.e. under constant amplitude loading) weighted according to the probability of occurrence $P_m(\sigma)$ of stress cycles at stress $\sigma_a = \sigma$ so that the damage rate under spectrum loading is equal to

$$\left(\frac{dD}{dn}\right)_s = \int_0^\infty \left(\frac{dD}{dn}\right)_{CA} P_m(\sigma)\, d\sigma \qquad (6)$$

then failure is predicted at $\sum \frac{n}{N} < 1$, i.e. due to the above effect along Miner's Rule should overestimate life.

The results of step tests on notched and plain specimens of steel and aluminium alloys (excluding alclad material) at zero mean stress indicate in most respects a consistent variation of relative damage rate $\left(\frac{dD}{d\,\frac{n}{N}}\right)$ with stress. In almost every case using a low-high sequence Miner's Rule has been found to underestimate the fatigue life, and vice versa for high-low tests[7,11,75-81]. In two investigations[82,83] where in both cases the high stress approached yield at the point of fatigue initiation, these effects were not found in either a steel or aluminium alloy. These tests therefore indicate that in most cases under

constant amplitude loading fatigue damage accumulates relatively faster early in the life at higher stress levels. An exception to the general rule is the case of alclad aluminium alloy. Of five investiations, one[10] showed no consistent sequence effect, and four[27,84-86] showed an effect opposite to that of plain aluminium alloy and steels.

Some life prediction methods have been based on accounting for the variation of relative damage rate with stress[7,13,15] and hence they predict lives shorter than those predicted by Miner's Rule when applied to spectrum loading.

That there is a variation in relative damage rate with stress in unclad aluminium alloy and steel specimens under fatigue loading has been confirmed by a number of investigators[68,87-89] using direct observation. Techniques were employed by means of which a record was made of the stage at which a detectable crack occurred. The observed direction of the variation in relative damage rate with stress confirmed that implied by the step tests. Other observations have shown[7,68,90,91] that for notched and plain specimens in a range of materials the number of fatigue origins increases with stress, so that at high stresses multi-origin failures occur, with single origin failures at low stresses. Further, the changeover from single to multi-origined failures has been shown to occur over a relatively narrow stress range[7,90] and a discontinuity in the S-N curve has been detected in this region for a number of materials[90].

The occurrence of a change in the number of nuclei with stress demonstrates that the variation in relative damage rate exists alongside an actual change in the fatigue process, showing that equation (6) is not strictly true. Differences in fatigue mechanism with stress have been studied metallographically[92].

In the case of plain alclad specimens, crack detection techniques have shown[88] a variation of relative damage rate with stress opposite to that of the bare material, a fact which is consistent with the particular behaviour of alclad specimens in the step tests.

Fig.43 demonstrates how $\sum \frac{n}{N}$ may be expected to vary for two-level step and block programme tests with an assumed difference in relative damage rate between the two levels, neglecting any change of fatigue mechanism with stress. In this figure it can be seen that $\sum \frac{n}{N}$ is always less than unity for two-level block programmes tests, demonstrating the proof in Ref.74

referred to earlier in this section. Calculations are given in Appendix G. The curves for the step tests are similar to those found in the actual tests mentioned earlier. As a typical example, Fig.44 shows results which have been obtained[75] by means of step tests on steel specimens at four levels designated A, B, C and D in descending order of amplitude. AB refers to a step test starting at level A and finishing at level B . Assessment of the actual values of $\sum \frac{n}{N}$ to be expected due to this factor alone is complicated by the fact that damage against percentage life curves constructed from two-level step test data do not always show a simple increase of damage with number of cycles. A strengthening effect has been found for low-high tests[7,75-79,93] on both aluminium alloy and steel specimens, i.e. in a step test the life at the second level exceeded the life at that level for a virgin specimen. The result of this factor is to necessitate the drawing of damage curves with 'negative damage' in some circumstances. Fig.45 shows the damage curves obtained from Fig.44, assuming a straight line relationship for level A , and demonstrates the negative damage implied by the strengthening effect. Fig.46 shows the calculated results to be expected from two-level block programme tests on the specimens, neglecting the strengthening effect by assuming the damage rate to be zero when in fact it was negative. The object of this is to obtain a rough estimate of the contribution to $\sum \frac{n}{N}$ of variations in damage rate alone. The figure shows that the minimum possible value of $\sum \frac{n}{N}$ was 0.67 between levels A and D , a value which is unrealistically low due to the assumption made about the strengthening effect. For spectrum tests with levels A and D the predicted $\sum \frac{n}{N}$ would in any case be closer to unity. In this case then, for spectrum tests the effect of difference in relative damage rate is not likely to be large.

It can be concluded from the foregoing discussions that the effect of variation in relative damage rate with stress is to reduce the fatigue life from that value predicted by Miner's Rule. The amount of reduction is not likely to be large for spectrum loading, and 20% reduction on life can probably be considered as an extreme value. However, since the variation in relative damage rate with stress exists alongside an actual change in fatigue mechanism with stress, there is also the question of interaction between mechanisms at different stress levels to be considered, i.e. equation (6) may not hold strictly. Such interactions may increase or decrease $\sum \frac{n}{N}$ and it is not possible at present to draw any conclusions on the magnitudes of such effects. One such effect, referred to here as the 'strengthening effect' is also discussed in Appendix C.

Appendix B

RESIDUAL STATIC STRENGTH AT FAILURE

A second factor also tending to make lives unconservative as predicted by the rule is the effect of residual static strength at failure. If a well-mixed spectrum of loads is applied to a component, it will fail at approximately the highest load in the spectrum and will have, at failure, a value of residual strength given by that load. Under the smaller component loads in the spectrum alone, however, failure would occur at a lower value of residual strength. This implies a state of greater damage, so any calculation using Miner's Rule will be based on lives under constant amplitude loading to final failure at a damage state equal to or greater than that which is associated with failure under spectrum loading. Hence, $\sum \frac{n}{N}$ should then be less than unity. Rules attempting to account for this factor have also been derived[4,5].

It is possible to make an assessment of the magnitude of this effect in at least one specific case. Work has been carried out[94] by means of which the state of residual strength of aluminium alloy bolted joints with steel side plates was determined throughout the fatigue life under programmed loading, representing aircraft gust loading at a positive mean stress. The results of this work are given in Fig.47. The highest and mean stress levels in the load programme are shown and an extrapolation of the curve of residual static strength against percentage life shows that the static strength was dropping at such a rate that had the specimens not failed, the static strength at 104% of the achieved life would have dropped to the strength for expected failure at the mean stress alone. Therefore, in this case the drop in static strength would affect the achieved life by less than 4%. The achieved $\sum \frac{n}{N}$ for these specimens was between 2.2 and 8.4 [24]. Clearly in this case the effect on the achieved life would only be large if loads approaching the uncracked ultimate strength of the specimen were contained in the load spectrum. This conclusion, however, does not necessarily follow for other structural configurations where the shape of the residual strength against percentage life curve may be different.

Appendix C

EFFECT OF LOW-LEVEL STRESS CYCLES

The effect of low-level stress cycles is difficult to assess, since under different circumstances such cycles may be beneficial or damaging.

At first sight it would appear that cycles of stress in the spectrum which lie below the initial fatigue limit should be damaging, since after a crack has formed in a component, its effective fatigue limit might be expected to drop and the lower-level stress cycles become effective. Investigations have been carried out[80,91,95,96] in which steel specimens were subjected to cyclic pre-stressing above the fatigue limit. Subsequently the pre-stressed specimens were used to obtain complete S-N curves. In all cases this treatment was found to lower the effective fatigue limit which confirms that the above situation can apply in some circumstances. The same behaviour has also been found to apply to an aluminium alloy[80]. In Refs.11, 15 and 80 cumulative damage rules are described which account for this behaviour.

It has, however, been shown for steels[91] that cyclic pre-stressing at a single stress level below the initial fatigue limit can actually raise the effective fatigue limit. In addition, when subjected to a stress history in which the stress started at a low alternating stress level and was raised in increments to a value above the fatigue limit, steel specimens have at that raised level survived many times the endurance of virgin specimens. This second phenomenon is known as coaxing. Aluminium alloy specimens do not exhibit this property[76,78] However it has been shown[97,98] that periodic stressing below the fatigue limit (i.e. two-level block programme test with one stress below the fatigue limit) can increase the life at the higher level for aluminium alloy specimens. $\sum \frac{n}{N}$ values greater than one have been obtained also in programmed tests on steel specimens with large numbers of cycles below the fatigue limit[99].

Coaxing in steel specimens has been attributed to strain ageing[100,101]. Aluminium alloys, which are not strain ageing materials, do not show coaxing behaviour. It has, however, been shown[7,75,76,78,79] that both steel and aluminium alloy specimens show similar strengthening behaviour in low-high step tests, where the low stress is above the initial fatigue limit. This suggests that there exists a mechanism in addition to coaxing, by means of which damage at high stress levels is suppressed by cycles of low amplitude. This is unlikely to involve macroscopic residual stresses as described in section 3, since the action of these is to change $\sum \frac{n}{N}$ by the effect of high on low stress cycles.

It is naturally of interest to summarise the circumstances under which strengthening effects ensure that cycles below the initial fatigue limit do no damage, or are, on balance, beneficial. Whilst it is not possible to make an authoritative general statement on this point, one trend is discernible. When under spectrum loading conditions (block programmed loading in Refs.97 and 99) there are large numbers of cycles below the fatigue limit, and no cycles exceed about 105% of the fatigue strength at 10^7 cycles $\sum \frac{n}{N}$ is commonly greater than one for steel and aluminium alloy specimens. However, there are reasons to believe that where fretting is present the damaging effect of cycles below the fatigue limit will be enhanced Appendix E. In any case it would be unwise to rely on the strengthening effect in design, since the net effect on Miner's Rule in a balance between a favourable and an unfavourable effect. If a design case is chosen such that there is a net unfavourable effect and the number of cycles below the initial fatigue limit is extremely large, the effect on life could also be large.

Appendix D

EFFECT OF STRAIN HARDENING

Plastic deformation of metals due to a single monotonically increasing load generally results in strain hardening. This term is used to describe a process which gives rise to an increase in indentation hardness and yield stress. Cyclic plastic straining on the other hand can result in either strain hardening or softening[102,103], determined in this case by an increase or decrease respectively in stress amplitude under constant strain conditions (or vice versa for strain amplitude under constant stress loading). It has been shown[102] for a number of metals subjected to different heat treatments that in general cyclic strain hardening occurs under reversed plastic loading where $\frac{\sigma_u}{\sigma_y} > 1.4$, and cyclic strain softening occurs where $\frac{\sigma_u}{\sigma_y} < 1.2$. 2024 aluminium alloy has been shown[103] to exhibit slight cyclic strain hardening properties under plastic strain cycling.

Low-level stress cycling (i.e. generally below the yield point) has also been shown to give rise to both strain hardening and strain softening. In one investigation[104] a range of metals in the annealed condition were shown to exhibit cyclic strain hardening properties under such loading, whereas in the cold drawn condition the opposite was true. As for the common engineering materials, mild steel shows marked cyclic strain softening behaviour and has been found to develop considerable plastic flow at alternating stresses of 75% of the initial yield point corresponding to failure in about 10^6 cycles. For 26S aluminium alloy the same effect was found at stresses for failure in the same number of cycles, but the effect was very much smaller[41].

Since some of the mechanical properties of materials are changed, (e.g. indentation hardness, σ_y) when strain hardening occurs it is not unreasonable to suppose that the fatigue resistance might also be affected. If this is so then the process is important in cumulative damage, because high stress cycles may affect subsequent damage under lower stress cycles and vice versa. The effect of static plastic pre-straining on subsequent fatigue performance is of interest here. It has been shown that for plain specimens of aluminium alloys 7075-T6 [105] and L65 [106] large plastic prior straining reduced fatigue strength. For mild steel the opposite effect was found[106]. In another programme[107] the same effects were found as before for L65 and mild steel, but in this case the specimens were cut from bars which had been previously strained plastically in compression.

It is difficult to separate the effects of strain hardening associated with microscopic residual stress systems, on cumulative damage behaviour from those due to geometric residual stresses, since the introduction of the latter is usually accompanied by plastic deformation and hence by strain hardening at the points of fatigue initiation. For instance, in the investigation described in Ref.40 (see section 3.3) some of the difference in lives between the specimens with and without residual stresses (Fig.6) may well be connected with strain hardening. However the fact that in general the direction of the change in life for preloaded notched aluminium alloy specimens depends on the direction of the initial applied load implies that geometric residual stresses are most important in this case.

The marked cyclic strain softening behaviour of mild steel provides an explanation for the cycle by cycle drop in residual stresses in this material found in Ref.40.

Appendix E

THE EFFECT OF FRETTING

Fretting[108] is essentially a process by which damage is caused at points where there is repeated movement between metal surfaces in contact. Its effect when acting at an area from which fatigue damage may originate is to speed the initiation of the fatigue process. It was found during constant amplitude tests[62] on aluminium alloy specimens, in which fatigue damage initiated from areas of fretting caused by removable metal pads, that fretting damage was fully developed after only one-fifth of the fatigue life. Removal of the fretting pads after this point had no effect of fatigue life. Fretting has a very large effect on fatigue strength, and strength reduction factors of 10 have been obtained[109]. The largest strength reduction factors are usually obtained at higher mean stresses, factors being lower at zero mean stress[62,109].

Fretting may be expected to affect cumulative damage behaviour in a number of ways. First, since fretting shortens crack initiation time, crack propagation should become a greater proportion of the total fatigue life. Consequently the residual static strength at a given proportion of the fatigue life is lower for a specimen failing from an area of fretting than for a plain or simple notched specimen. The effect on $\sum \frac{n}{N}$ of residual static strength (Appendix B) is therefore greater. It also follows, from the fact that a greater proportion of the fatigue life is spent cracked that in this case the damaging effect of cycles below the fatigue limit is also likely to be greater. Secondly, a change in the residual strength against cycles curve implies a corresponding change in the shape of the damage against cycles curves. This change may affect $\sum \frac{n}{N}$ (see Appendix A). A third way in which fretting may affect $\sum \frac{n}{N}$ is connected with the effects of residual stresses. Since fretting reduces fatigue strength (and hence $\sigma_{af\ell}$), when fretting is present the ratio $M = \frac{\sigma_y}{K_t \sigma_{af\ell}}$ must increase. As was discussed in section 3.5, this ratio is important in determining the effectiveness of residual stresses and so will affect $\sum \frac{n}{N}$. To take a particular example, due to the increase in M, mild steel specimens with notches and fretting (e.g. lugs) may be more susceptible to the effects of mean stress and preloading than those with notches alone.

There are also other possible effects of fretting which act in opposition and are both also connected with residual stresses. Since the effect of such

stresses is to change the mean stress at the point of fatigue initiation, it is to be expected that the damaging effect of the fretting would increase or decrease depending on whether the local mean stress is raised or lowered. This is due to the fact that fretting has been shown to be more damaging in terms of percentage reduction in fatigue strength at positive mean stresses than at zero mean stress[62,109]. Thus in this respect fretting should tend to enhance residual stress effects by effectively changing the shape of the Goodman diagram. On the other hand, fretting reduces crack initiation time and geometric residual stresses affect only the initiation and to a lesser extent immediately following crack growth (section 3.3), so in this instance residual stress effects should be reduced.

Finally, it is possible that fretting may be intrinsically more or less damaging under variable amplitude loading than under constant amplitude loading. It appears that no tests have been carried out in which a comparison was made between identical specimens under the two types of loading so it is impossible to draw any definite conclusions on this point.

Appendix F

CRACK PROPAGATION CONSIDERATIONS

The fatigue process in plain specimens has been classified into two stages[110]. Stage I starts from the surface of the materials and is dependent upon the maximum resolved shear stress. Crack growth occurs along the plane of maximum shear stress, at 45° to the maximum tensile stress. The stress state at the tip of the crack changes as the crack begins to propagate from a biaxial to a triaxial state of stress. The effect of this is to reduce the ratio $\frac{\text{maximum shear stress}}{\text{maximum tensile stress}}$ and to change the fatigue mechanism to Stage II behaviour. Crack growth in this second mode occurs, at least initially, at right angles to the direction of maximum tensile stress, and is characterised by striation markings at right angles to the direction of growth and a 1/1 relationship between number of striations and number of cycles. All the investigations referred to in this section apply to Stage II crack propagation in fluctuating tension.

Two-level constant amplitude tests have been carried out on cracked panel specimens of 2024-T3 alclad material[111]. It was found that when the stress was changed from a high to a low level, crack propagation was retarded for some time, gradually accelerating to the value which would have been expected from a constant amplitude test at the lower level alone. An opposite though smaller effect was found when changing from a low to a high level, i.e. after the change the crack propagation rate accelerated to a rate somewhat beyond the value to be expected from the higher level before settling down to the value expected from constant amplitude tests. It was also found that single tensile loads in the middle of a constant amplitude loading pattern caused a temporary retardation. Single negative loads did not accelerate crack growth, but if applied after a single tensile load they reduced the retardation due to that load. The retardation of the crack growth rate in the high-low sequence was attributed to a region of residual compressive stress induced at the crack tip by the high initial loading. It was also assumed that the action of any succeeding negative load was to destroy the residual stresses in the region by local yielding. The overall effect gave values of $\sum \frac{n}{N}$ greater than one for crack propagation rates under programmed and subsequently (Ref.69) under random loading to a gust load spectrum.

Under Gaussian random loading however it has been found[112] that under direct stress conditions in certain cases crack propagation rates can be

predicted with acceptable accuracy by the application of a linear summation of constant amplitude crack propagation rates. This difference in result may be connected with the higher $\frac{\sigma_p}{\sigma_r}$ value in the case of the gust load spectrum.

Appendix G

EXAMPLE OF THE EFFECT OF VARIATION IN RELATIVE DAMAGE RATE WITH STRESS

For the purpose of development of cumulative damage rules an expression for damage has been assumed[7] for loading under constant amplitude conditions at stress level σ_{ai} :

$$D = \left(\frac{n_i}{N_i}\right)^{X_i} \tag{7}$$

where D = damage

$\frac{n_i}{N_i}$ = cycle ratio - percentage of life consumed at the ith level

X_i = an exponent which varies with alternating stress level.

Assume a two-level block programme test is carried out between levels σ_{a1} and σ_{a2} . Let the cycles of the two amplitudes be well-mixed and let p_1 p_2 be the proportions of cycles at levels σ_{a1} and σ_{a2} respectively. ($p_1 + p_2 = 1$.)

From (7) under constant amplitude loading

$$\frac{dD}{dn_i} = \frac{X_i}{N_i}\left(\frac{n_i}{N_i}\right)^{X_i-1} .$$

Therefore under two-level block programmed loading

$$\frac{dD}{dn_b} = p_1 \frac{X_1}{N_1}\left(\frac{n_1}{N_1}\right)^{X_1-1} + p_2 \frac{X_2}{N_2}\left(\frac{n_2}{N_2}\right)^{X_2-1}$$

where n_b is the number of cycles applied under block programmed loading conditions.

Substitute (7) therefore

$$N_b = \int_o^1 \frac{dD}{\frac{p_1 X_1}{N_1} D^{\left(1-\frac{1}{X_1}\right)} + \frac{p_2 X_2}{N_2} D^{\left(1-\frac{1}{X_1}\right)}}$$

therefore

$$\sum \frac{n}{N} = \int_o^1 \frac{\left[\frac{p_1}{N_1} + \frac{p_2}{N_2}\right] dD}{\frac{p_1}{N_1} X_1 D^{\left(1-\frac{1}{X_1}\right)} + \frac{p_2 X_2}{N_2} D^{\left(1-\frac{1}{X_2}\right)}}$$

Let

$$C = \text{linear damage at level 1}$$

$$= \frac{\frac{p_1}{N_1}}{\left[\frac{p_1}{N_1} + \frac{p_2}{N_2}\right]}$$

therefore

$$\sum \frac{n}{N} = \int_o^1 \frac{dD}{C X_1 D^{\left(1-\frac{1}{X_1}\right)} + (1 - C) X_2 D^{\left(1-\frac{1}{X_2}\right)}}$$

Let

$$D = (D')^{X_1}$$

therefore

$$\sum \frac{n}{N} = \int_0^1 \frac{X_1 (D')^{(X_1-1)} \, dD'}{C\, X_1\, D'^{(X_1-1)} + (1-C)\, X_2\, D'^{\left(X_1-\frac{X_1}{X_2}\right)}}$$

$$= \int_0^1 \frac{dD'}{C + (1-C)\frac{X_2}{X_1}\, D'^{\left(1-\frac{X_1}{X_2}\right)}} \quad . \tag{8}$$

Therefore $\sum \frac{n}{N}$ depends only on $\frac{X_2}{X_1}$ for two-level programmed tests. Equation (8) has been evaluated by computer programme. The results are shown in Fig.43.

For step tests in the order 1-2 assuming n_1 counts at level 1 [29].

$$\text{Remaining life at level 2} = N_2\left[1 - \left(\frac{n_1}{N_1}\right)^{\frac{X_1}{X_2}}\right]$$

therefore

$$\frac{\text{achieved life}}{\text{life predicted from Miner's Rule}} = \frac{n_1 + N_2\left[1 - \left(\frac{n_1}{N_1}\right)^{\frac{X_1}{X_2}}\right]}{n_1 + N_2\left[1 - \frac{n_1}{N_1}\right]} \tag{9}$$

and

$$\sum \frac{n}{N} = \frac{n_1}{N_1} + 1 - \left(\frac{n_1}{N_1}\right)^{\frac{X_1}{X_2}} \tag{10}$$

And vice versa for tests in the order 2-1 .

An evaluation of equation (10) is also shown in Fig.43.

Note that for step tests the ratio $\frac{\text{achieved life}}{\text{predicted life}}$ is not equal to $\sum \frac{n}{N}$ except when $\sum \frac{n}{N} = 1$. This is because if Miner's Rule does not hold, the component fails under a different load spectrum (i.e. different proportions of counts at levels 1 and 2) from that which it would fail under if Miner's Rule did hold.

Table 1

SUMMARY OF RESULTS OF INVESTIGATIONS USING GAUSSIAN RANDOM LOADING

(PLAIN SPECIMENS AND NOTCHED SPECIMENS AT ZERO MEAN STRESS)

Ref. No.	Investigator	Mean stress (ksi)	Material	K_t	$\sum \frac{n}{N}$ at life below		Bending or direct	$\frac{n_o}{n_p}$
					10^5	10^6		
48	Fuller	0	2024-T3	Plain specimen	0.23	0.15	B	0.96
48	Fuller	0	2024-T3	Plain specimen	0.30	0.17	B	0.75
48	Fuller	0	2024-T3	Plain specimen	0.30	0.18	B	0.95
49	Hooke & Head	0	24-ST	Notched	-	0.40*	B	0.84
50	Swanson	16	2024-T4	1.0	0.12	0.04	D	0.96
51	Kowalewski	0	W3115.5 (2024)	1.77	0.7	1.0	B	0.91
52	Fralich	0	7075-T6	Sharply notched	4.5	1.7	B	>0.95
53	Clevenson Steiner	0	2024-T4	2.2	0.15	0.04	D	0.83 - 0.64
54	Smith Malme	0	2024	1.9	0.8	0.4	B	?
56	Fralich	0	SAE 4130	Sharply notched	0.6	0.6	B	>0.95
57	Marsh Mackinnon	13.5	Mild steel	Sharply notched	0.6	0.5	D	>0.95
58	Booth Wright Smith	0	EN 1A Mild steel	Plain specimen	-	0.4	B	0.78
58	Booth Wright Smith	0	EN 15 Mild steel	Plain specimen	-	0.4	B	0.78

* at 3.4×10^6 cycles to failure

Table 2

MEASURED CHEMICAL COMPOSITION AND TENSILE PROPERTIES OF DTD 5014 ALUMINIUM ALLOY

CHEMICAL COMPOSITION (per cent)

Cu	Mg	Si	Fe	Mn	Zn	Ni	Ti
2.26	1.38	0.25	1.06	0.06	0.02	1.02	0.06

Balance aluminium

Average tensile properties

UTS	58.5 tsi
0.1% proof	50.8 tsi
Elongation	13%

Table 3

STATIONARY RANDOM FATIGUE TEST RESULTS

MEAN STRESS = 10 ksi

Stress ksi rms	Spec. No.	Life (N)
1.0	1213-F78R	$1.79\ 10^7$
1.0	0408-F84R	$1.35\ 10^7$
1.0	1214-F85R	$4.00\ 10^7$
1.0	0409-F86R	$2.20\ 10^7$
1.0	1806-F367R	$6.92\ 10^6$
1.0	1922-F370R	$7.90\ 10^6$
1.0	2119-F371R	$8.20\ 10^6$
1.0	2007-F372R	$9.50\ 10^6$
1.0	0119-F399R	$7.27\ 10^6$
1.0	0222-F408R	$9.01\ 10^6$
1.5	0404-F76R	$3.70\ 10^6$
1.5	1216-F82R	$3.97\ 10^6$
1.5	2121-F350R	$2.70\ 10^6$
1.5	1711-F373R	$3.20\ 10^6$
1.5	2403-F374R	$2.70\ 10^6$
1.5	2314-F437R	$2.29\ 10^6$
1.5	2811-F439R	$3.66\ 10^6$
1.5	3616-F441R	$2.75\ 10^6$
1.5	3221-F443R	$1.78\ 10^6$
2.0	0411-F74R	$1.26\ 10^6$
2.0	1203-F80R	$1.08\ 10^6$
2.0	2407-F349R	$9.80\ 10^5$
2.0	2318-F366R	$2.11\ 10^6$
2.5	0414-F72R	$9.00\ 10^5$
2.5	1217-F81R	$8.72\ 10^5$
2.5	2321-F348R	$9.30\ 10^5$
3.0	0419-F73R	$8.66\ 10^5$
3.0	1220-F77R	$6.56\ 10^5$
3.0	0418-F142R	$8.96\ 10^5$
3.5	0403-F75R	$8.00\ 10^5$
3.5	1202-F79R	$8.40\ 10^5$
3.5	1215-F83R	$7.56\ 10^5$
3.5	0410-F87R	$8.30\ 10^5$
3.5	1619-F345R	$8.38\ 10^5$
3.5	2215-F365R	$6.91\ 10^5$

Table 4

CONSTANT AMPLITUDE FATIGUE TEST RESULTS

MEAN STRESS = 10 ksi

Stress ksi rms	Spec. No.	Life (N)
1.0	1405-F92S	$6.40\ 10^{7}\rightarrow$
1.0	0813-F107S	$3.67\ 10^{7}\rightarrow$
1.2	0802-F206S	$6.67\ 10^{7}\rightarrow$
1.5	1411-F89S	$3.38\ 10^{6}$
1.5	0804-F105S	$3.14\ 10^{7}\rightarrow$
1.5	0806-F141S	$3.55\ 10^{6}$
1.5	0822-F207S	$1.87\ 10^{7}\rightarrow$
1.6	1610-F20	$3.72\ 10^{6}$
2.0	1412-F96S	$1.86\ 10^{6}$
2.0	2306-F357S	$1.84\ 10^{6}$
2.0	2404-F362S	$1.05\ 10^{6}$
2.1	0816-F101S	$1.20\ 10^{6}$
2.5	1418-F94S	$8.10\ 10^{5}$
2.5	0819-F108S	$7.36\ 10^{5}$
3.0	1413-F95S	$5.98\ 10^{5}$
3.0	0817-F103S	$4.78\ 10^{5}$
3.0	2111-F363S	$4.36\ 10^{5}$
3.5	1403-F88S	$3.36\ 10^{5}$
3.5	0818-F102S	$3.36\ 10^{5}$
4.0	1409-F93S	$2.92\ 10^{5}$
4.0	0809-F100S	$2.36\ 10^{5}$
4.0	1308-F115S	$3.82\ 10^{5}$
4.5	0810-F99S	$3.60\ 10^{5}$
4.5	1414-F133S	$2.45\ 10^{5}$
5.0	1401-F91S	$2.06\ 10^{5}$
5.0	0811-F97S	$2.32\ 10^{5}$
5.0	1721-F364S	$1.62\ 10^{5}$
6.0	1402-F90S	$1.20\ 10^{5}$
6.0	0801-F104S	$1.50\ 10^{5}$
6.0	1522-F106S	$1.26\ 10^{5}$

Table 5

RANDOM PROGRAMMED LOADING FATIGUE TEST RESULTS

MEAN STRESS = 10 ksi

Stress ksi rms	Spec. No.	Life (N)
1.230	0805-F180RP	$1.26\ 10^7$
1.230	1211-F181RP	$8.36\ 10^6$
1.230	1602-F182RP	$1.68\ 10^7$
1.230	1003-F183RP	$1.05\ 10^7$
1.230	0914-F184RP	$8.11\ 10^6$
1.722	0803-F174RP	$3.18\ 10^6$
1.722	1204-F175RP	$6.33\ 10^6$
1.722	1613-F176RP	$8.58\ 10^6$
1.722	1011-F177RP	$4.34\ 10^6$
1.722	1007-F178RP	$3.07\ 10^6$
1.722	0918-F179RP	$7.52\ 10^6$

Table 6

STATIONARY RANDOM FATIGUE TEST RESULTS

MEAN STRESS = 16 ksi

Stress ksi rms	Spec. No.	Life (N)
1.0	1513-F30R	$6.46\ 10^6$
1.0	0708-F44R	$6.60\ 10^6$
1.0	0706-F147R	$9.68\ 10^6$
1.0	1813-F354R	$9.20\ 10^6$
1.5	1514-F32R	$2.62\ 10^6$
1.5	0719-F41R	$2.27\ 10^6$
1.5	2212-F352R	$1.80\ 10^6$
2.0	1511-F26R	$1.28\ 10^6$
2.0	0717-F43R	$1\ 10\ 10^6$
2.5	1519-F29R	$7.40\ 10^5$
2.5	0716-F37R	$8\ 50\ 10^5$
2 5	1912-F351R	$6.30\ 10^5$
3.0	1502-F27R	$4\ 60\ 10^5$
3.0	0702-F34R	$8.25\ 10^5$
3.0	0712-F45R	$4.48\ 10^5$
3.0	0714-F142R	$6.74\ 10^5$
3.0	1710-F376R	$5.40\ 10^5$
3.0	2004-F377R	$6\ 40\ 10^5$
3.5	1512-F28R	$4\ 20\ 10^5$
3.5	0713-F36R	$5.00\ 10^5$
3.5	2311-F383R	$3.60\ 10^5$
3.5	2112-F384R	$4.50\ 10^5$
3.5	0111-F385R	$4.45\ 10^5$
4.0	1515-F33R	$2.80\ 10^5$
4.0	0703-F39R	$2.60\ 10^5$
4.5	1503-F35R	$2.42\ 10^5$
4.5	0718-F42R	$2.34\ 10^5$
5 0	1501-F25R	$1.92\ 10^5$
5 0	0704-F40R	$1\ 54\ 10^5$
5.0	1420-F149R	$1.00\ 10^5$
5.0	2010-F329R	$1\ 30\ 10^5$
5.0	2313 F375R	$1.70\ 10^5$
6 0	1518 F38R	$9.60\ 10^4$

Table 7

CONSTANT AMPLITUDE FATIGUE TESTS RESULTS

MEAN STRESS = 16 ksi

Stress ksi rms	Spec. No.	Life (N)
1.0	1316-F137S	$2.32\ 10^{7}\rightarrow$
1.0	1105-F144S	$2.78\ 10^{7}\rightarrow$
1.0	1304-F148S	$1.64\ 10^{7}\rightarrow$
1.0	1604-F203S	$3.0\ 10^{7}\rightarrow$
1.2	0821-F202S	$3.56\ 10^{6}$
1.2	0720-F204S	$5.91\ 10^{6}$
1.5	1106-F17S	$2.25\ 10^{6}$
1.5	1320-F24S	$2.70\ 10^{6}$
1.5	2216-F380S	$2.30\ 10^{6}$
2.0	1305-F2S	$8.80\ 10^{5}$
2.0	1104-F13S	$1.14\ 10^{6}$
2.0	1114-F71S	$1.06\ 10^{6}$
2.5	1301-F8S	$6.30\ 10^{5}$
2.5	1116-F11S	$5.60\ 10^{5}$
2.5	1109-F16S	$5.40\ 10^{5}$
3.0	1120-F4S	$3.15\ 10^{5}$
3.0	1312-F12S	$3.10\ 10^{5}$
3.0	2309-F381S	$3.80\ 10^{5}$
3.0	3106-F410S	$3.08\ 10^{5}$
3.0	3703-F411S	$3.94\ 10^{5}$
3.0	2509-F412S	$3.50\ 10^{5}$
3.5	1110-F9S	$1.90\ 10^{5}$
3.5	1303-F15S	$2.00\ 10^{5}$
3.55	1307-F136S	$2.06\ 10^{5}$
4.0	1119-F6S	$1.60\ 10^{5}$
4.0	1314-F14S	$1.80\ 10^{5}$
4.5	1117-F10S	$1.05\ 10^{5}$
4.5	1318-F21S	$1.06\ 10^{5}$
5.0	1122-F1S	$1.00\ 10^{5}$
5.0	1317-F20S	$1.08\ 10^{5}$
6.0	1118-F7S	$5.60\ 10^{4}$
6.0	1302-F19S	$5.10\ 10^{4}$
6.0	1420-F119S	$4.90\ 10^{4}$
6.0	1916-F382S	$6.40\ 10^{4}$
7.0	1103-F18S	$4.20\ 10^{4}$
7.0	1306-F22S	$3.20\ 10^{4}$
7.0	1321-F135S	$4.48\ 10^{5}$
7.0	1101-F138S	$3.73\ 10^{4}$

Table 8

RANDOM PROGRAMMED LOADING FATIGUE TEST RESULTS

MEAN STRESS = 16 ksi

Stress ksi rms	Spec. No.	Life (N)
1.230	1015-F195RP	$6.51\ 10^6$
1.230	0911-F196RP	$9.01\ 10^6$
1.230	1605-F197RP	$8.11\ 10^6$
1.230	0820-F196RP	$7.79\ 10^6$
1.475	1507-F158RP	$4.15\ 10^6$
1.475	0709-F159RP	$5.54\ 10^6$
1.475	1311-F160RP	$7.92\ 10^6$
1.97	1509-F155RP	$2.72\ 10^6$
1.97	1422-F156RP	$2.76\ 10^6$
1.97	1309-F157RP	$2.43\ 10^6$
2.46	1410-F152RP	$2.19\ 10^6$
2.46	1520-F153RP	$1.67\ 10^6$
2.46	1310-F154-RP	$1.69\ 10^6$

Table 9

STATIONARY RANDOM FATIGUE TEST RESULTS

MEAN STRESS = 25 ksi

Stress ksi rms	Spec. No.	Life (N)
0.7	1805-F346R	$1.28\ 10^7$
0.9	1620-F343R	$5.88\ 10^6$
0.9	0908-F344R	$5.08\ 10^6$
1.0	1008-F57R	$6.82\ 10^6$
1.0	0507-F62R	$8.66\ 10^6$
1.0	0504-F69R	$1.68\ 10^7$
1.0	1013-F145R	$4.64\ 10^6$
1.0	2419-F332R	$5.27\ 10^6$
1.5	1022-F47R	$1.80\ 10^6$
1.5	0502-F54R	$1.34\ 10^6$
2.0	1002-F49R	$6.80\ 10^5$
2.0	0503-F56R	$1.26\ 10^6$
2.0	2206-F378R	$6.35\ 10^5$
2.0	1910-F379R	$7.30\ 10^5$
2.5	1001 F48R	$4.60\ 10^5$
2.5	0506-F67R	$4.10\ 10^5$
3.0	1017-F50R	$2.60\ 10^5$
3.0	0516-F58R	$3.56\ 10^5$
3.0	0520-F140R	$4.06\ 10^5$
3.0	1906-F328R	$3.70\ 10^5$
3.5	1010-F46R	$2.84\ 10^5$
4.0	1005-F53R	$2.34\ 10^4$
4.0	0508-F60R	$1.96\ 10^5$
4.0	3207-F427R	$2.00\ 10^5$
4.0	2708-F428R	$1.50\ 10^5$
4.0	3608-F429R	$2.20\ 10^5$
5.0	1004-F51R	$1.15\ 10^5$
5.0	0521-F61R	$1.60\ 10^5$
5.0	1702-F327R	$7.56\ 10^4$
5.0	3404-F432R	$5.40\ 10^4$
5.0	3518-F433R	$7.50\ 10^4$
5.0	3219-F434R	$9.38\ 10^4$
5.0	2904-F435R	$6.07\ 10^4$
6.0	1006-F52R	$7.50\ 10^4$
6.0	0519-F63R	$8.60\ 10^4$
6.0	2105-F325R	$8.20\ 10^4$
6.0	2218-F333R	$5.14\ 10^4$
6.0	2402-F334R	$5.00\ 10^4$
6.0	1808-F336R	$2.80\ 10^4$
6.0	1816-F337R	$3.50\ 10^4$
6.0	1810-F338R	$3.50\ 10^4$
6.0	1622-F340R	$4.50\ 10^4$
6.0	2210-F341R	$4.60\ 10^4$
7.0	1016-F55R	$2.80\ 10^4$
7.0	0517-F64R	$6.50\ 10^4$
7.0	1009-F66R	$5.50\ 10^4$
7.0	2421-F326R	$3.02\ 10^4$
7.0	2418-F330R	$3.70\ 10^4$
7.0	2106-F331R	$2.80\ 10^4$
7.0	2116-F339R	$2.50\ 10^4$

Table 10

CONSTANT AMPLITUDE FATIGUE TEST RESULTS

MEAN STRESS = 25 ksi

Stress ksi rms	Spec. No.	Life (N)
0.8	3113-F421S	$1.40\ 10^7$
0.8	2610-F422S	$6.90\ 10^6$
0.9	1601-F209S	$4.68\ 10^7$
1.0	0915-F125S	$4.78\ 10^6$
1.0	0313-F130S	$1.47\ 10^7$
1.0	1607-F199S	$5.38\ 10^6$
1.0	0812-F200S	$5.19\ 10^6$
1.0	0711-F201S	$5.68\ 10^6$
1.5	0318-F118S	$1.88\ 10^6$
1.5	0917-F120S	$1.60\ 10^6$
1.5	2417-F388S	$2.00\ 10^6$
1.75	0317-F116S	$1.34\ 10^6$
2.0	0316-F114S	$7.70\ 10^5$
2.0	0916-F124S	$6.30\ 10^5$
2.5	0301-F109S	$3.74\ 10^5$
2.5	0905-F117S	$2.74\ 10^5$
3.0	0315-F112S	$2.09\ 10^5$
3.0	0914-F121S	$2.14\ 10^5$
3.5	0321-F122S	$1.16\ 10^5$
3.5	0902-F123S	$1.14\ 10^5$
3.5	2217-F387S	$1.20\ 10^5$
4.0	0322-F111S	$1.24\ 10^5$
4.0	0903-F126S	$7.20\ 10^4$
5.0	0314-F110S	$5.00\ 10^4$
5.0	0921-F127S	$4.25\ 10^4$
6.0	0919-F128S	$3.75\ 10^4$
6.0	0311-F129S	$3.55\ 10^4$
6.0	2319-F386S	$3.30\ 10^4$
7.0	0906-F131S	$3.08\ 10^4$
7.0	0310-F132S	$2.40\ 10^4$
7.0	0907-F134S	$2.62\ 10^4$
7.0	0913-F139S	$3.15\ 10^4$

Table 11

RANDOM PROGRAMMED LOADING FATIGUE TEST RESULTS

MEAN STRESS = 25 ksi

Stress ksi rms	Spec. No.	Life (N)
1.230	1616-F170RP	$3.18\ 10^6$
1.230	1505-F171RP	$2.83\ 10^6$
1.230	0715-F172RP	$3.72\ 10^6$
1.230	0707-F173RP	$4.67\ 10^6$
1.97	1606-F167RP	$1.81\ 10^6$
1.97	1508-F168RP	$2.24\ 10^6$
1.97	0705-F169RP	$1.23\ 10^6$
2.70	0701-F164RP	$8.82\ 10^5$
2.70	1504-F165RP	$9.11\ 10^5$
2.70	1421-F166RP	$6.44\ 10^5$
2.70	0814-F192RP	$6.10\ 10^5$*
2.70	1609-F193RP	$6.62\ 10^5$*
2.70	1021-F194RP	$7.60\ 10^5$*
3.44	1506-F161RP	$2.14\ 10^5$
3.44	1416-F162RP	$2.24\ 10^5$
3.44	1322-F163RP	$1.56\ 10^5$
3.44	1521-F185RP	$3.30\ 10^5$*
3.44	1612-F186RP	$2.77\ 10^5$*
3.44	1218-F188RP	$2.82\ 10^5$*
3.44	0808-F190RP	$2.84\ 10^5$*
3.44	1201-F191RP	$2.65\ 10^5$

NOTE * - Test started on highest component rms level

Table 12

STATIONARY RANDOM PARTIAL DAMAGE TEST RESULTS

MEAN STRESS = 10 ksi

Spec. No.	Seconds to stopoff	% stopoff	Failing load (ton)	Failing stress (ksi)	
2003-F294RS	10810	41.8	3.97	58.1	
1708-F297RS	10810	41.8	4.10	60.0	
2117-F298RS	7207	27.8	3.97	58.1	
2209-F299RS	7207	27.8	4.09	59.9	
2415-F300RS	3603	13.9	4.12	60.4	
1819-F301RS	3603	13.9	4.10	60.0	Stress = 1.5 ksi
2203-F355RS	16700	64.5	3.85	56.2	Nom. life = 2.9×10^6
1907-F356RS	16700	64.5	2.25	32.9	
2401-F436RS	15530	60.0	2.27	33.2	
2910-F440RS	15530	60.0	2.88	42.2	
3701-F442RS	15530	60.0	1.58	23.1	
3515-F444RS	10350	40.0	3.55	51.9	
3410-F445RS	10350	40.0	3.58	52.4	
3107-F446RS	10350	40.0	2.68	39.2	
0604-F302RS	4324	60.6	4.00	58.5	
2013-F303RS	4324	60.6	3.97	58.1	
2302-F304RS	2882	40.4	3.86	56.5	Stress = 3.5 ksi
1720-F305RS	2882	40.4	3.86	56.5	Nom. life = 8.0×10^5
2420-F306RS	1441	20.2	3.94	57.6	
1919-F307RS	1441	20.2	4.10	60.0	

Table 13

CONSTANT AMPLITUDE PARTIAL DAMAGE TEST RESULTS

MEAN STRESS = 10 ksi

Spec. No.	Seconds to stopoff	% stopoff	Failing load (ton)	Failing stress (ksi)	
0618-F255SS	8110	62.8	2.54	37.2	
2408-F256SS	8110	62.8	2.55	37.3	
0620-F257SS	2702	20.9	3.98	58.3	
1701-F258SS	5415	42.0	3.16	46.2	Stress = 2.0 ksi
2014-F259SS	5405	41.8	3.18	46.5	Nom. life = 1.45×10^6
2410-F260SS	2702	20.9	3.61	52.9	
3720-F415SS	5180	40.0	4.04	59.1	
3521-F416SS	7770	60.1	1.48	21.6	
1802-F261SS	559	22.4	4.12	60.3	
0611-F262SS	559	22.4	3.96	58.0	
2414-F263SS	1117	44.7	4.04	59.2	
2213-F264SS	1117	44.7	3.59	52.5	Stress = 40 ksi
1918-F265SS	1675	67.0	2.90	42.4	Nom. life = 2.8×10^5
2305-F266SS	1675	67.0	2.52	36.8	
3218-F413SS	1000	40.0	4.03	59.0	
2913-F414SS	1500	60.0	3.25	47.5	
2002-F268SS	108	8.6	4.08	59.6	
2412-F269SS	108	8.6	4.10	60.0	
0609-F270SS	216	17.3	4.01	58.6	
2205-F271SS	216	17.3	4.14	60.5	
1915-F272SS	324	26.0	4.08	59.6	Stress = 6.0 ksi
1820-F273SS	324	26.0	4.12	60.3	Nom. life = 1.4×10^5
2107-F402SS	500	40.0	4.01	58.6	
2308-F403SS	500	40.0	4.06	59.4	
1714-F404SS	750	60.0	3.01	44.0	
2006-F406SS	750	60.0	3.40	49.8	

Table 14

STATIONARY RANDOM PARTIAL DAMAGE TEST RESULTS

'LAX STRESS = 16 ksi

Spec. No.	Seconds to stopoff	% stopoff	Failing load (ton)	Failing stress (ksi)	
2413-F274RS	4504	25.2	4.11	60.1	
2207-F276RS	4504	25.2	4 13	60.5	
2101-F277RS	9009	50.5	3.72	54.9	Stress = 1.5 ksi
2304-F278RS	9009	50.5	3.78	55.4	Nom. life = 2.0×10^6
1818-F279RS	9009	50.5	4.10	60.0	
2118-F280RS	13510	75.5	3.94	57.6	
0607-F281RS	13510	75 5	3.58	52 4	
1902-F282RS	631	16.8	4.12	60.3	
0606-F283RS	1893	50 5	3.44	50.4	
1713-F284RS	1893	50.5	3.98	58.3	
2005-F285RS	1261	33.6	4.08	59.7	Stress = 3.5 ksi
2122-F286RS	1261	33.6	4.01	58.6	Nom. life = $4.2. \times 10^5$
2303-F287RS	631	16.8	4.12	60.3	
2809-F430RS	2622	70.0	3.36	49.1	
2915-F431RS	2622	70.0	3.72	54.4	
1901-F288RS	1027	76.6	3.67	53.7	
2315-F289RS	1027	76.6	2.76	40.4	
2416-F290RS	684	51.0	3.91	58.1	
1719-F291RS	684	51.0	4.00	58.5	Stress = 5.0 ksi
2104-F292RS	342	25.5	4.13	60.4	Nom. life = 1.5×10^5
0605-F293RS	342	25.5	4.03	59.0	
0216-F310RS	1025	76.5	3.75	54.9	
2011-F361RS	964	71.9	3.69	54.0	
2307-F400RS	965	71.9	3.68	53.8	

Table 15

CONSTANT AMPLITUDE PARTIAL DAMAGE TEST RESULTS

MEAN STRESS = 16 ksi

Spec. No.	Seconds to stopoff	% stopoff	Failing load (ton)	Failing stress (ksi)	
1019-F215SS	13450	60.2	3.00	43.9	
0920-F216SS	8980	40.2	3.52	51.5	
1012-F217SS	4484	20.1	3.85	56.4	
0722-F224SS	13450	60.2	2.38	34.9	Stress = 1.5 ksi
0213-F227SS	4509	20.2	3.65	53.4	Nom. life = 2.5×10^6
0101-F228SS	9009	40.4	3.76	54.9	
0417-F229SS	13450	60.2	2.36	34.6	
0710-F230SS	13450	60.2	3.38	49.5	
1614-F212SS	1442	77.0	3.70	54.2	
0909-F220SS	1081	57.6	3.64	53.3	
1621-F221SS	1081	57.6	3.10	45.4	Stress = 3.5 ksi
0202-F222SS	0721	38.5	4.05	59.4	Nom. life = 2.1×10^5
0116-F223SS	0721	38.5	3.84	56.2	
0610-F225SS	360	19.2	4.02	58.9	
0416-F226SS	360	19.2	4.08	59.6	
0211-F231SS	243	60.4	3.73	54.6	
0621-F232SS	243	60.4	3.83	56.1	
0622-F233SS	171	42.4	3.92	57.4	Stress = 6.5 ksi
0103-F234SS	171	42.4	4.06	59.5	Nom. life = 4.5×10^4
0220-F235SS	81	20.1	4.12	60.4	
0602-F236SS	81	20.1	4.03	59.0	

Table 16

STATIONARY RANDOM PARTIAL DAMAGE TEST RESULTS

MEAN STRESS = 25 ksi

Spec. No.	Seconds to stopoff	% stopoff	Failing load (ton)	Failing stress (ksi)	
1817-F308RS	7568	56.5	4.08	59.8	
2020-F311RS	7568	56.5	3.27	47.9	
2411-F312RS	5045	37.6	3.94	57.6	Stress = 1.5 ksi
2221-F313RS	5045	37.6	3.96	58.0	Nom. life = 1.5×10^6
2103-F314RS	2522	18.9	4.14	60.6	
2310-F315RS	2522	62.8	4.14	60.6	
1707-F316RS	1405	62.8	3.82	55.9	
1811-F317RS	1405	62.8	2.84	41.6	
2422-F318RS	937	42.0	4.09	59.9	
1904-F319RS	937	42.0	4.11	60.1	
2312-F321RS	468	21.0	4.13	60.5	Stress = 3.5 ksi
1815-F322RS	468	21.0	4.09	59.9	Nom. life = 2.5×10^5
2406-F358RS	669	29.9	4.06	59.4	
1706-F389RS	616	27.6	3.94	57.6	
0201-F390RS	616	27.6	4.14	60.6	
1909-F394RS	1400	62.6	3.64	53.3	
2320-F395RS	1400	62.6	3.37	49.3	
1911-F391RS	196	29.5	4.03	59.0	
1510-F392RS	196	29.5	4.04	59.1	
2204-F396RS	322	48.5	3.77	55.2	
2012-F397RS	322	48.5	3.61	52.9	
2019-F398RS	482	72.6	3.39	49.6	
0613-F399RS	482	72.6	3.28	48.0	Stress = 5.0 ksi
3201-F423RS	failed at 645	97.2			Nom. life = 7.5×10^3
2908-F424RS	686	103.3	3.75	54.9	
3417-F425RS	failed at 675	100.1			
2806-F426RS	686	103.3	3.07	44.9	

Table 17

CONSTANT AMPLITUDE PARTIAL DAMAGE TEST RESULTS

MEAN STRESS = 25 ksi

Spec. No.	Seconds to stopoff	% stopoff	Failing load (ton)	Failing stress (ksi)	
0118-F237SS	8649	60.9	2.26	33.1	
0219-F238SS	8649	60.9	3.14	46.0	
0619-F239SS	2837	20.2	4.05	59.3	Stress = 1.5 ksi
0415-F240SS	2837	20.2	4.05	59.3	Nom. life = 1.6×10^6
0105-F241SS	5765	40.6	3.30	48.3	
0617-F242SS	5765	40.6	3.64	53.4	
0218-F243SS	72	6.7	4.12	60.3	
0113-F244SS	72	6.7	4.12	60.3	
0616-F245SS	144	13.4	3.97	58.1	
0209-F246SS	144	13.4	4.04	59.1	
0109-F247SS	216	20.2	4.40	63.4	
0614-F248SS	216	20.2	3.83	56.1	Stress = 3.5 ksi
2202-F407SS	670	62.5	3.49	51.1	Nom. life = 1.2×10^5
2507-F417SS	428	39.9	3.73	54.6	
2715-F418SS	428	39.9	2.72	39.8	
2814-F419SS	643	60.0	2.91	42.6	
2602-F420SS	643	60.0	3.63	53.1	
0210-F249SS	54	20.2	4.11	60.1	
0110-F250SS	54	20.2	4.08	59.7	
0601-F251SS	108	40.3	4.05	59.4	
0203-F252SS	108	40.3	4.12	60.3	Stress = 6.5 ksi
0115-F253SS	159	59.4	4.01	58.6	Nom. life = 3×10^4
0615-F254SS	159	59.4	3.40	49.8	
2009-F407SS	155	57.8	3.80	55.6	

Table 18

Predicted $\sum \frac{n}{N}$ values, allowing for failure at the highest load in the spectrum

Random loading

Mean stress (ksi)	Alternating stress (ksi rms)	$\sum \frac{n}{N}$
10	2.5	0.95
10	3.5	0.95
16	2.5	0.96
16	3.5	0.95
16	5.0	0.95
25	1.5	0.95
25	3.5	0.90
25	5.0	0.87

Table 19

PARAMETERS FOR PROGRAMMED RANDOM LOADING

Level	P	rms levels in terms of σ/λ	rms stress levels (ksi)									
1	0.71	0.79	0 996	1.197	1.395	1.595	1.795	1.984	2.19	2.39	2.59	2.79
2	0 26	1.233	1.557	1.868	2.18	2.49	2.80	3.11	3.42	3.74	4.04	4.36
3	0.03	1.982	2.50	3.00	3.50	4.00	4.50	5.00	5.50	6.00	6.50	7.00
λ			1.261	1.515	1.767	2.02	2.27	2.52	2.78	3.03	3.28	3.54
Overall rms (ksi)			1.230	1.475	1.722	1.97	2.21	2.46	2.70	2.95	3.20	3.44

REFERENCES

No.	Author	Title, etc.
1	H. W. Liu H. T. Corten	Fatigue damage under varying stress amplitudes. NASA Technical Note D647, November 1960
2	H. J. Grover	An observation concerning the cycle ratio in cumulative damage. Symposium on fatigue of aircraft structures. ASTM Special Technical Publication No.274 (1960)
3	A. M. Freudenthal R. A. Heller	On stress interaction in fatigue and a cumulative damage rule. Journal of Aerospace Science, Vol.26, No.7, July 1959
4	R. R. Gatts	Cumulative fatigue damage with random loading. Journal of Basic Engineering, September 1962
5	S-R. Valluri	A theory of cumulative damage in fatigue. ARL 182, December 1961
6	C. R. Smith	Linear strain theory and the Smith Method for predicting the fatigue life of structures for spectrum type loading. ARL 64-55, April 1964
7	S. M. Marco W. L. Starkey	A concept of fatigue damage. ASME Transactions, May 1954
8	W. T. Kirkby P. R. Edwards	A method of fatigue life prediction using data obtained under random loading conditions. R.A.E. Technical Report 66023 (ARC 28247) (1966)
9	A. M. Freudenthal	Fatigue of materials and structures under random loading. WADC - University of Minnesota Conf. on Acoustical Fatigue. WADC Technical Report 59-676, March 1961
10	M. A. Miner	Cumulative damage in fatigue. Journal of Appl. Mech. Vol.12, No.3, p.A159/A164, September 1945

REFERENCES (Contd.)

No.	Author	Title, etc.
11	S. S. Manson A. J. Nachtigall J. C. Freche	A proposed new relation of cumulative fatigue damage in bending. Proc. ASTM, Vol.61 (1961)
12	H. T. Corten T. J. Dolan	Cumulative fatigue damage. Int. Conf. Fatigue of Metals, September 1956
13	F. E. Richart Jnr. N. M. Newmark	An hypothesis for the determination of cumulative damage in fatigue. Proc. ASTM (1948)
14	H. W Liu H. T. Corten	Fatigue damage during complex stress histories. NASA Technical Note D-256, November 1959
15	D. L. Henry	A theory of fatigue-damage accumulation in steel. Trans. ASME (1955)
16	C. R. Smith	A method for estimating the fatigue life of 7075-T6 aluminium alloy aircraft structures. NAEC-ASL-1096, December 1965
17	F. Ripp	Calculation of fatigue life by Grumman method, and comparison with test data. Grumman aircraft Report GE-168, July 1967
18	G. V. Deneff	Fatigue prediction study. WADD Technical Report 61-153, January 1962
19	J. R. Fuller	Cumulative fatigue damage due to variable-cycle loading. Noise Control, July/August 1961
20	R. A. Heller	Reduction of the endurance limit as a result of stress interaction in fatigue. WADD Technical Report 60-752, February 1961
21	A. Palmgren	Die Lebensdauer von Kugellagen. Zeitschrift Verdin Deutscher Ingenieure, Vol.68, (1924)

REFERENCES (Contd.)

No.	Author	Title, etc.
22	W. J. Critchlow A. J. McCulloch L. Young M. A. Melcon	An engineering evaluation of methods for the prediction of fatigue life in airframe structures. Technical Report ASD-TR-61-434, March 1962
23	R. A. Heller M. Seki A. M. Freudenthal	The influence of residual stresses on the random fatigue life of notched specimens. ASD-TDR-62-1075, December 1962
24	H. Yeomans	Programme loading fatigue tests on a bolted joint. R.A.E. Technical Note Structures 327, (1963)
25	H. F. Hardrath	Cumulative damage. Tenth Sagamore Army Matls. Conf., August 1963
26	W. A. P. Fisher	Programme fatigue tests on notched bars to a gust load spectrum. A.R.C. C.P.498 (1958)
27	J. Schijve F. A. Jacobs	Fatigue tests on notched and unnotched clad 24S-T sheet specimens to verify the cumulative damage hypothesis. NLL Report M.1982, April 1955
28	E. C. Naumann R. L. Schott	Axial-load fatigue tests using loading schedules based on manoeuvre-load statistics. NASA Technical Note D-1253, May 1962
29	W. A. P. Fisher	Some fatigue tests on notched specimens with programme loading for a 'ground attack' aircraft. A.R.C. C.P.497 (1958)
30	J. Schijve F. A. Jacobs	Research on cumulative damage in fatigue of riveted aluminium alloy joints. NLL Report M.1999, January 1956
31	T. J. Dolan	Residual stress, strain hardening and fatigue. 'Internal Stresses and Fatigue of Metals', Ed. G. M. Rassweiler and W. L. Grube. Pub. Elsevier (1959)

REFERENCES (Contd.)

No.	Author	Title, etc.
32	P. R. Edwards	An experimental study of the stress histories at stress concentrations in an aluminium alloy specimen under variable amplitude loading sequences. RAE Technical Report 70004 (ARC 32233) (1970)
33	J. H. Crews, Jnr. H. F. Hardrath	A study of cyclic plastic stresses at a notch root SESA Paper No.963, May 1965
34	L. Mordfin N. Halsey	Programmed manoeuvre - spectrum fatigue tests of aircraft beam specimens. ASTM STP 338 (1962)
35	R. B. Heywood	The influence of preloading on the fatigue life of aircraft components and structures. A.R.C. C.P.232 (1955)
36	K. Gunn R. McLester	Effect of prestressing on the fatigue strength of notched test-pieces of naturally-aged and fully-heat-treated aluminium alloy DTD 364 B. Aluminium Laboratories Limited Report B-RR-649-59-30, July 1959
37	G. Forrest	Some experiments on the effects of residual stresses on the fatigue of aluminium alloys. Journal Inst. Met., Vol.72, Part 1 (1946)
38	D Rosenthal G. Sines	Effect of residual stress on the fatigue strength of notched specimens. Proc. ASTM (1951)
39	J. Schijve F. A. Jacobs	Programme-fatigue test on aluminium alloy lug specimens with slotted holes and expanded holes. NLL Report TN M.2139, November 1964
40	E. J. Pattinson D. S. Dugdale	Fading of residual stresses due to repeated loading. Metallurgia, November 1962
41	P. G. Forrest	Influence of plastic deformation on notch sensitivity in fatigue. Int. Conf. Fatigue of Metals 1956 (1956)

REFERENCES (Contd.)

No.	Author	Title, etc.
42	A. A. Blatherwick	Stress redistribution during bending fatigue. J. Exp. Mechanics, April 1961
43	E. A. Roberts	Cumulative damage and static overloading effects on the fatigue properties of a high-strength structural steel. Part 2. Cumulative damage tests. S & T Memo 18/65, September 1965
44	F. H. Hooke	On the effects of mean stress and of preloading on the fatigue life of a high tensile structural steel (Ducol W25) Part 1. University of Nottingham, Report CD/4, September 1958
45	F. H. Hooke	Ditto. Part 2. Further experiments. S & T Memo 21/59, November 1959
46	E. Broek J. Schjive	The influence of the mean stress on the propagation of fatigue cracks in aluminium alloy sheet. NLR Technical Note M 2111, January 1963
47	F. J. Bradshaw C. Wheeler	The effect of environment on fatigue crack propagation. R.A.E. Technical Report 65073 (ARC 27169) (1965)
48	J. R. Fuller	Research on techniques of establishing random type fatigue curves for broad band sonic loading. SAE Paper 671C, April 1963
49	A. K. Head F. H. Hooke	Random noise fatigue testing. Int. Conf. on Fatigue of Metals (1956)
50	S. R. Swanson	An investigation of the fatigue of aluminium alloy due to random loading. UTIA Report No.84, February 1963
51	J. Kowalewski	Uber die Beziehungen zwischen der Lebensdauer von Bauteilen bei unregelnafzig schwankenden und bei geordneten Belastungsfolgen. DVL Bericht No.249, September 1963

REFERENCES (Contd.)

No.	Author	Title, etc.
52	R. W. Fralich	Experimental investigation of effects of random loading on the fatigue life of notched canilever-beam specimens of 7075-T6 aluminium alloy. NASA Memo 4-12-59L, June 1959
53	S. A. Clevenson R. Steiner	Fatigue life under random loading for several power spectral shapes. NASA Technical Report R-266, September 1967
54	P. W. Smith C. I. Malme	Fatigue tests of a resonant structure with random excitation. J.Ac. Soc. of America, Vol.35, No.1, January 1963
55	S. R. Swanson	A review of the current status of random load testing in America. ICAF meeting Stockholm, May 1969
56	R. W. Fralich	Experimental investigation of effects of random loading on the fatigue life of notched cantilever-beam specimens of SAE 4130 normalized steel. NASA Technical Note D-663, February 1961
57	K. J. Marsh J. A. Mackinnon	Random loading and block loading fatigue tests on sharply notched mild steel specimens. J. Mech Eng. Sci., Vol.10, No.1, February 1968
58	R. T. Booth D. H. Wright N. P. Smith	Variable-load fatigue tests on small specimens. Second Report: A comparison of loading patterns and the influence of occasional high loads. MIRA Report 1969/9, April 1969
59	R. P. Frick G. A. Gurtman H. D. Meriwether	Experimental determination of residual stresses in an orthotropic material. J. Materials, Vol.2, No.4, December 1967
60	K. Gunn	Effect of yielding on the fatigue properties of test pieces containing stress concentrations. Aluminium Laboratories Limited Report, B-RR-396-55-30 April 1955

REFERENCES (Contd.)

No.	Author	Title, etc.
61	J. O. Smith	The effect of range of stress on the fatigue strength of metals. Bulletin Univ. of Illinois, Vol.XXXIX, No.26, February 1942
62	A. J. Fenner J. E. Field	A study of the onset of fatigue damage due to fretting. N.E. Coast Inst. of Engineers and Shipbuilders Meeting at Newcastle upon Type, January 1960
63	E. Gassner W. Schutz	Evaluating vital vehicle components by programme fatigue tests. FISITA Congress, May 1962
64	E. Gassner W. Schutz	Assessment of the allowable design stresses and the corresponding fatigue life. ICAF Symposium, June 1965
65	E. C. Naumann	Evaluation of the influence of load randomization and of air-ground-air cycles on fatigue life. NASA Technical Note D-1584, October 1964
66	Royal Aeronautical Society	Data sheets on fatigue.
67	J. S. Bendat	Principles and applications of random noise theory. Wiley, New York (1958)
68	J. Schijve F. A. Jacobs	Fatigue crack propagation in unnotched and notched aluminium alloy specimens. NLR Report M 2128, May 1964
69	J. Schijve	Cumulative damage problems in aircraft structures and materials. NLR MP 69005, May 1969
70	A. M. Freudenthal	Cumulative damage under random loading. Int. Conf. Fatigue of Metals (1956)

REFERENCES (Contd.)

No.	Author	Title, etc.
71	S. R. Swanson	A survey of the fatigue aspects in the application of ultra high-strength steels. DMIC Report 210, October 1964
72	J. R. Heath-Smith F. Kiddle	Influence of ageing and creep on fatigue of structural elements in an Al 6% Cu alloy. R.A.E. Technical Report 67093(ARC 29543) (1967)
73	R. C. A. Thurston	Propagating and non-propagating fatigue cracks in metals. Department of Mines and Technical Surveys, Ottawa Information Circular IC 115, January 1960
74	Lloyd Kaecnele	Review and analysis of cumulative fatigue damage theories. Rand Corporation. Memorandum RM-3650-PR. August 1963
75	W. H. Erickson C. E. Work	A study of the accumulation of fatigue damage in steel. Proc. ASTM, Vol.61 (1961)
76	D. Webber J C. Levy	*Cumulative damage in fatigue with reference to* scatter in results. S & T Memo 15/56, August 1958
77	W. C. Brueggeman M. Mayer Jnr. W. H. Smith	Axial fatigue tests at two stress amplitudes of 0.032 inch 24S-T sheet specimens with a circular hole. NACA Technical Note 983, July 1945
78	T. J Dolan H. F Brown	Effect of prior repeated stressing on the fatigue life of 75S-T aluminium. Proc. ASTM, June 1952
79	W. K. Rey	A study of cumulative fatigue damage at elevated temperatures. NACA Technical Note 4284, September 1958

REFERENCES (Contd.)

No.	Author	Title, etc.
80	S. S Manson A. J. Nachtigall C. R. Ensign J. C. Freche	Further investigation of a relation for cumulative fatigue damage in bending. Journal Eng. Ind., February 1965
81	K. Gunn	The fatigue properties of two aluminium alloys tested under variable stress conditions. Aluminium Laboratories Limited B-RR-420-55-30, August 1955
82	H. J. Grover S. M. Bishop L. R. Jackson	Fatigue strength of aircraft materials; axial load fatigue tests on unnotched sheet specimens of 24S-T3, and 75S-T6 aluminium alloy, and of SAE 4130 steel. NASA Technical Note 2324, March 1951
83	H. G. Baron D. J. Campion	Surface effects and cumulative damage in low endurance fatigue tests on hot-rolled steel plate. RARDE Memo (M) 58/63, December 1963
84	I. Smith D. M. Howard F. C. Smith	Cumulative fatigue damage of axially loaded alclad 75S-T6 and alclad 24S-T3 aluminium alloy sheet. NACA Technical Note 3293, September 1955
85	P. A. T. Gill	Some aspects of high-frequency fatigue. M.Sc. Thesis, University of Southampton, March 1963
86	M. T. Lowcock T. R. G. Williams	Effects of random loading on the fatigue life of aluminium alloy L73. AASU Report No.225 (1962)
87	A. V. de Forest	The rate of growth of fatigue cracks. Trans ASME Vol.58, (1936)
88	M. S. Hunter W. G. Fricke Jnr.	Metallographic aspects of fatigue behaviour of aluminium. Proc. ASTM, Vol.54, June 1954
89	S. S. Manson	Interfaces between fatigue, creep and fracture. Int. J. Fracture Mechanics, Vol.2, No.1, pp.327-363, (1966)

REFERENCES (Contd.)

No.	Author	Title, etc.
90	T. R. G. Williams	Significance of the discontinuity in the S-N curve. Thermal and high strain fatigue (Proc. of Conf. - Inst. of Metals and Iron and Steel Inst.) (1967)
91	J. A. Bennett	A study of the damaging effect of fatigue stressing on X4130 steel. Proc. ASTM (1946)
92	R. L. Segall P. G. Partridge	Dislocation arrangements in aluminium deformed in tension or by fatigue. Phil. Mag. No.44, August 1959
93	J. A. Bennett J. L. Baker	Effect of prior static and dynamic stresses on the fatigue strength of aluminium alloys. N.B.S. Journal of Research, Vol.45, pp.449-457 (1950)
94	W. T. Kirkby G. R. Eynon	The residual static strength of a bolted joint cracked in fatigue. R.A.E. Technical Report 66111 (ARC 29863) (1966)
95	G. W. Brown C. E. Work	An evaluation on the influence of cyclic pre-stressing on the fatigue limit. Proc. ASTM (1963)
96	J. B. Kommers	The effect of overstress in fatigue on the endurance life of steel. Proc. ASTM (1945)
97	T. J. Dolan F. E. Richart Jnr. C. E. Work	The influence of fluctuations in stress amplitude on the fatigue of metals. Proc. ASTM (1949)
98	H. T. Corten G. M. Sinclair T. J. Dolan	An experimental study of the influence of fluctuating stress amplitude on fatigue life of 75S-T6 aluminium. Proc. ASTM (1954)
99	K. J. Marsh	Cumulative fatigue damage under a symmetrical saw-tooth loading programme. NEL Report No.136, March 1964

REFERENCES (Contd.)

No.	Author	Title, etc.
100	G. M. Sinclair	An investigation of the coaxing effect in fatigue of metals. Proc. ASTM 1952 (1952)
101	J. C. Levy S. L. Kanitkhar	Strain ageing and the fatigue limit of steel. J. Iron and Steel Institute, April 1961
102	R. W. Smith M. H. Hirshberg S. S. Manson	Fatigue behaviour of materials under strain cycling in low and intermediate life range. NASA Technical Note D-1574, April 1963
103	T. Endo J. Morrow	Monotonic and completely reversed cyclic stress-strain and fatigue behaviour of representative aircraft materials. NAEC-ASL 1105, June 1966
104	N. H. Polakowski A. Palchoudhuri	Softening of certain cold-worked metals under the action of fatigue loads. Proc. ASTM 1954, June 1954
105	F. H. Vitovec	Effect of static prestrain on fatigue properties. Proc. ASTM 1958, June 1958
106	N. E. Frost	The effect of cold work on the fatigue properties of two steels. Metallurgia, September 1960
107	N. E. Frost	The fatigue strength of specimens cut from pre-loaded blanks. Metallurgia, June 1958
108	R. H. Comyn C. W. Furlani	Fretting corrosion, a literature survey. Harry Diamond Laboratories. U.S. Army Matls. Command Technical Report 1169, December 1963
109	J. E. Field D. M. Waters	Fretting fatigue strength of EN26 steel. Effects of mean stress, slip range and clamping conditions. NEL Report No.275, February 1967

REFERENCES (Contd.)

No.	Author	Title, etc.
110	P. J. E. Forsyth	A two stage process of fatigue crack growth. Crack Propagation Symposium, Cranfield, September 1961
111	J. Schijve D. Broek P. de Rijk	Fatigue crack propagation under variable-amplitude loading. NLR Technical Note M2094, December 1961
112	S. R. Swanson	Random load fatigue testing: a state of the art survey. MTS Systems Corp. Report, June 1967

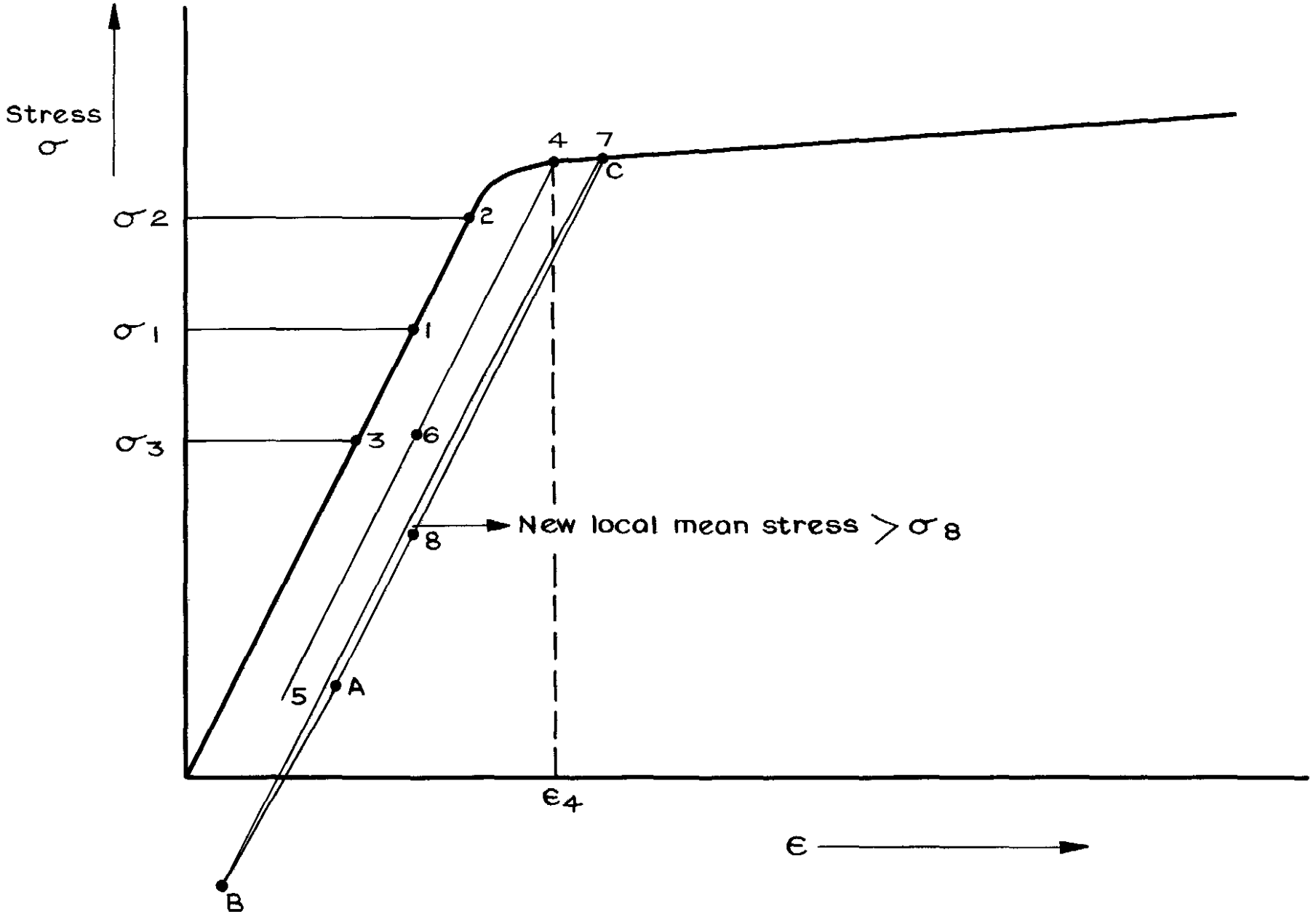

Fig.1 Idealised stress/strain history at notch root

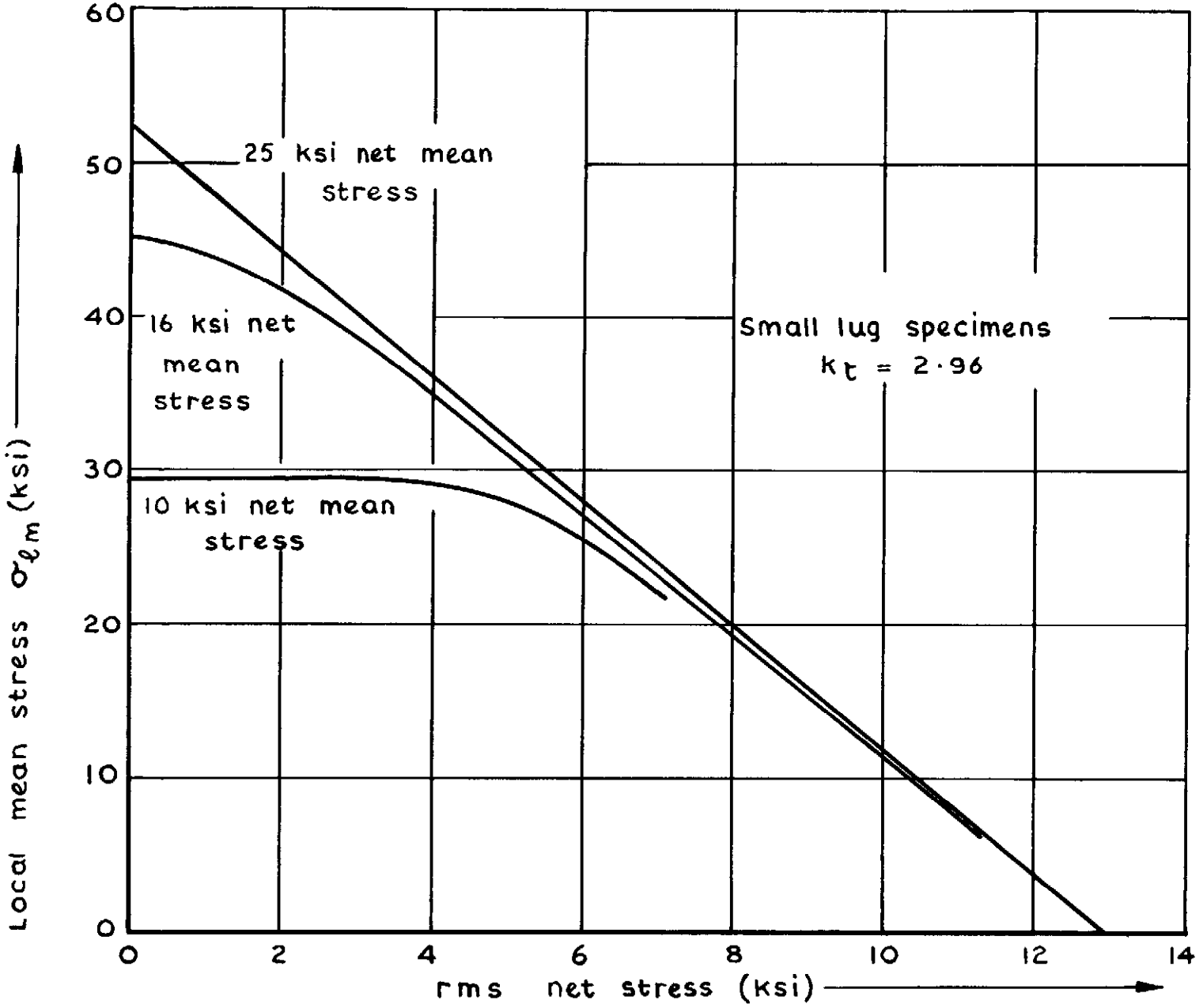

Fig.2 Calculated variation in $\sigma_{\ell m}$ for small lug specimens under constant amplitude loading neglecting Bauschinger effect

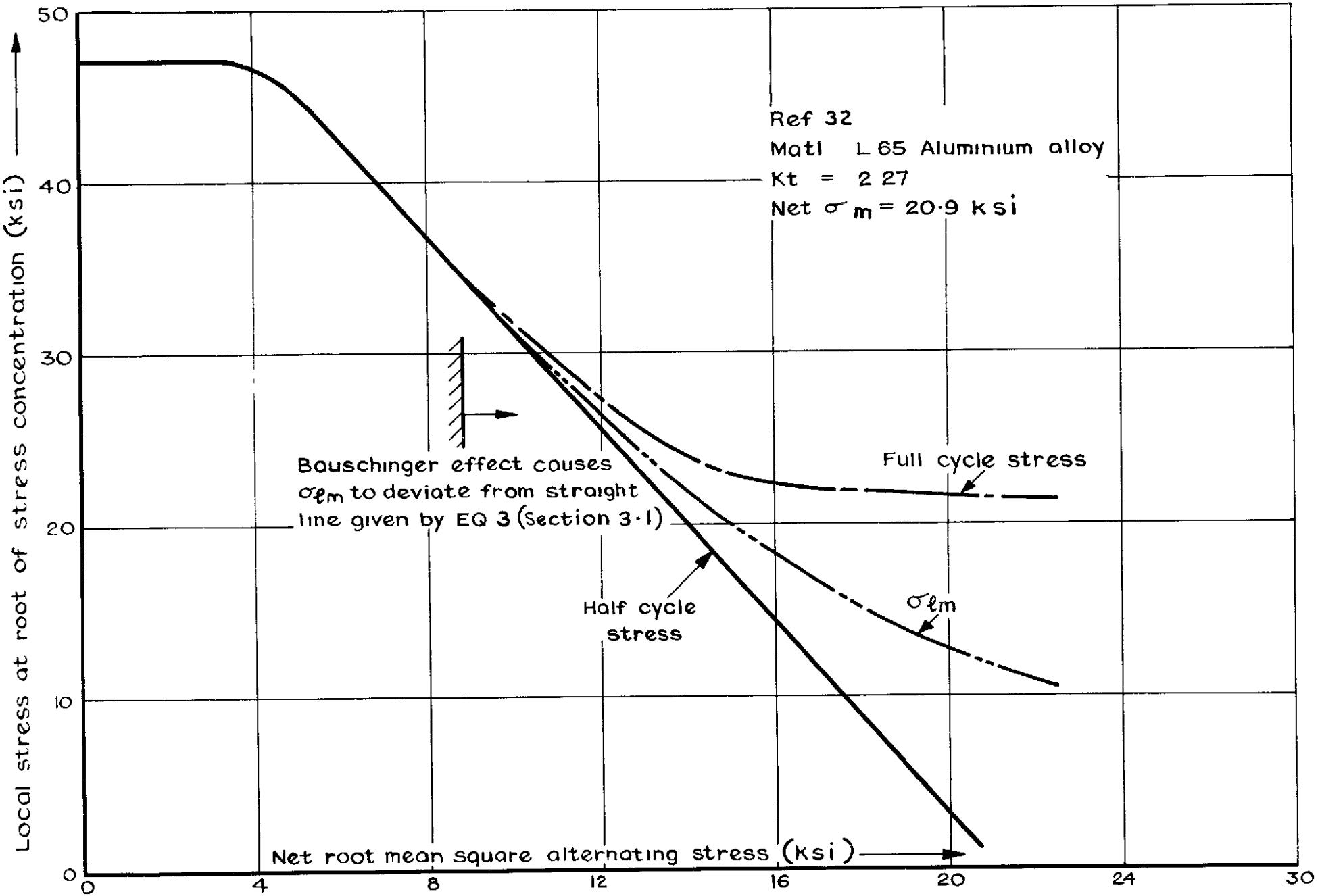

Fig. 3 Measured local stresses at stress concentration under constant amplitude loading

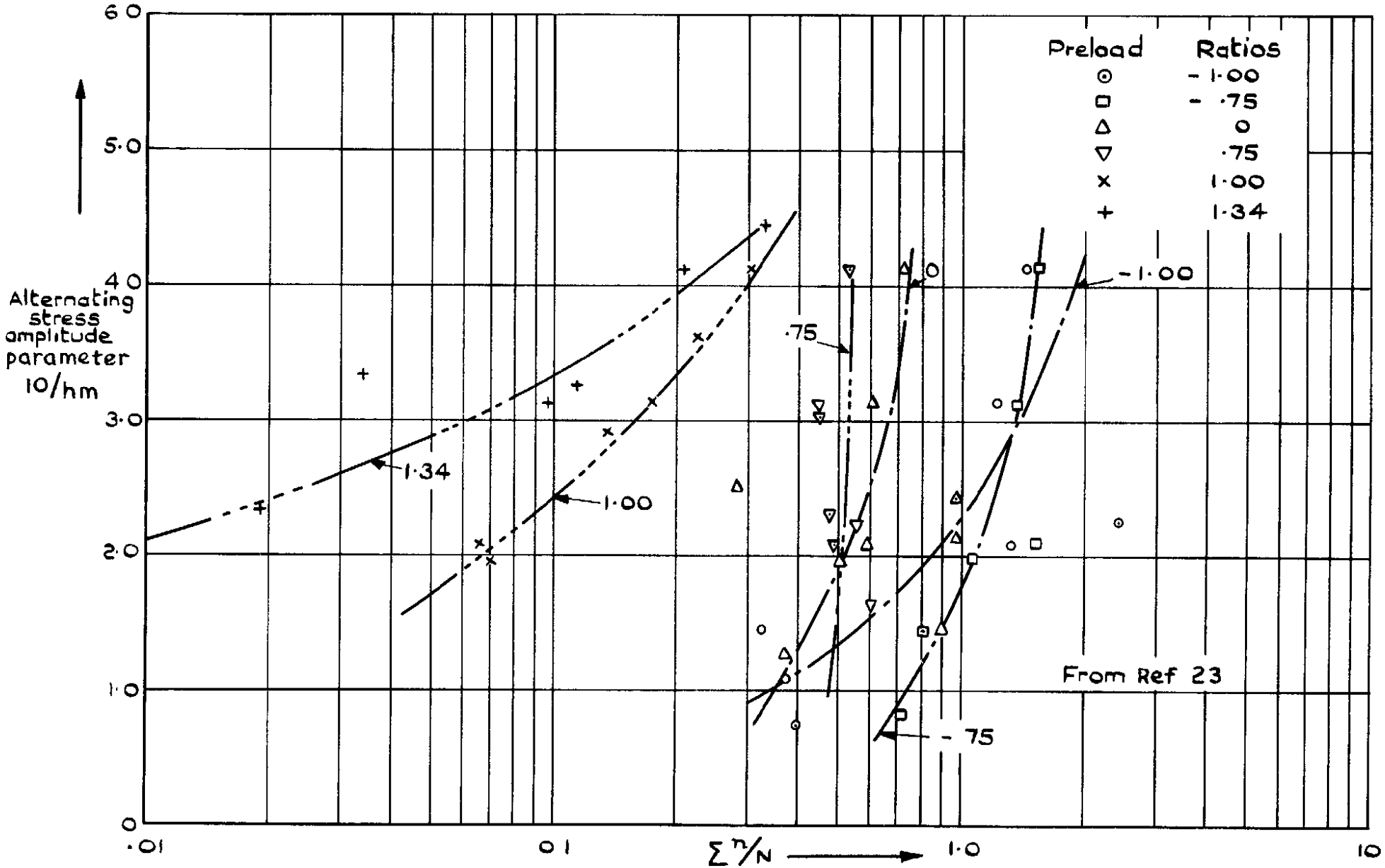

Fig.4 $\Sigma n/N$ for notched preloaded specimens of 7075-T6

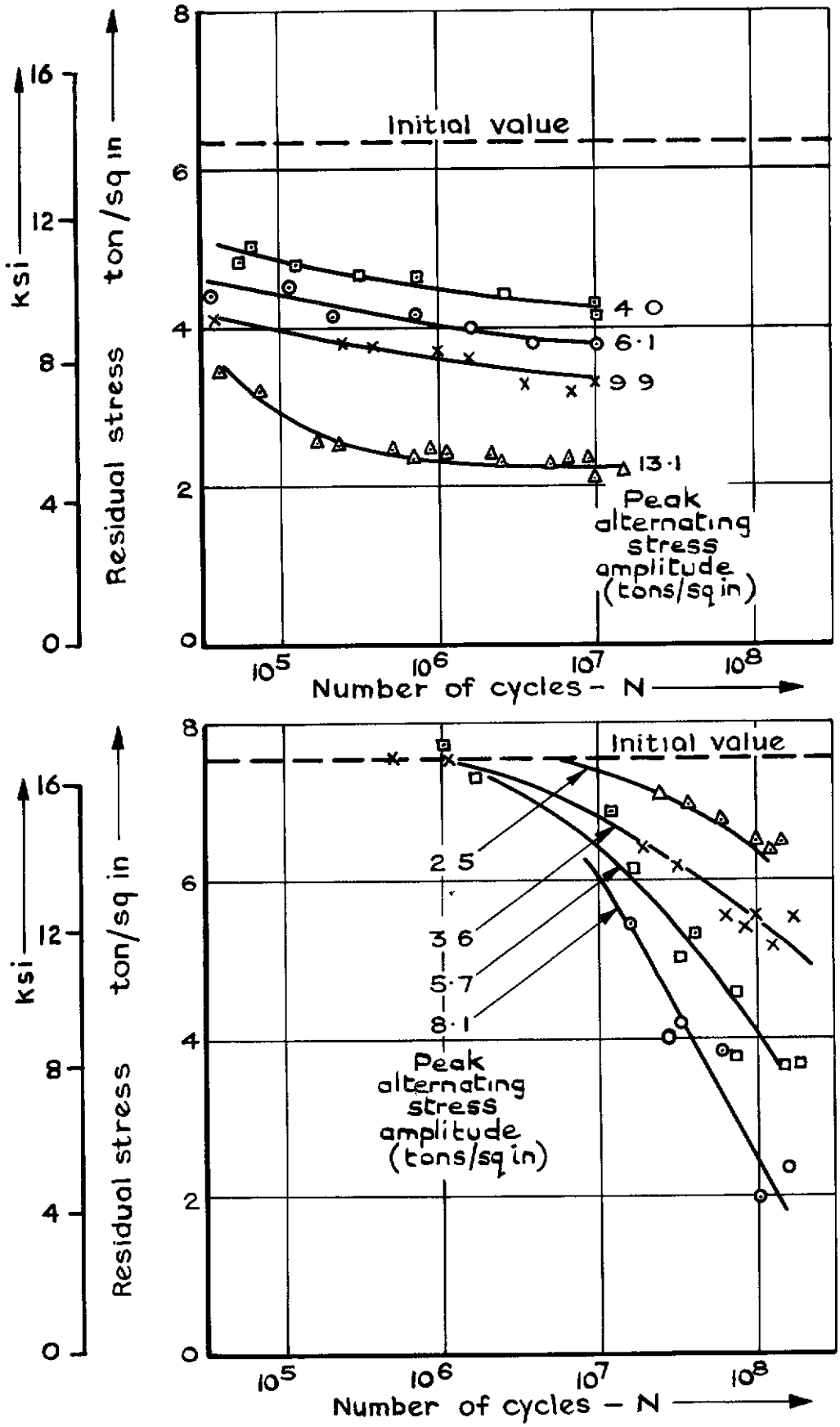

Fig. 5 Fading of residual stress after various amounts of cyclic stressing; top mild steel; bottom aluminium alloy (Ref 40)

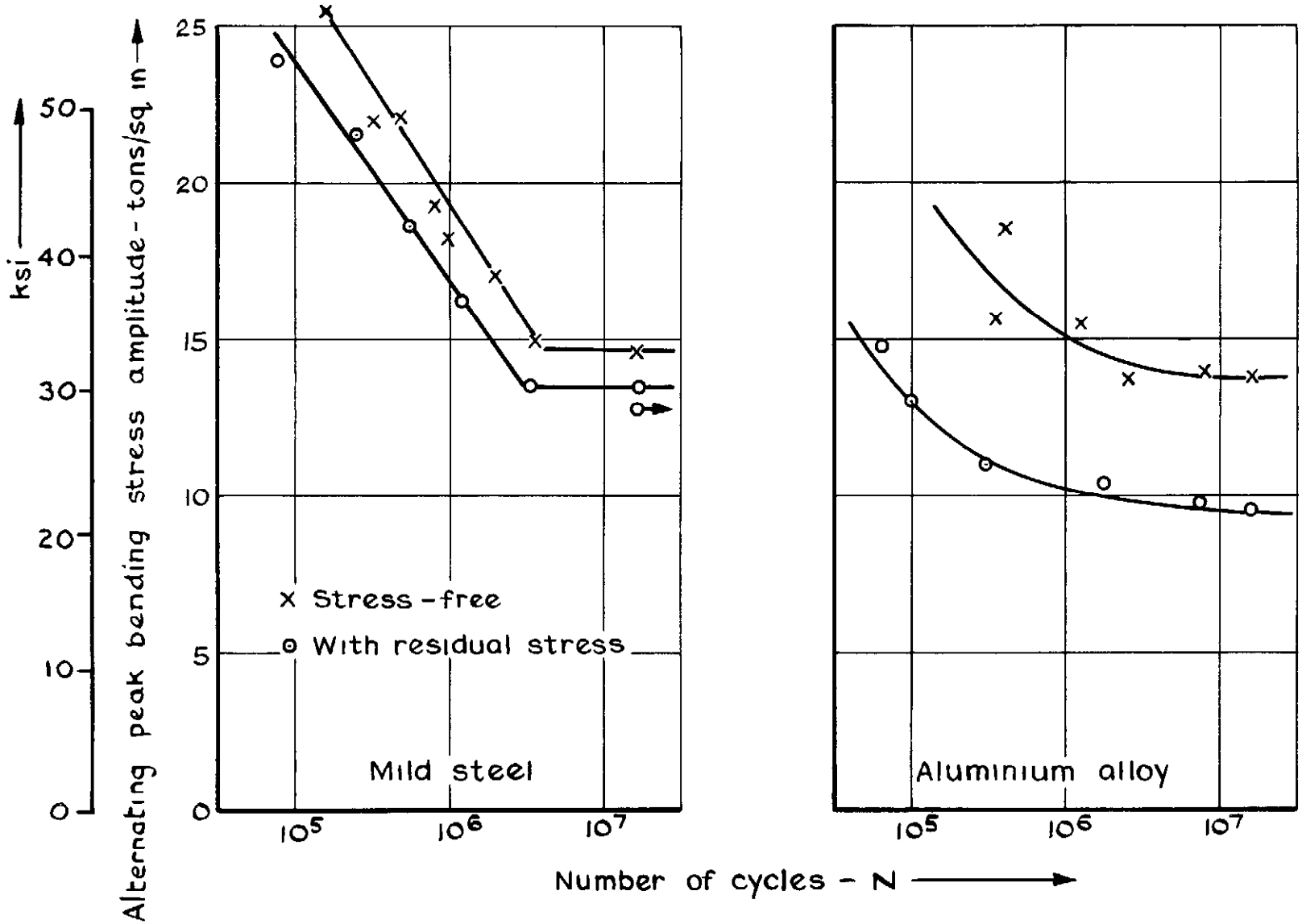

Fig. 6 Effect of residual stress on bending fatigue strength. (Ref 40)

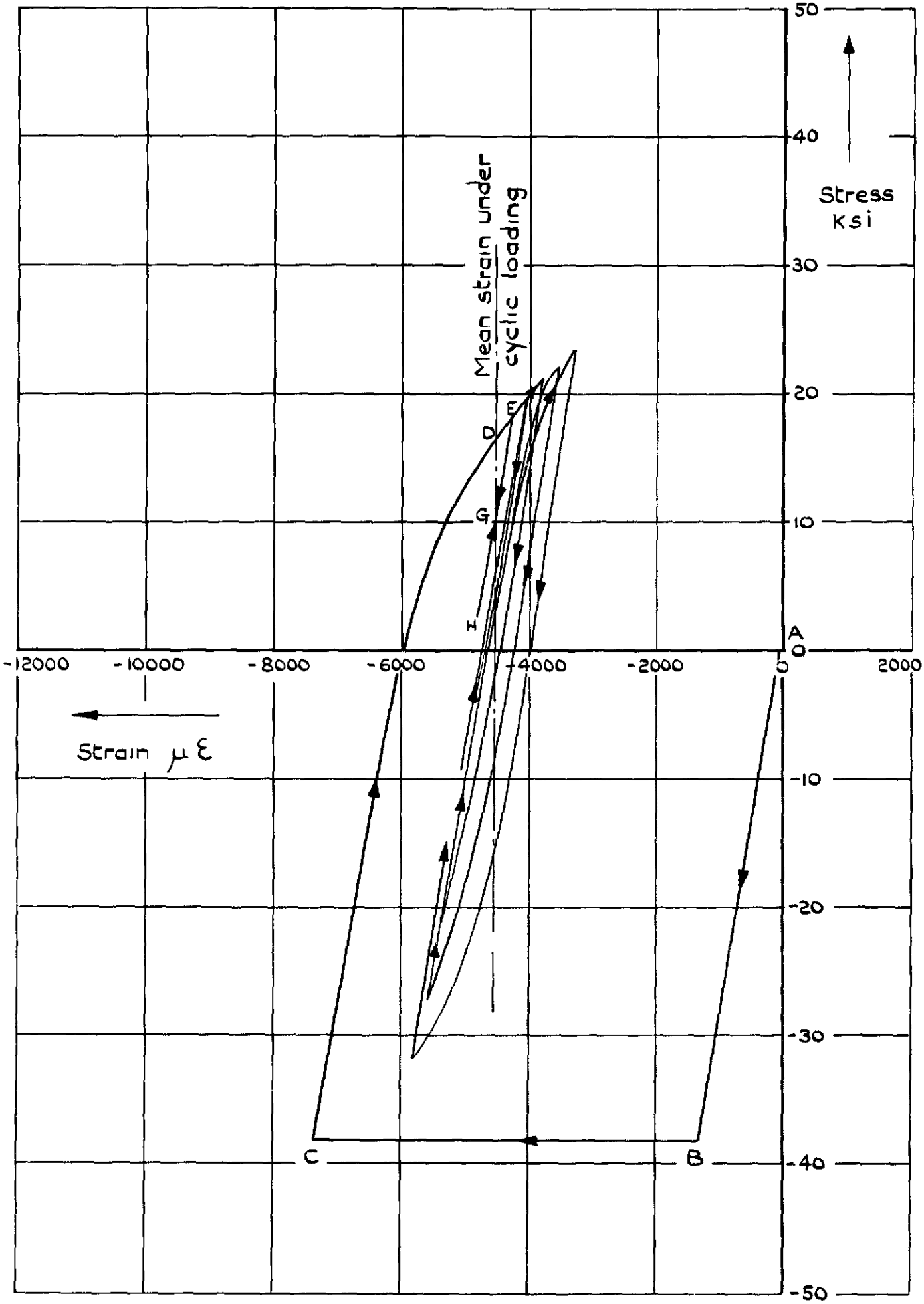

Fig. 7 Behaviour of annealed mild steel

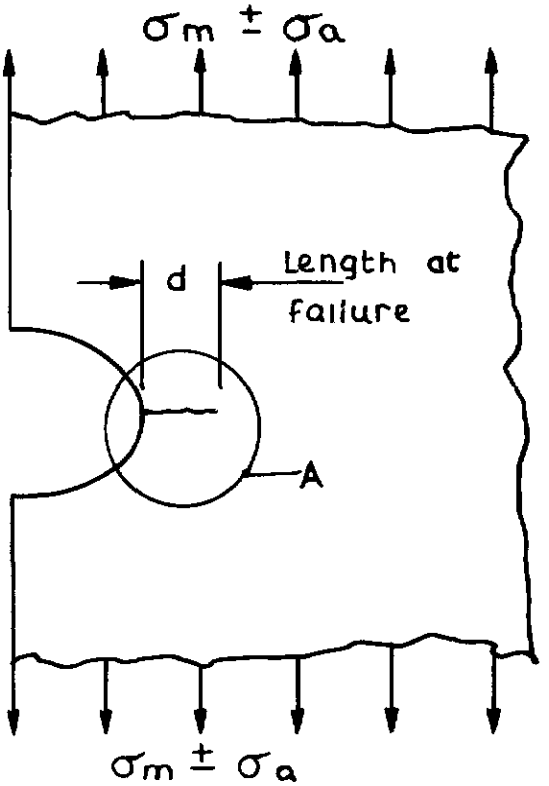

a Crack growing from notch in an infinite sheet

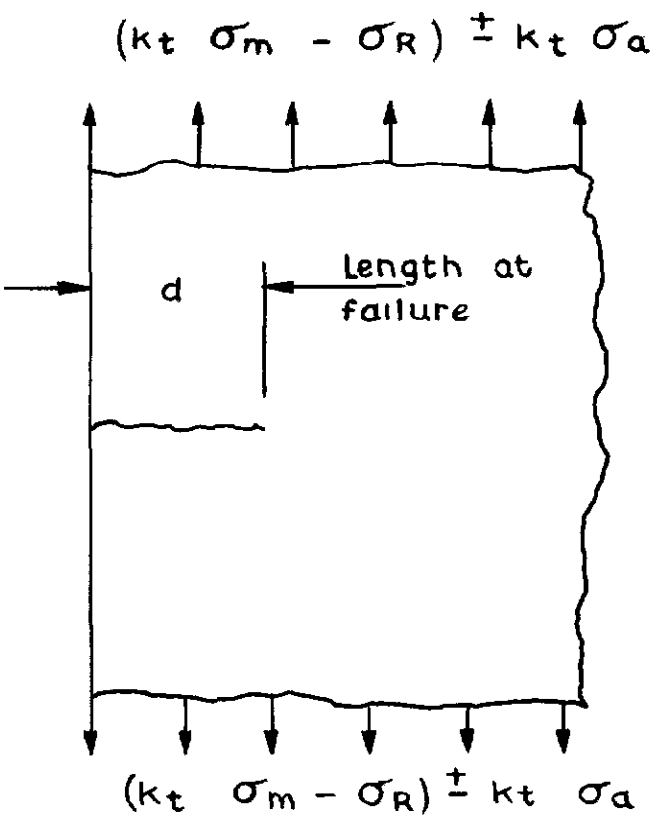

b Effective conditions at A for very large notch

Fig. 8 a & b Crack growing from notch root

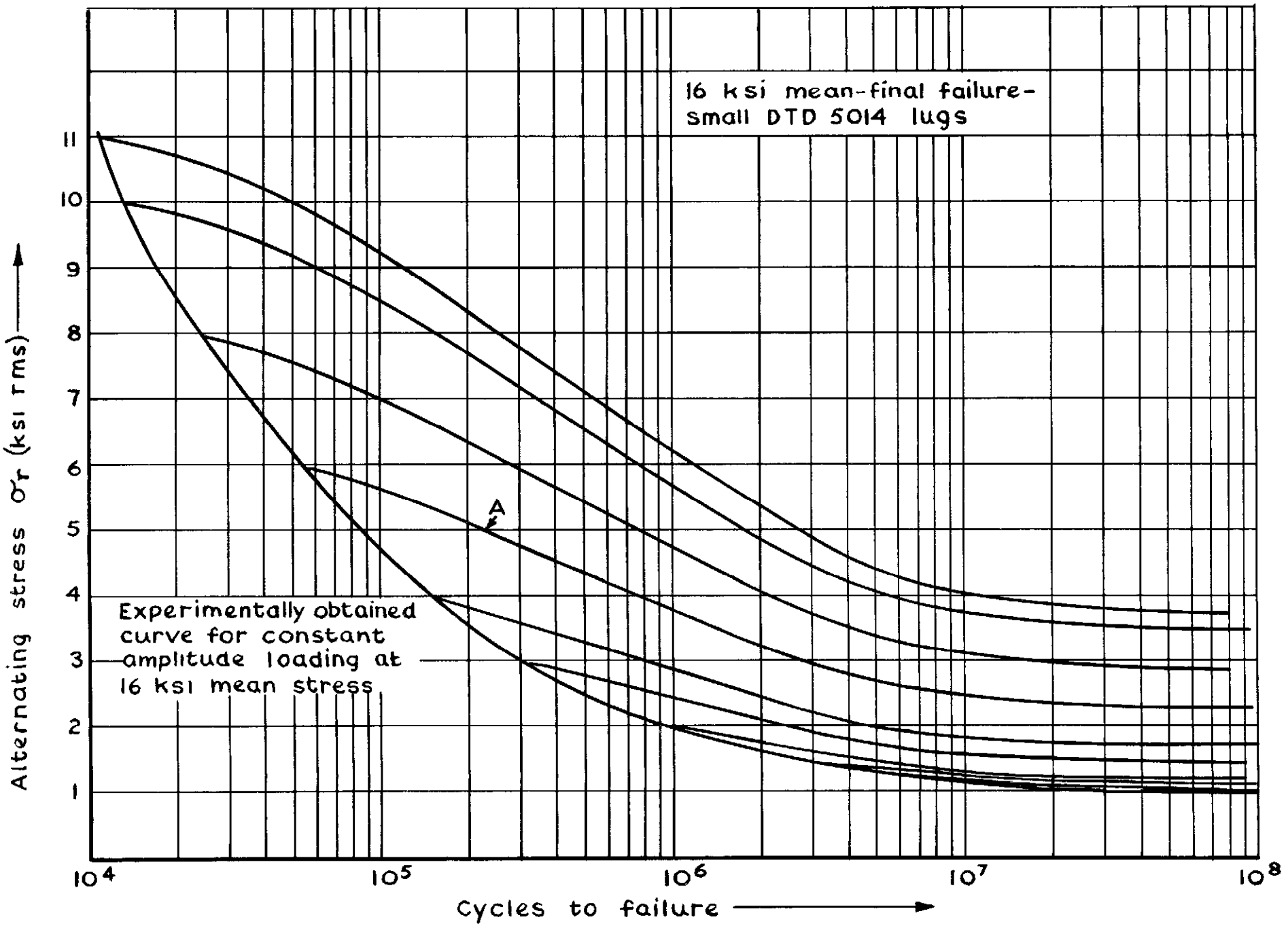

Fig. 9 Set of fictitious S–N curves

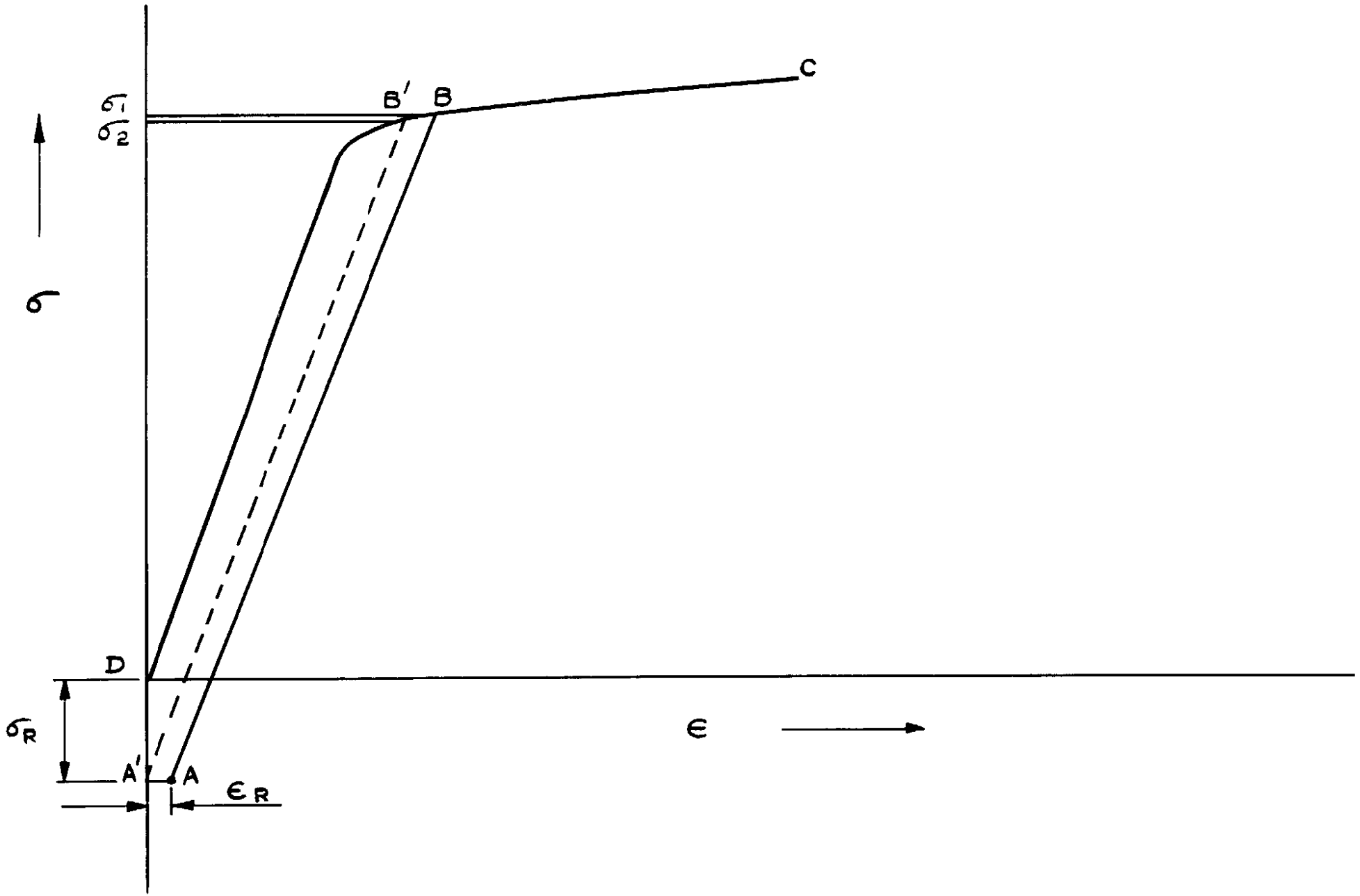

Fig. 10 Method of accounting for residual stresses due to manufacture

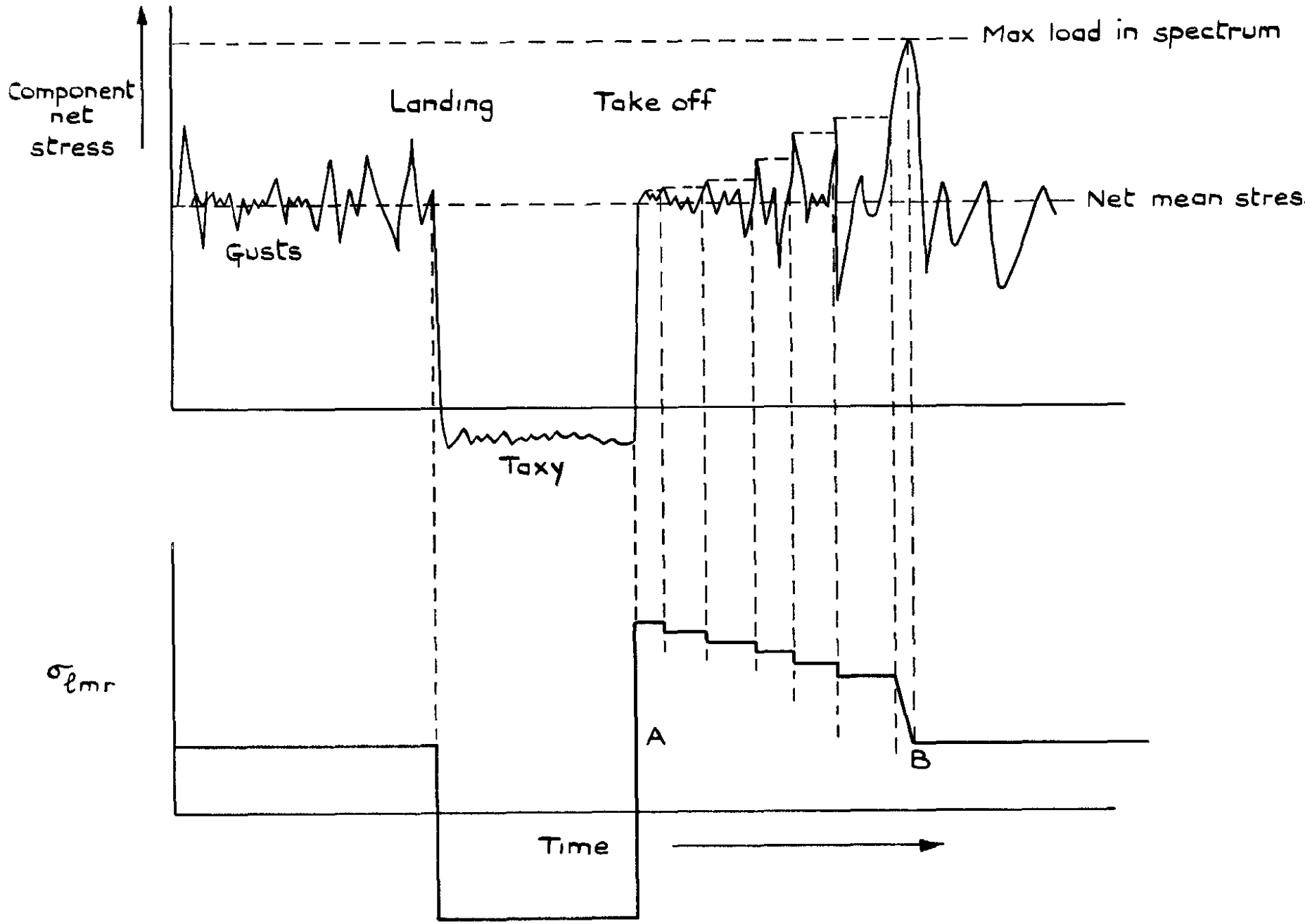

Fig.11 Variation of $\sigma_{\ell mr}$ during landing/take off sequence (diagrammatic)

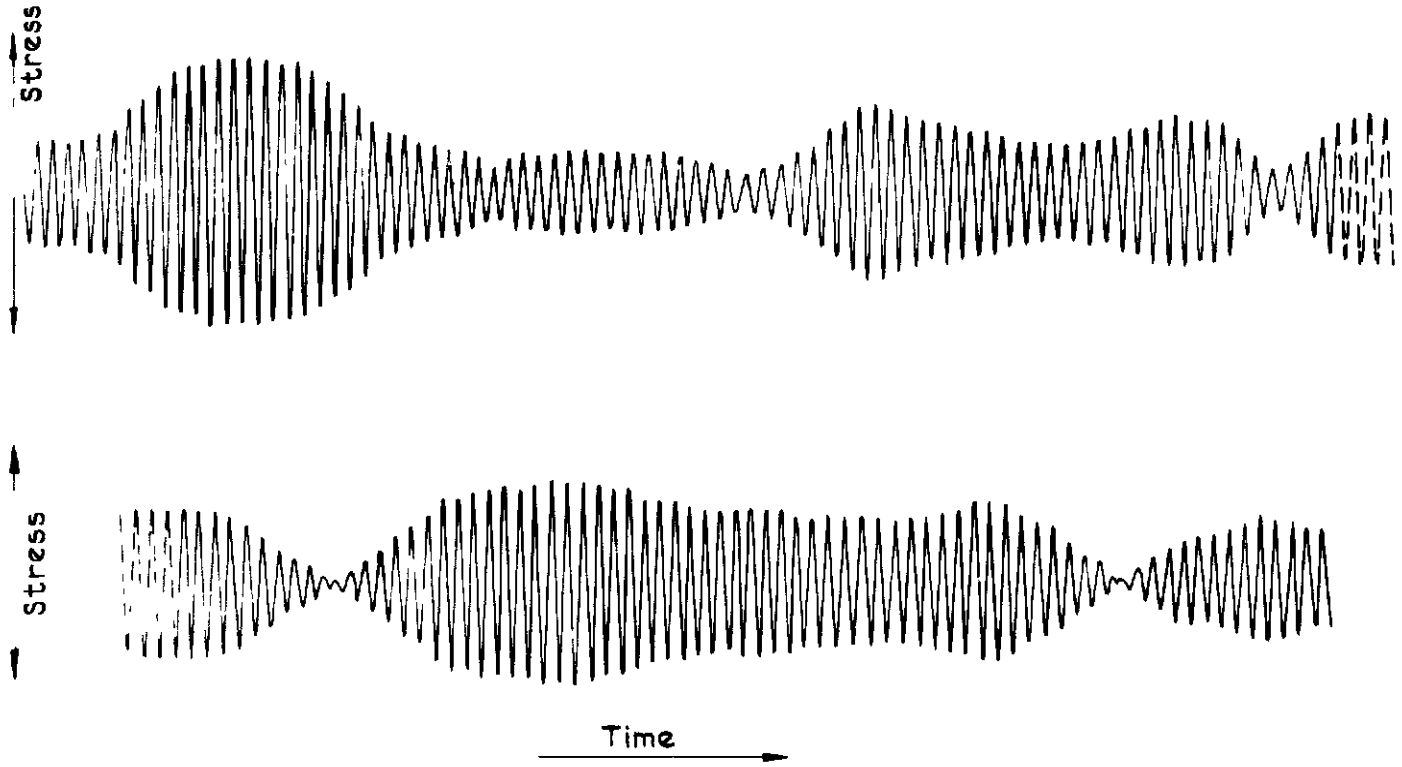

Fig. 12 a Random stress – time waveform

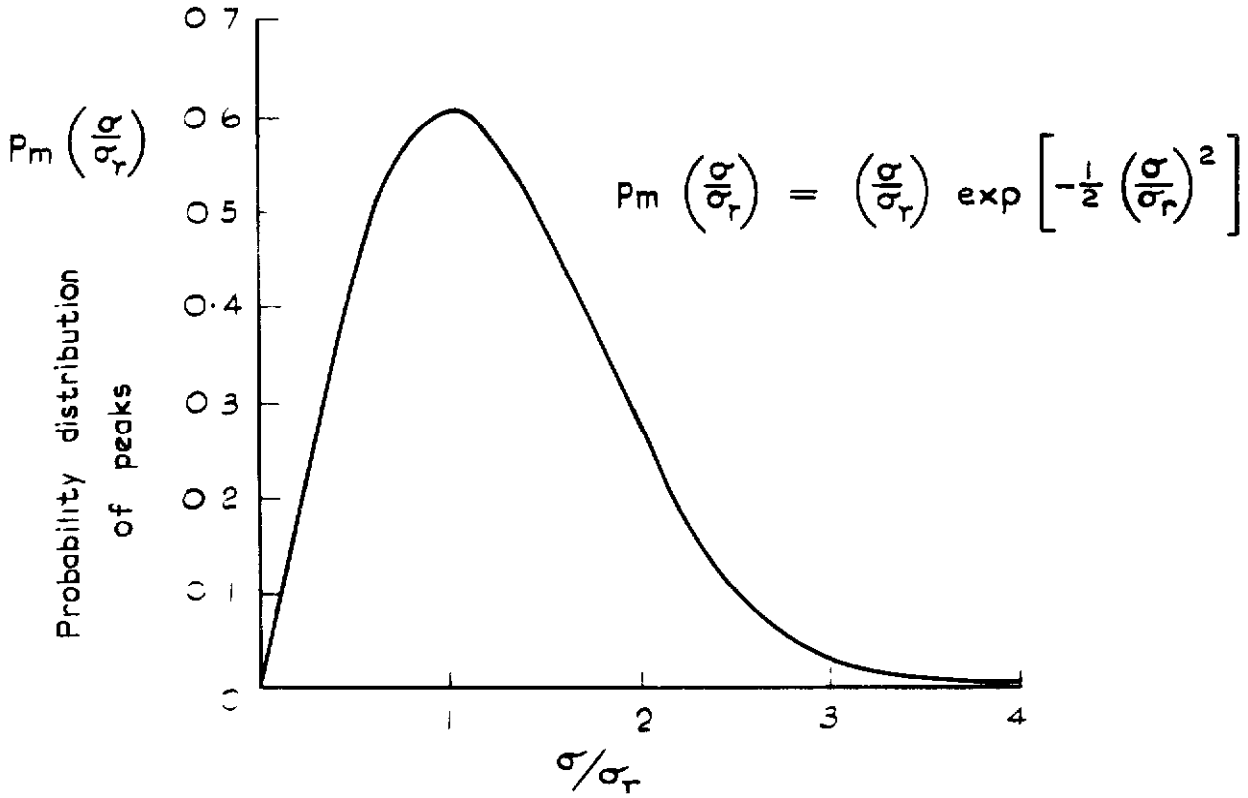

Fig. 12 b Rayleigh distribution

Fig 13. Fatigue machine

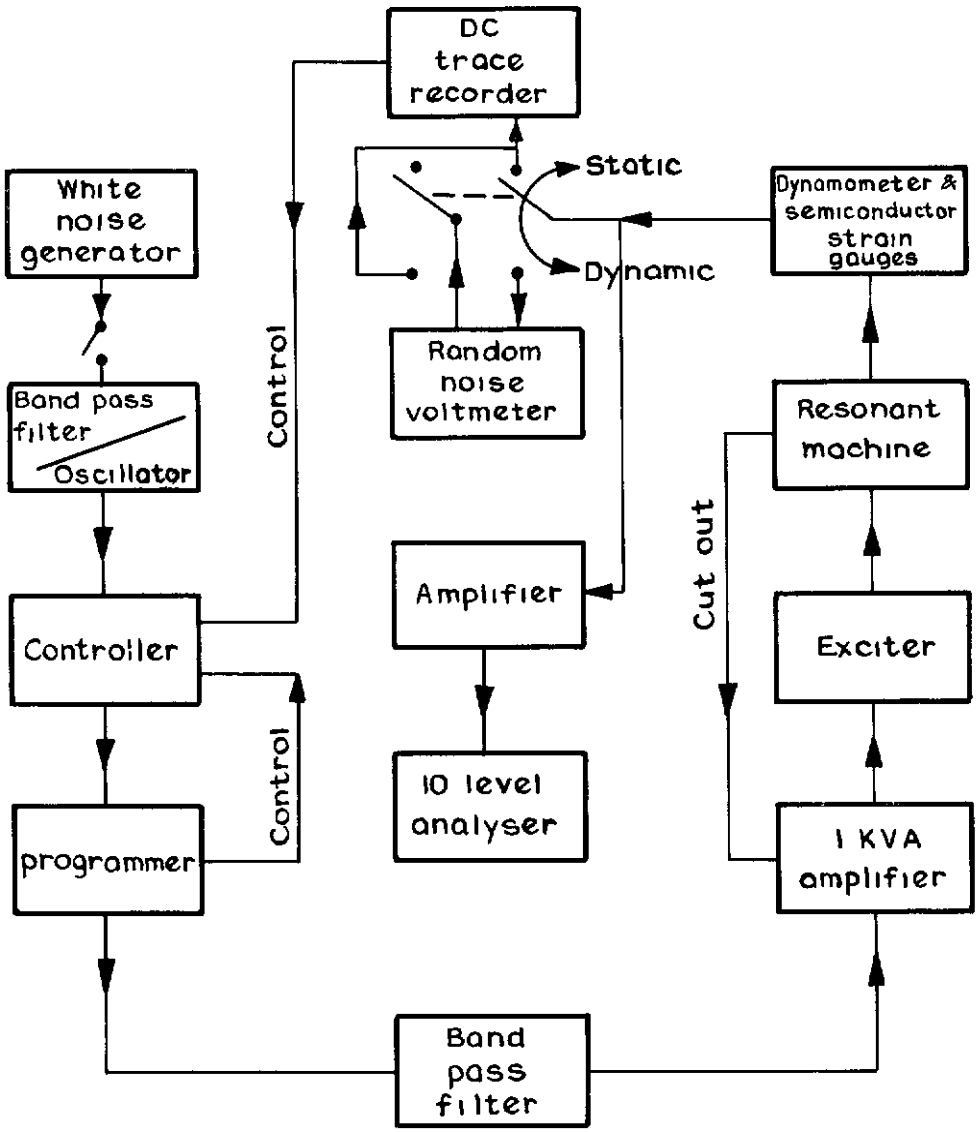

Fig. 14 Block diagram of fatigue machine and associated equipment

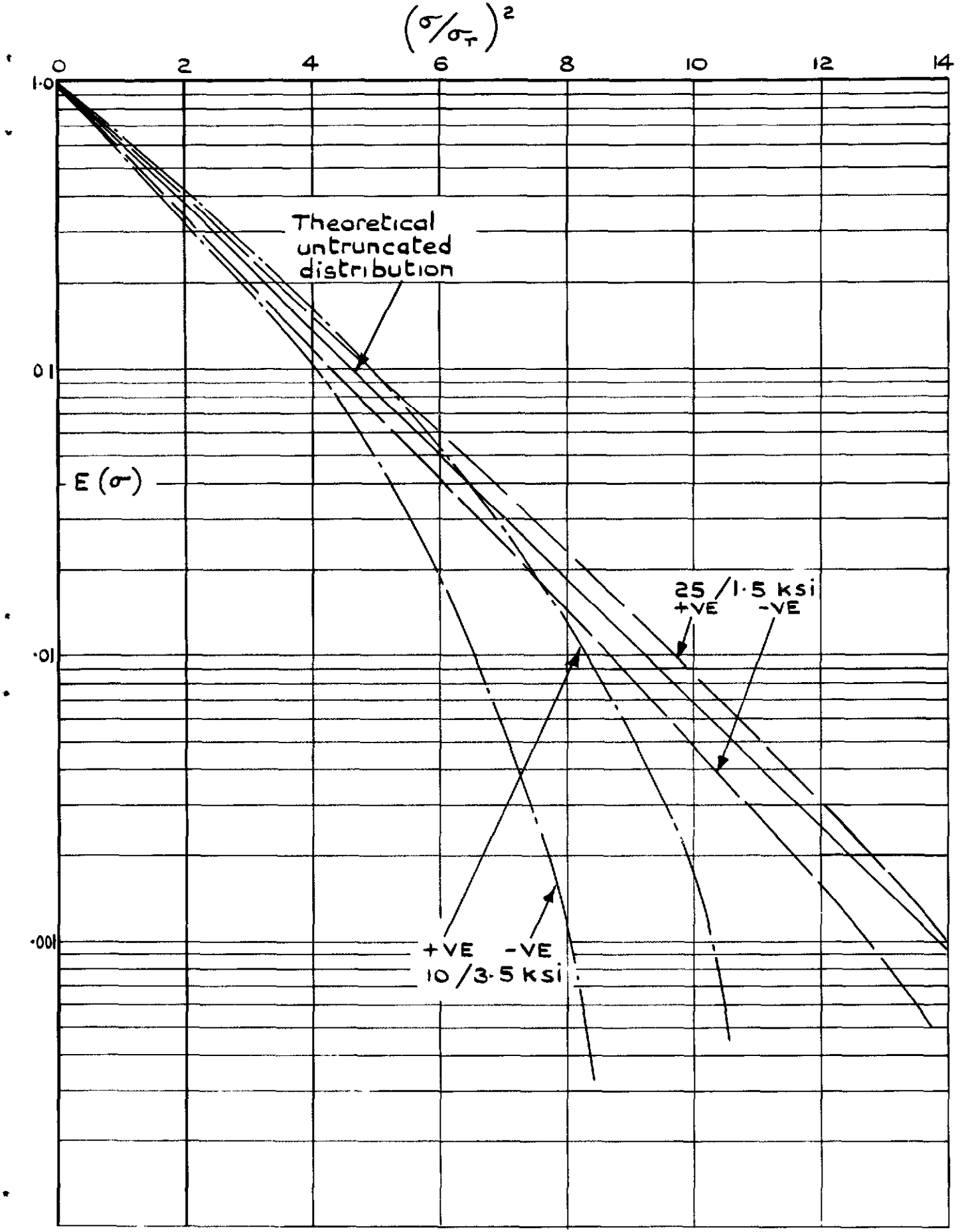

Fig. 15 Typical measured amplitude spectra (stationary random loading)

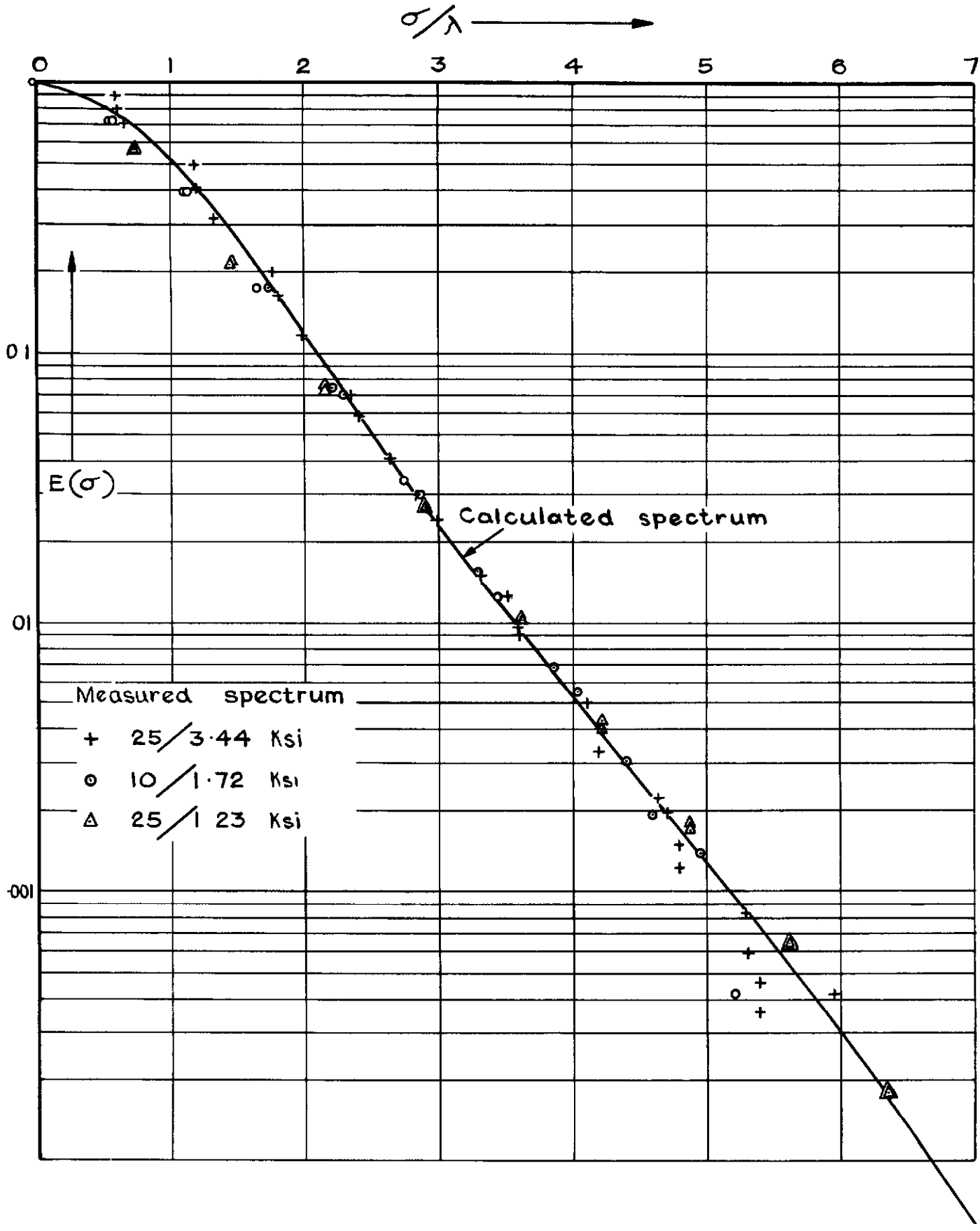

Fig. 16 Typical measured amplitude spectra (random programmed loading)

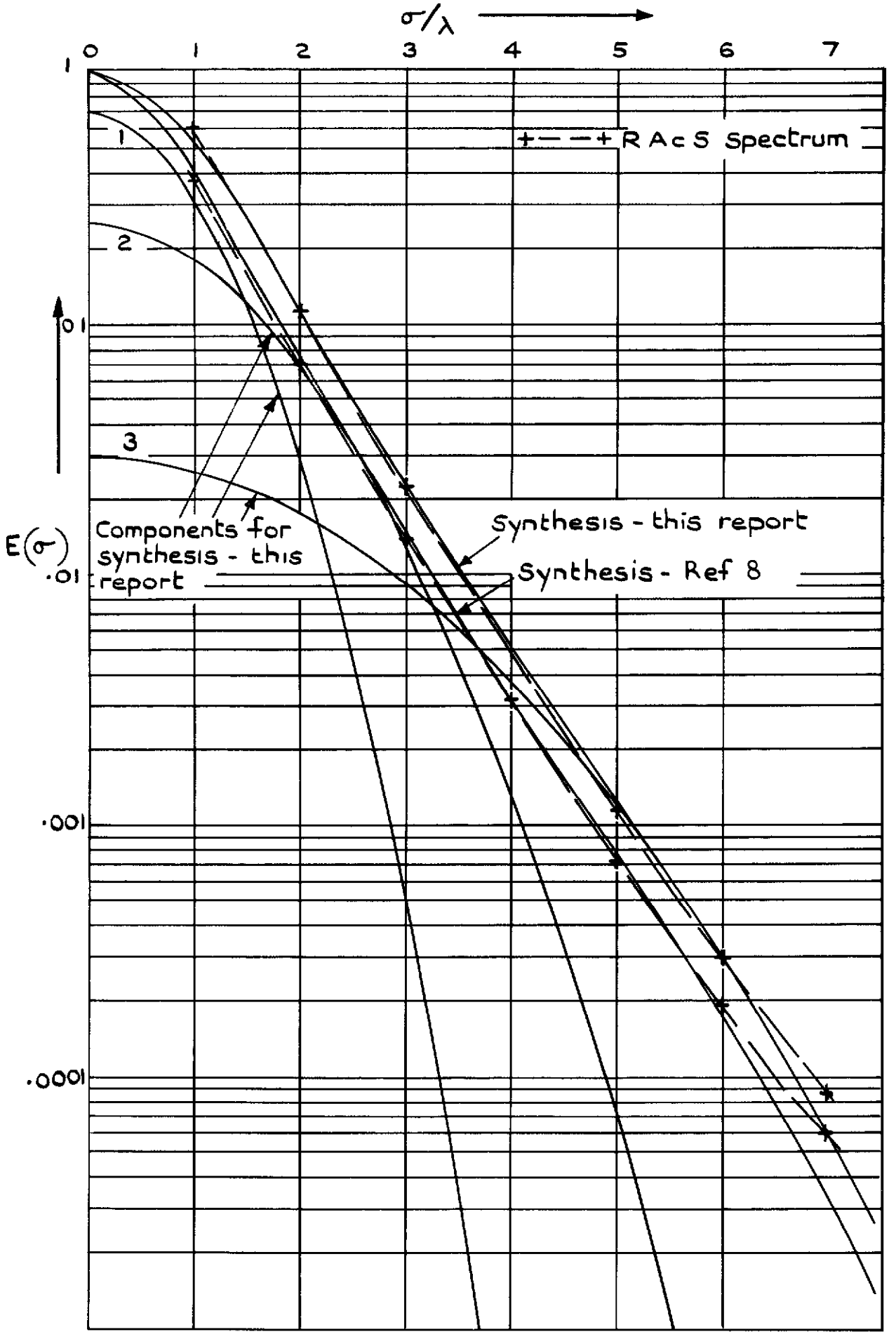

Fig. 17 Random programmed stress synthesis

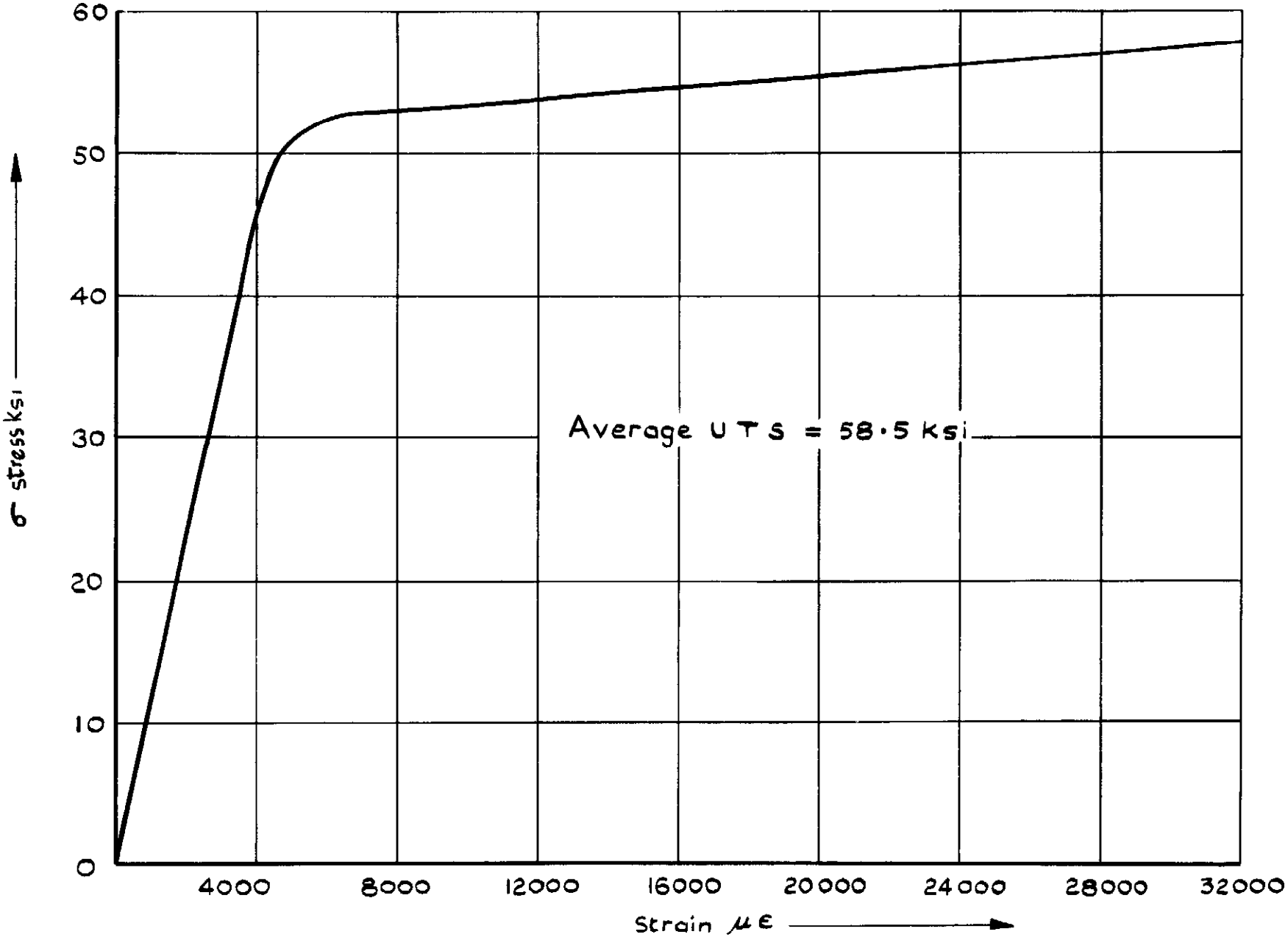

Fig. 18 Average tensile curve for DTD 5014

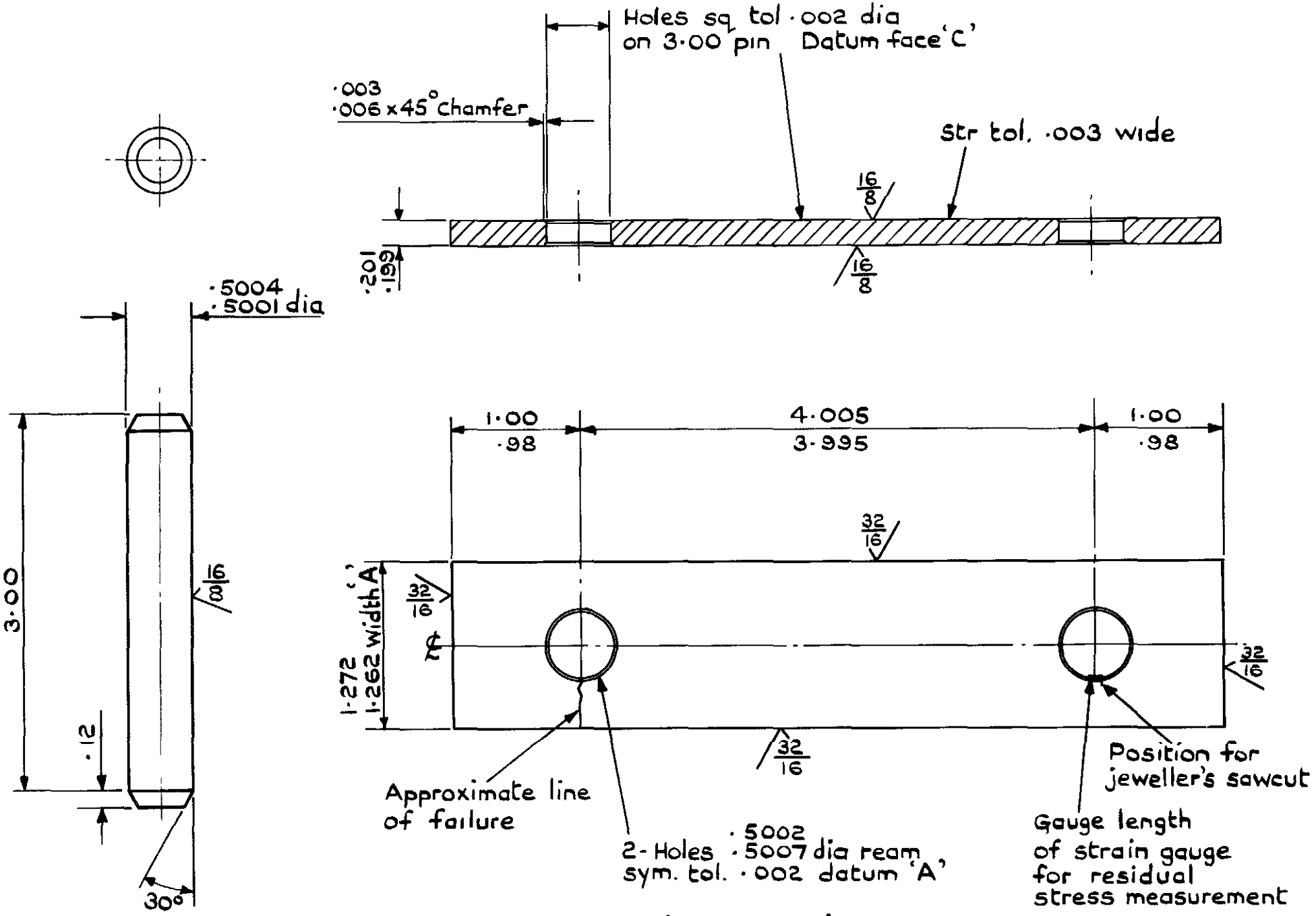

Fig.19 Lug specimen and pin

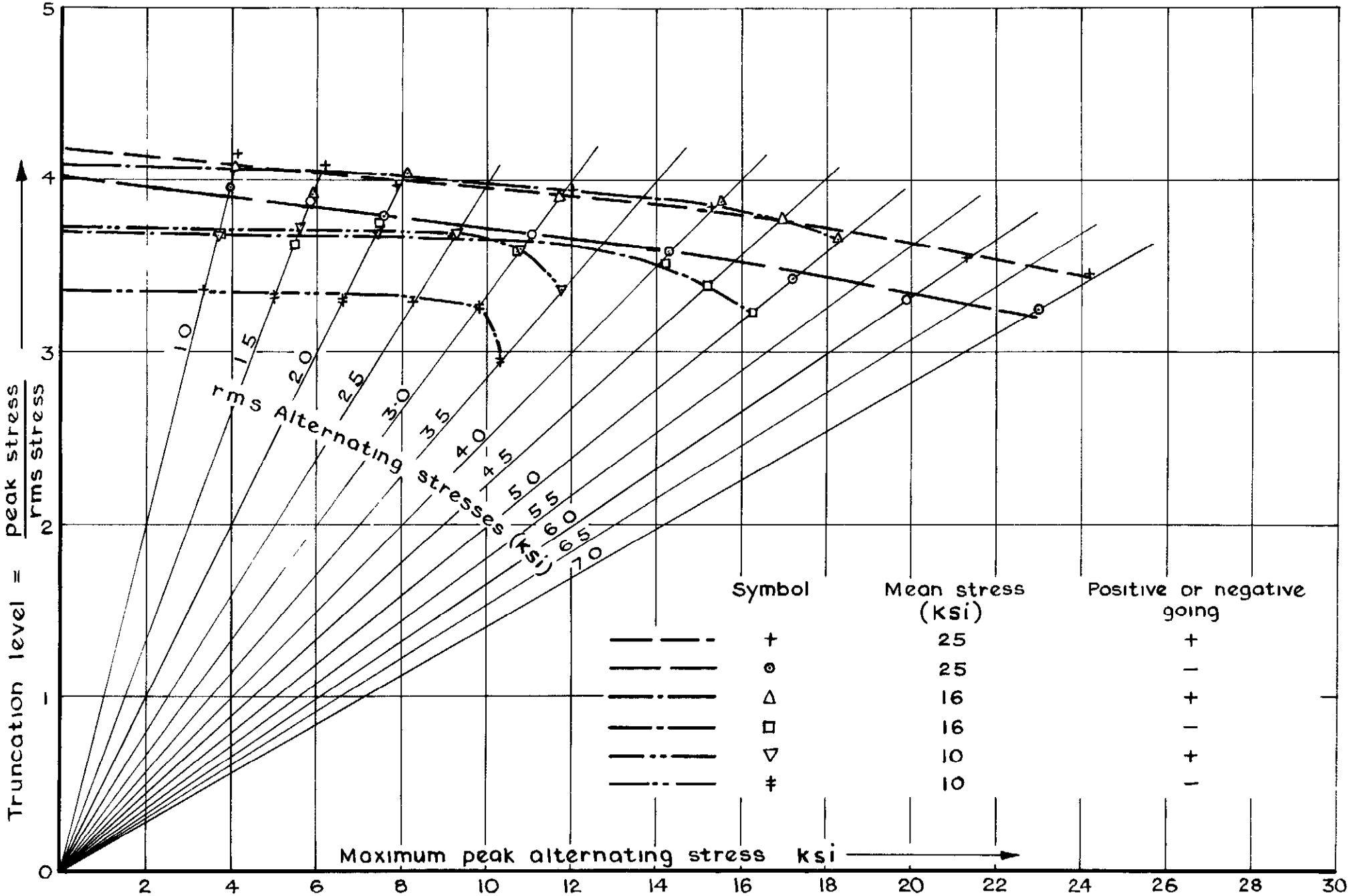

Fig. 20 Measured truncation levels against maximum peak dynamic stress

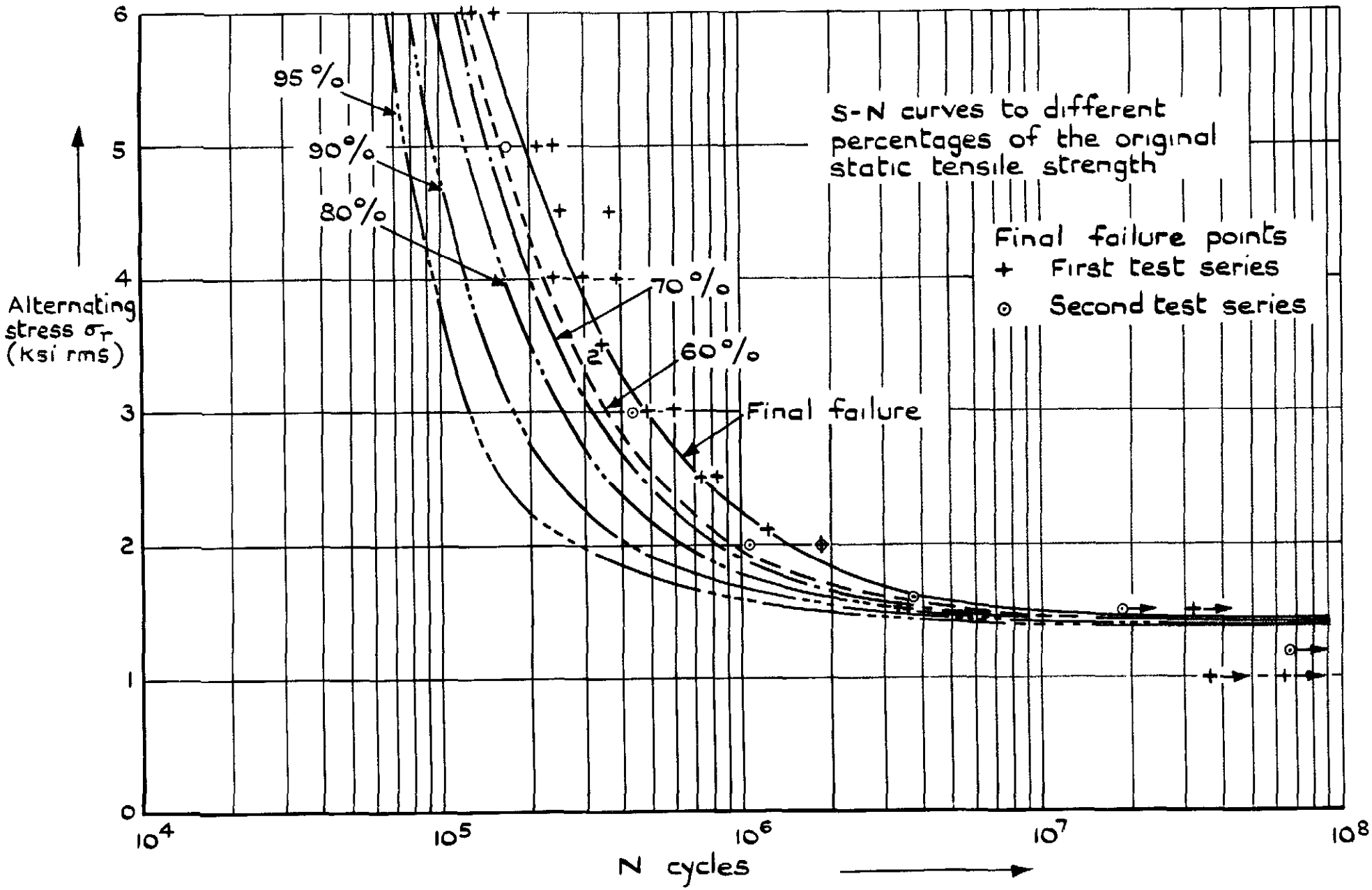

Fig. 21 Constant amplitude test results at 10 ksi mean stress

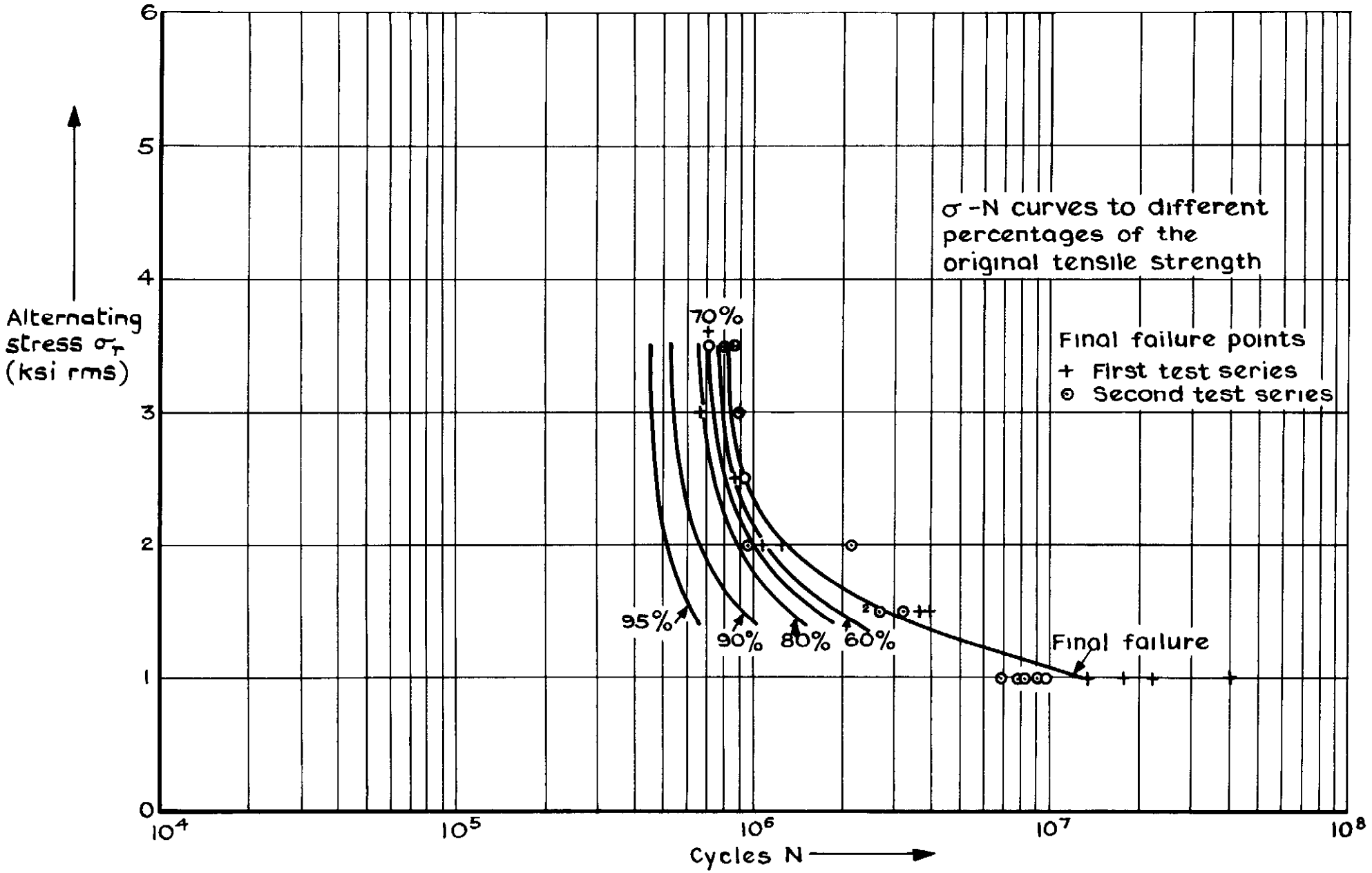

Fig. 22 Stationary random test results at 10 ksi mean stress

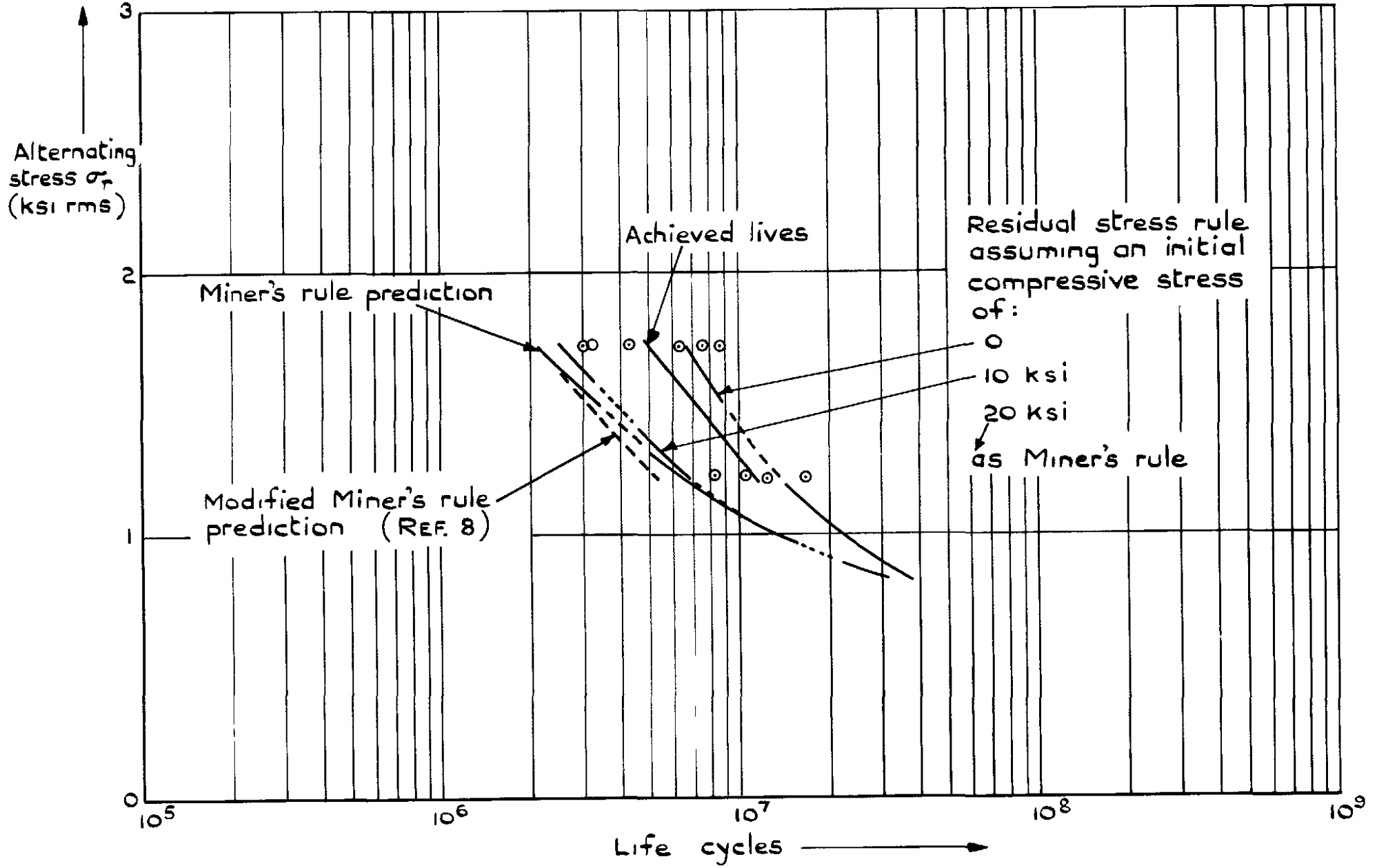

Fig. 23 Random programmed tests to final failure at 10 ksi mean stress

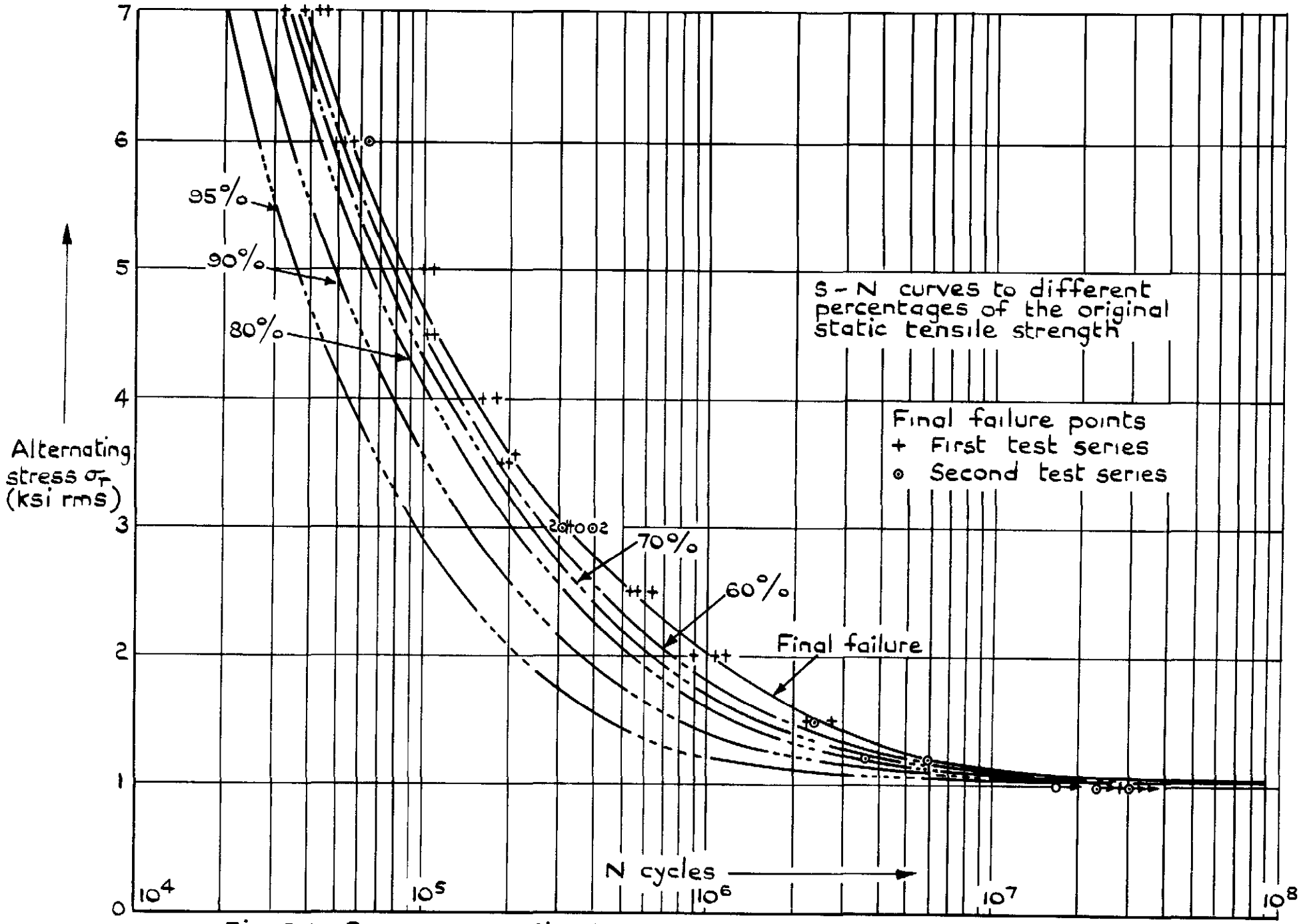

Fig. 24 Constant amplitude test results at 16 ksi mean stress

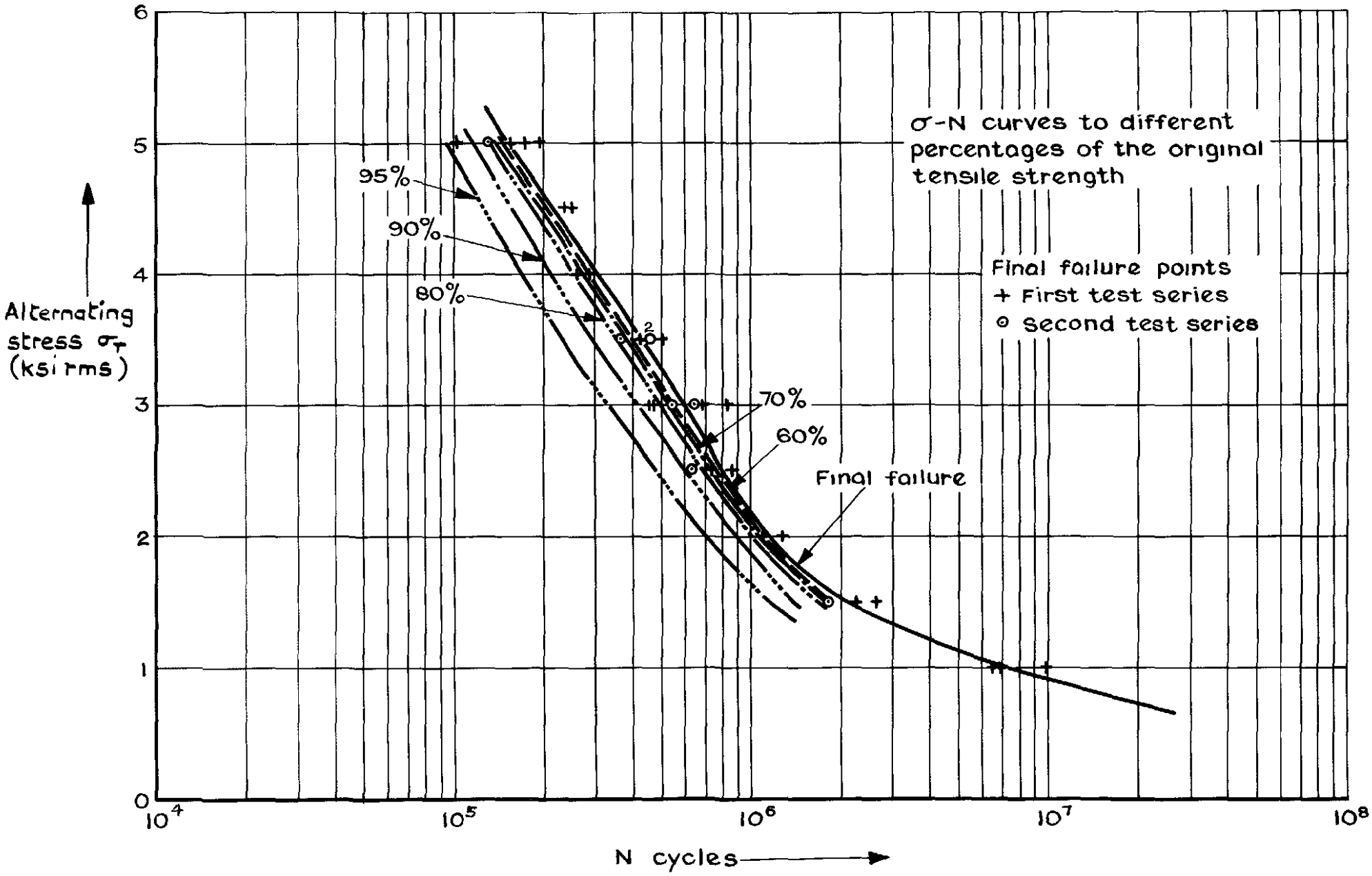

Fig. 25 Stationary random test results at 16 ksi mean stress

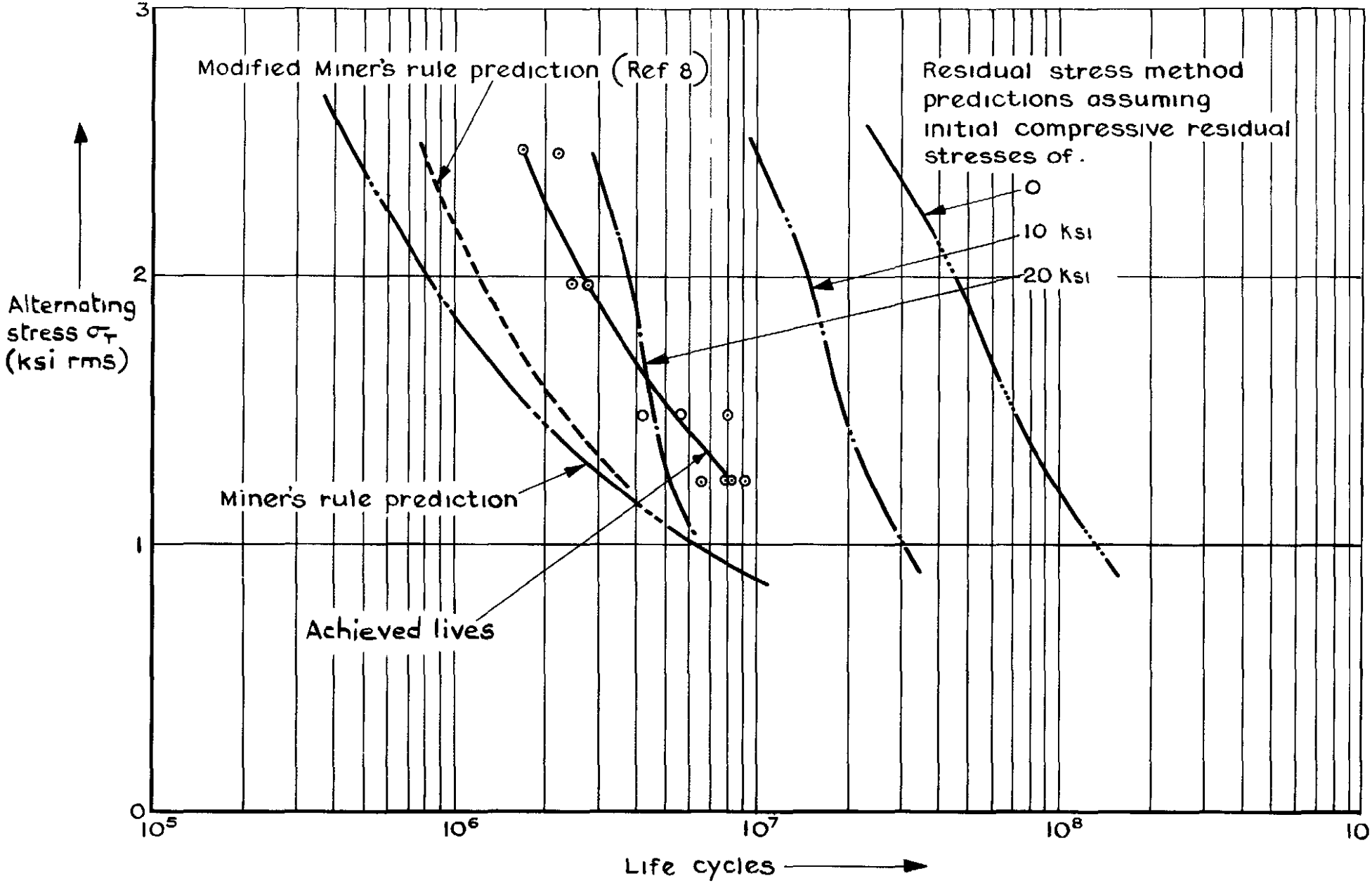

Fig. 26 Random programmed tests at 16 ksi mean stress.

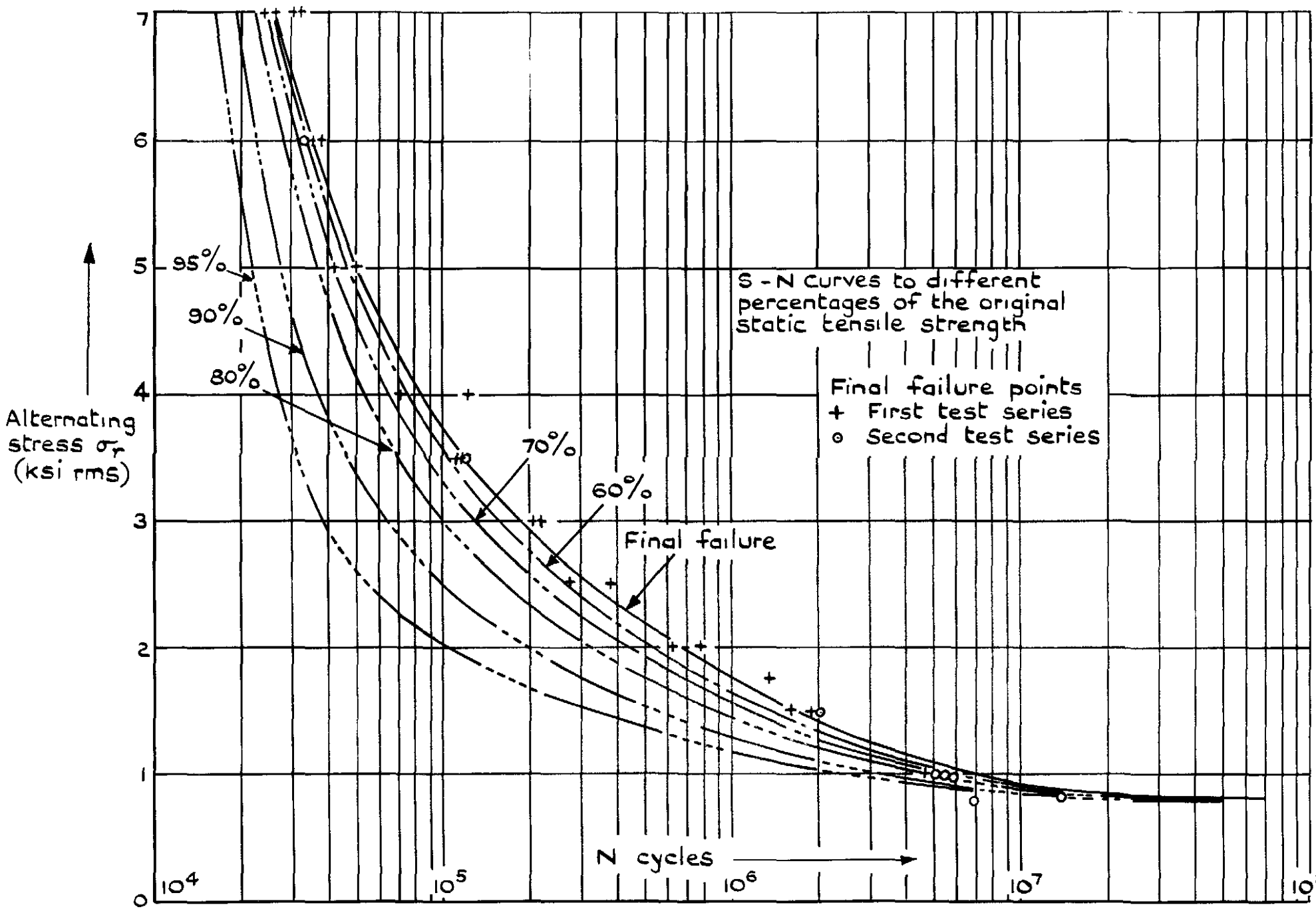

Fig. 27 Constant amplitude test results at 25 ksi mean stress

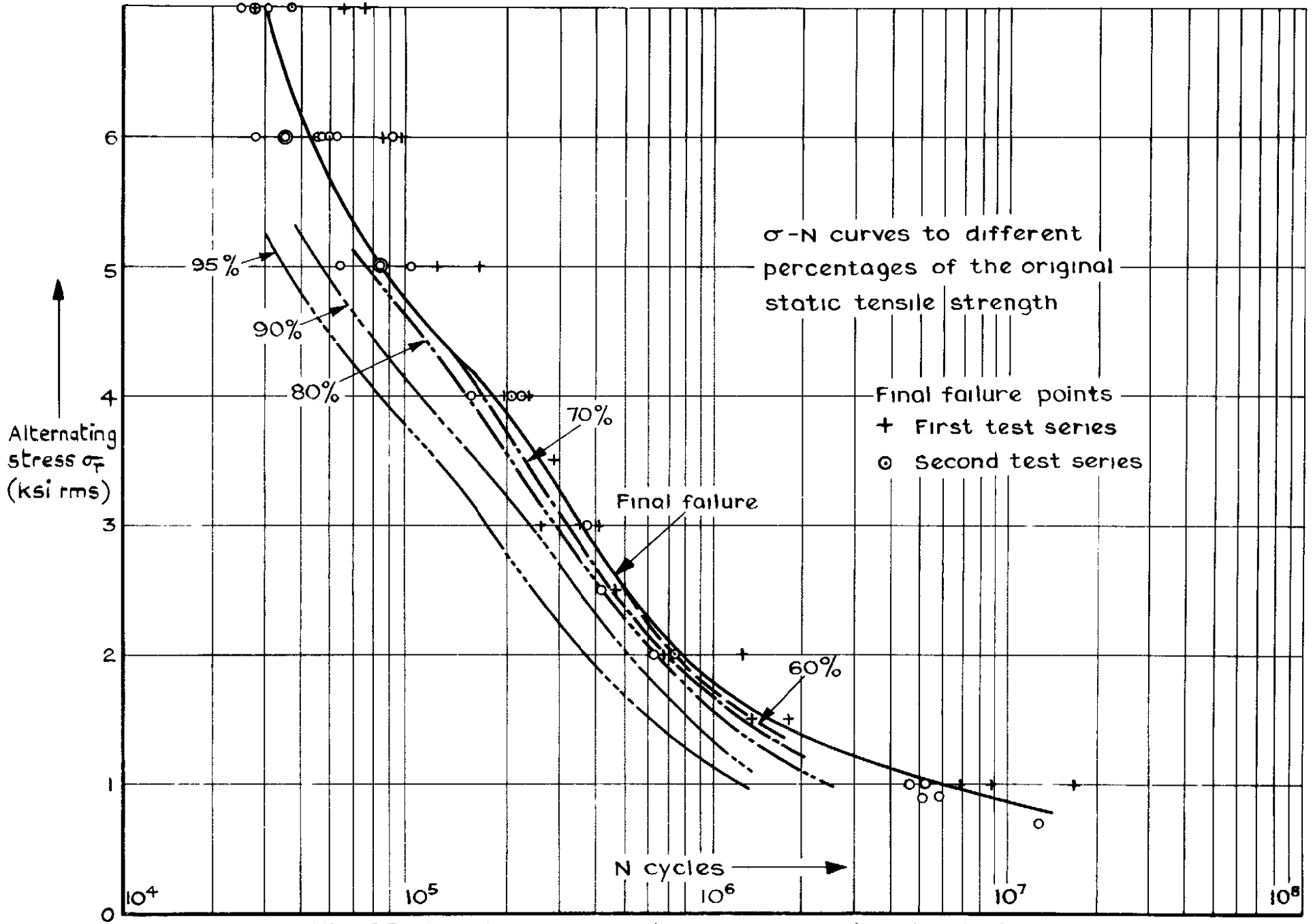

Fig. 28 Stationary random test results 25 ksi mean

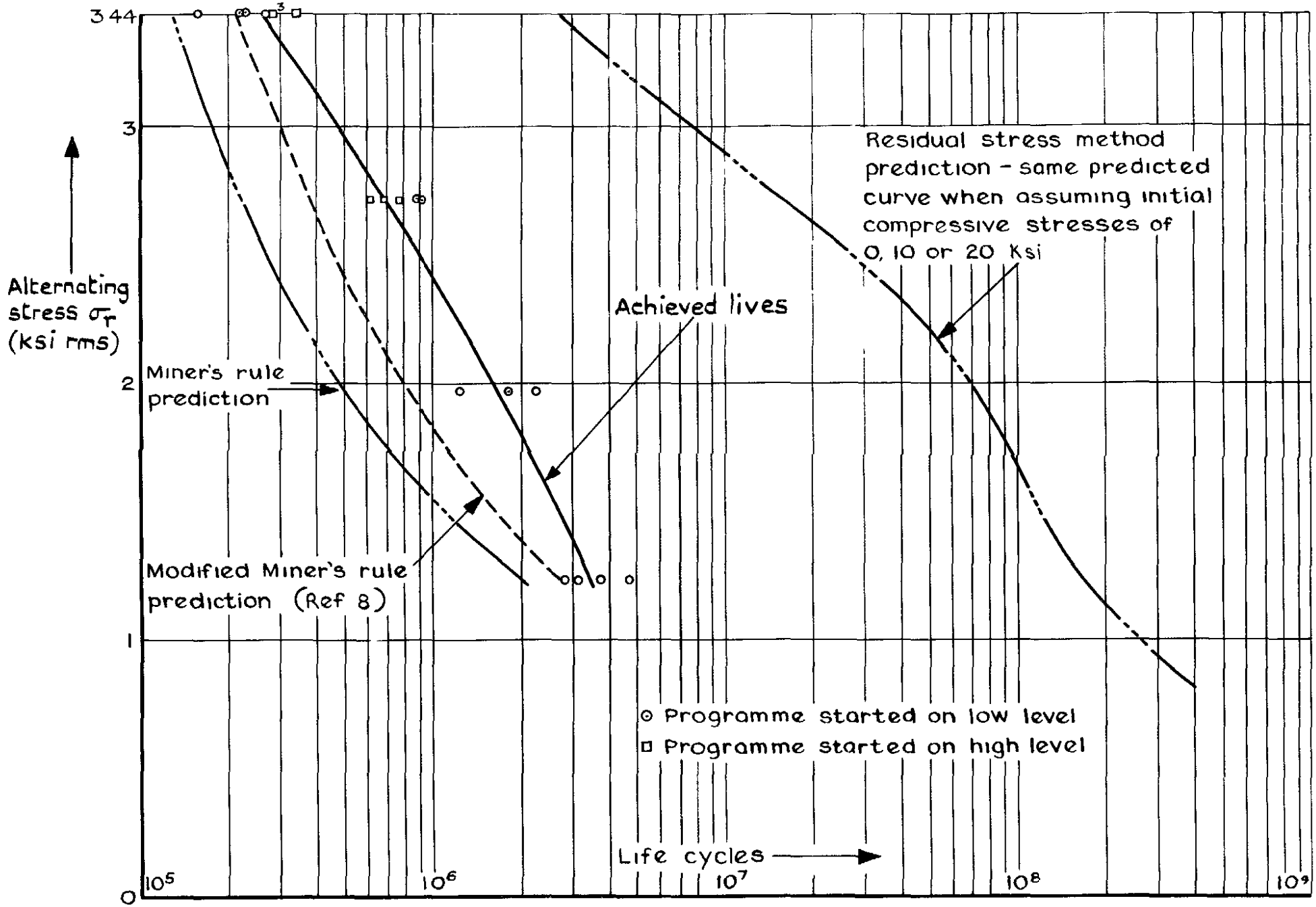

Fig.29 Random programmed tests 25 ksi mean stress

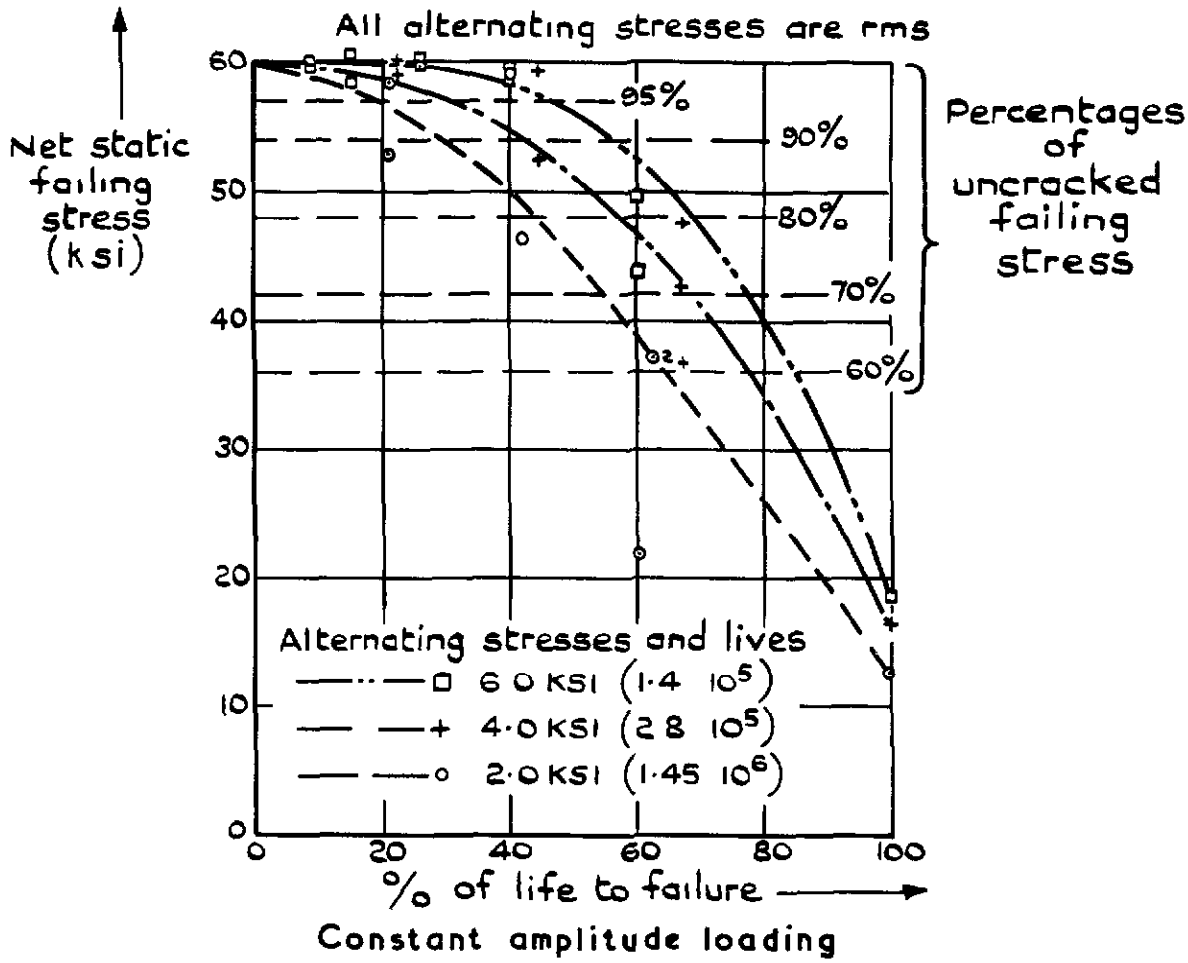

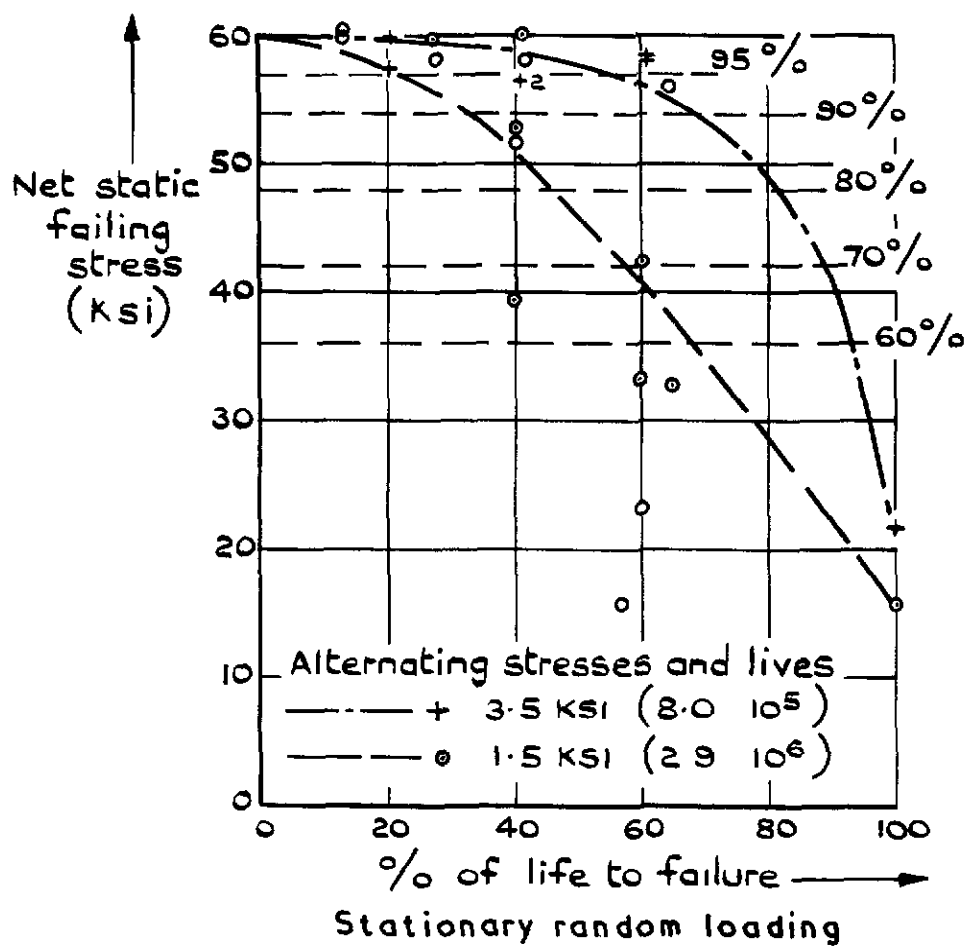

Fig. 30 Partial damage tests – 10 ksi mean small DTD 5014 lugs

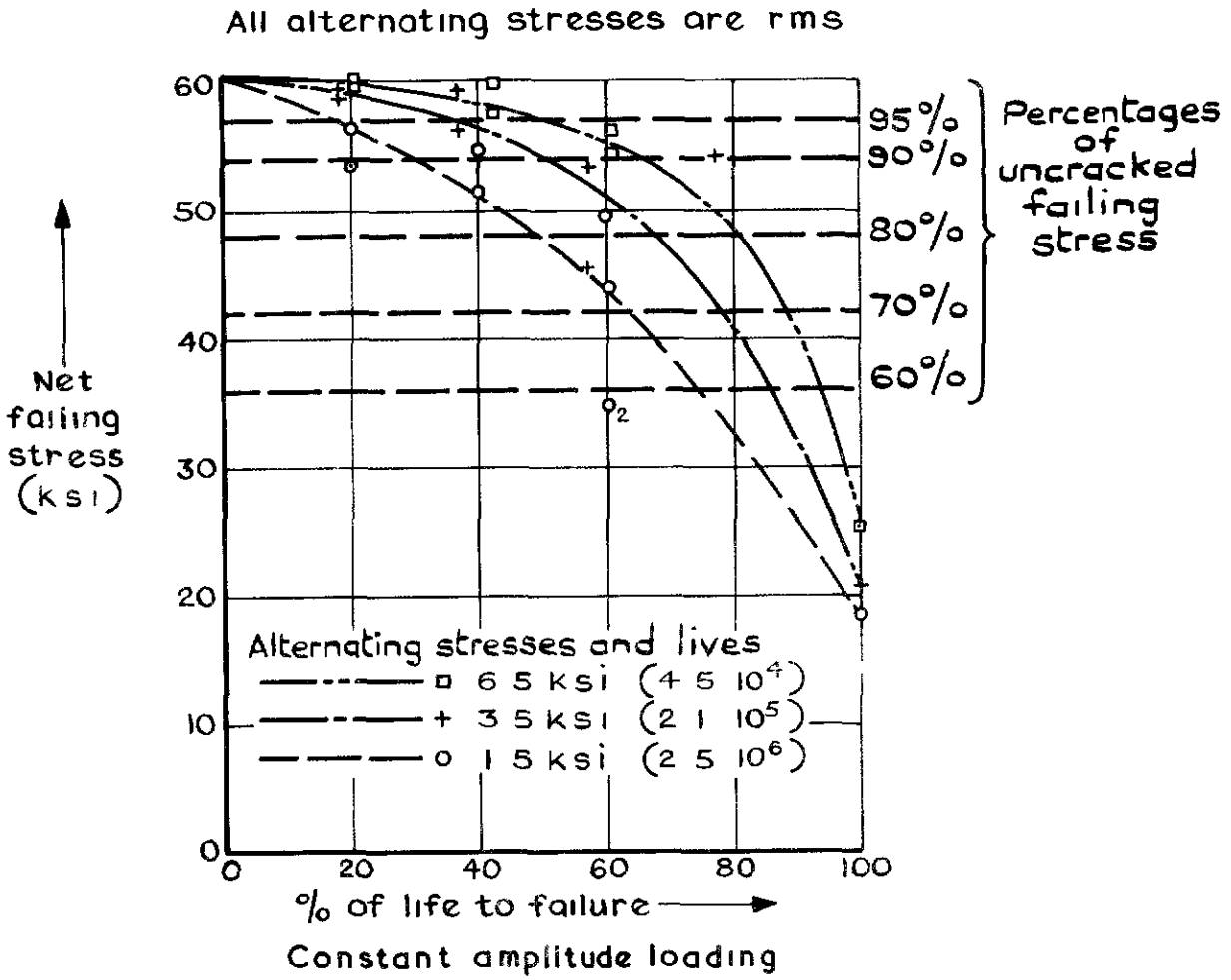

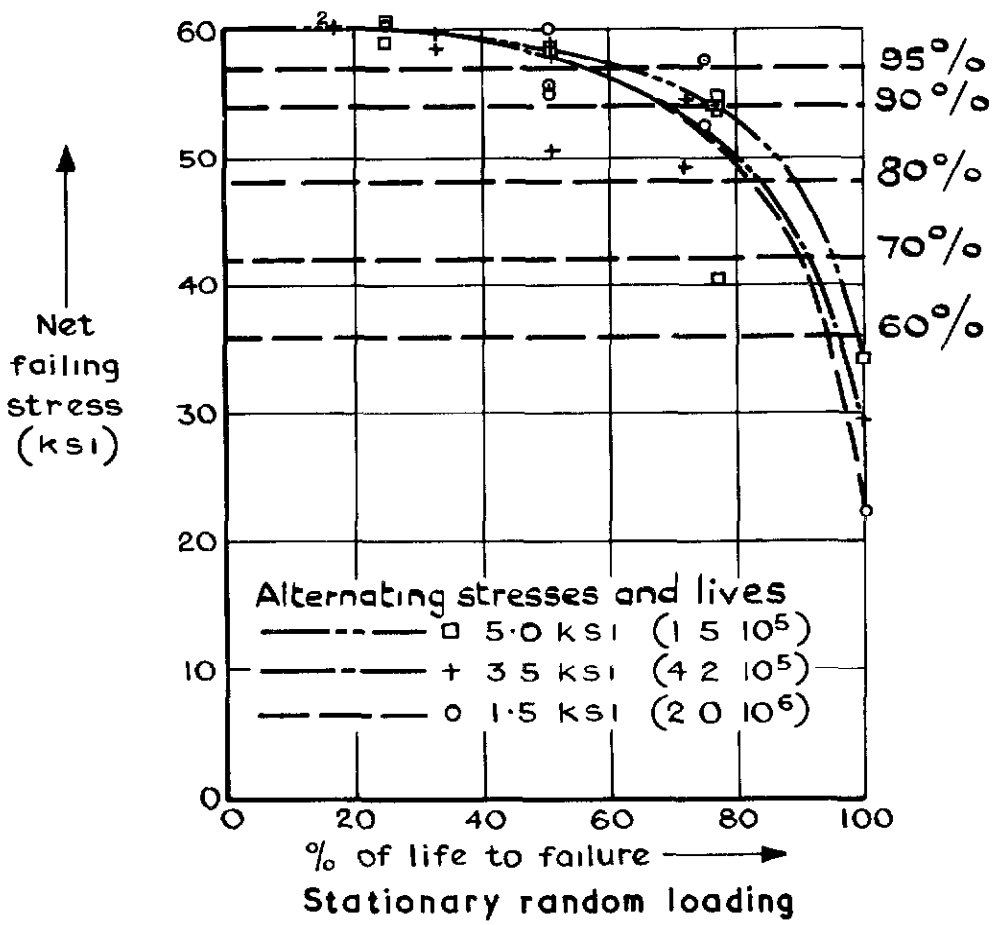

Fig. 31 Partial damage tests–16 ksi mean small DTD 5014 lugs

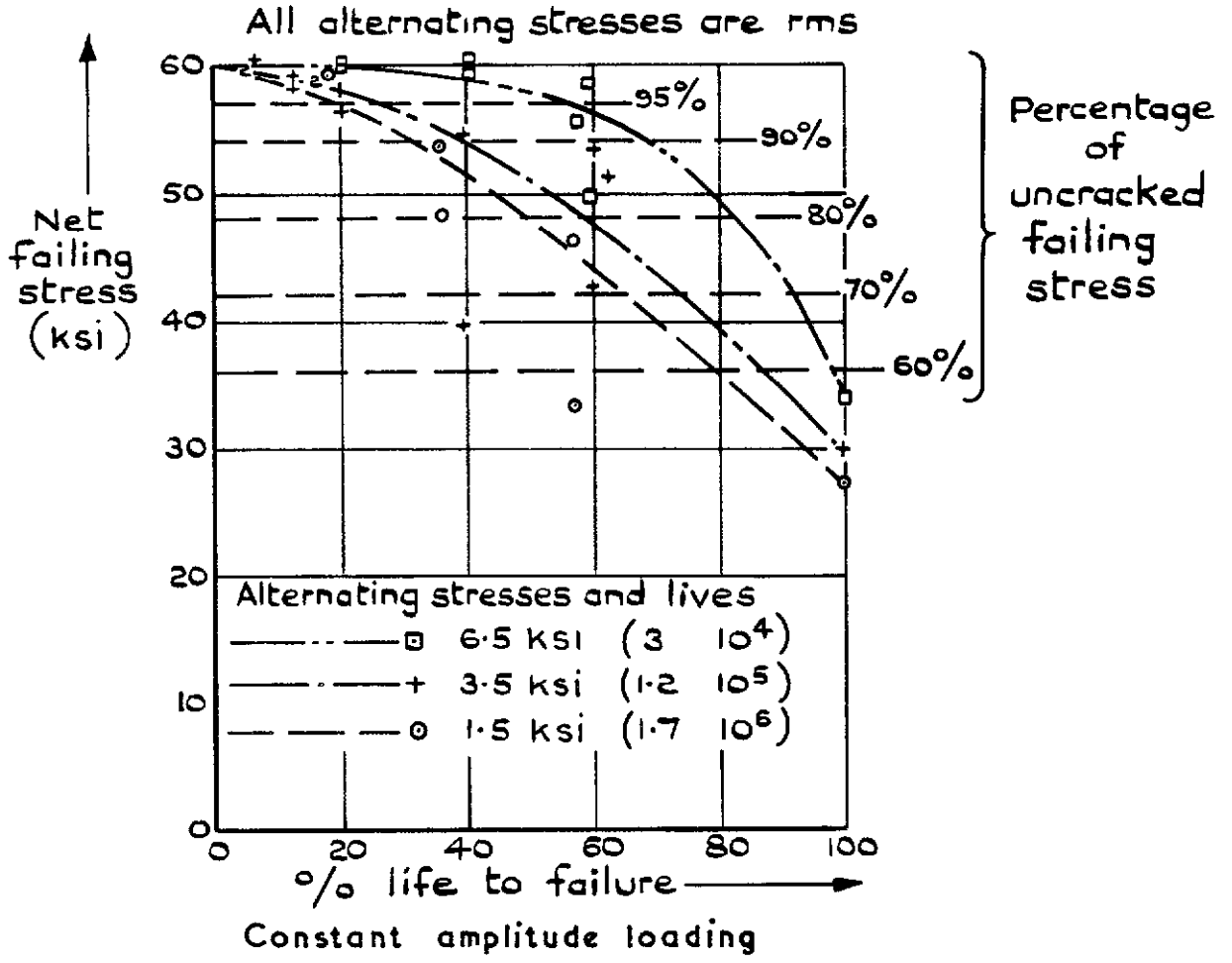

Fig. 32 Partial damage tests 25 ksi mean small DTD 5014 lugs

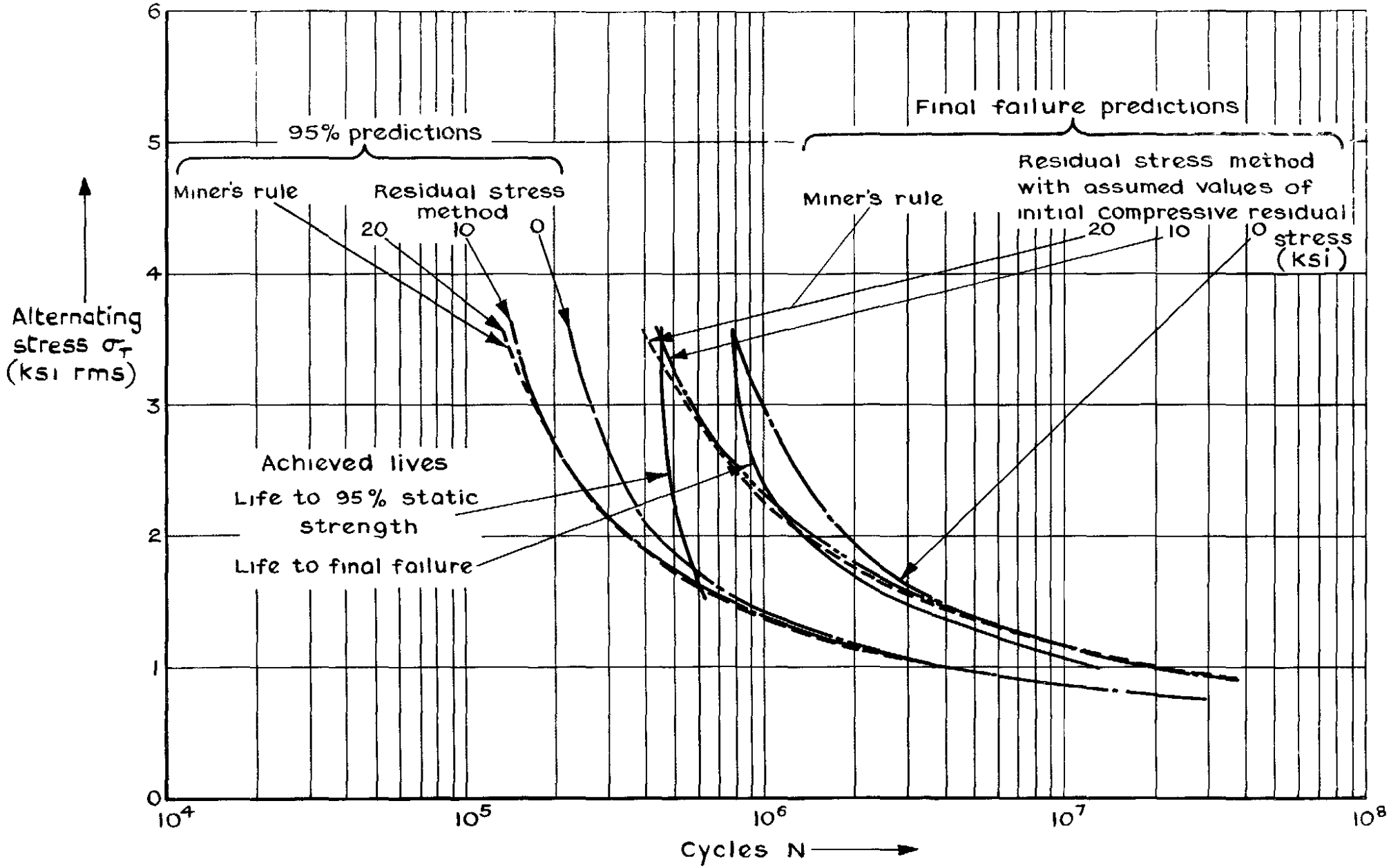

Fig. 33 Performance of cumulative damage rules for stationary random loading at 10 ksi mean stress

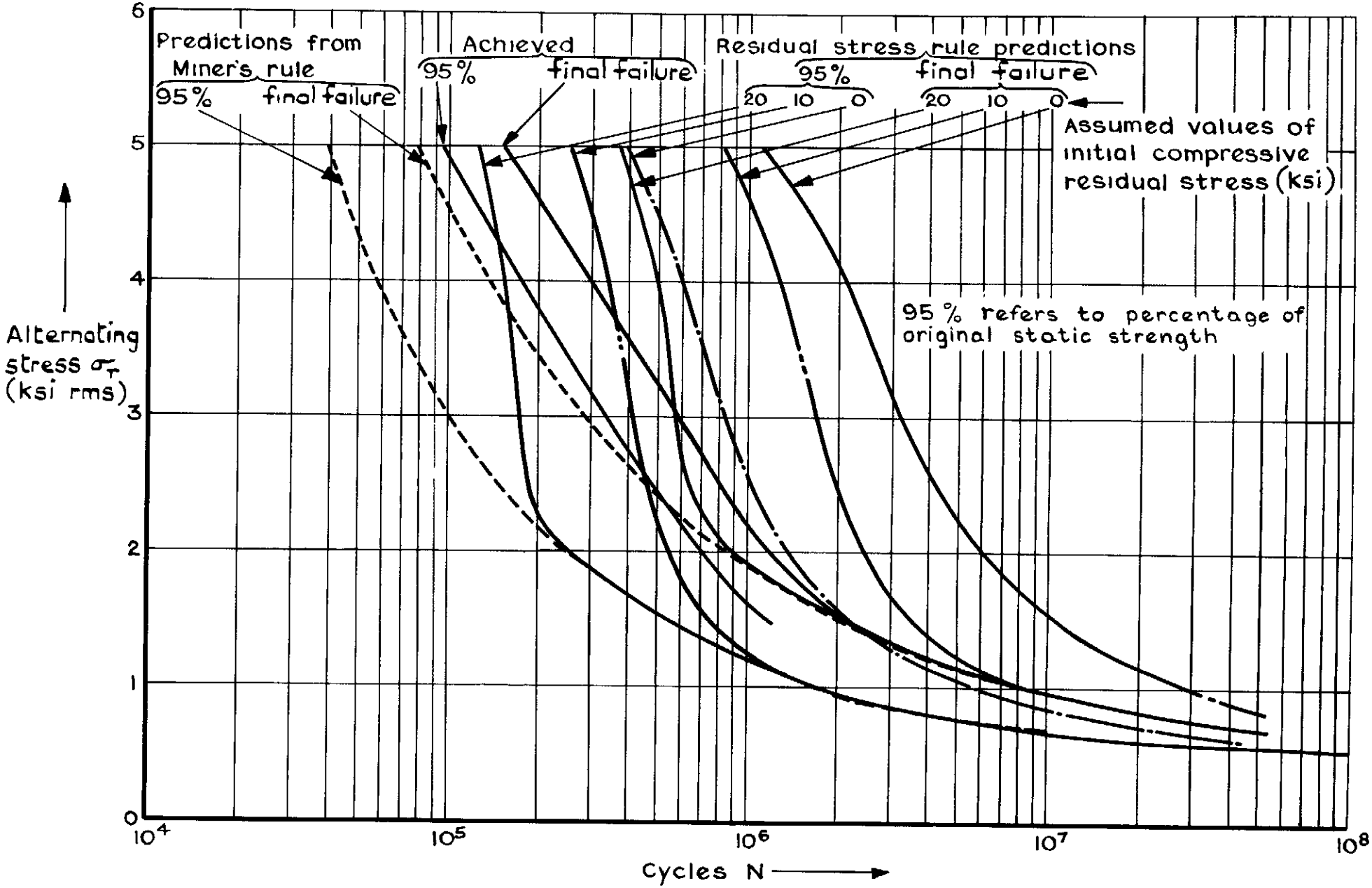

Fig. 34 Performance of cumulative damage rules for stationary random loading at 16 ksi mean stress

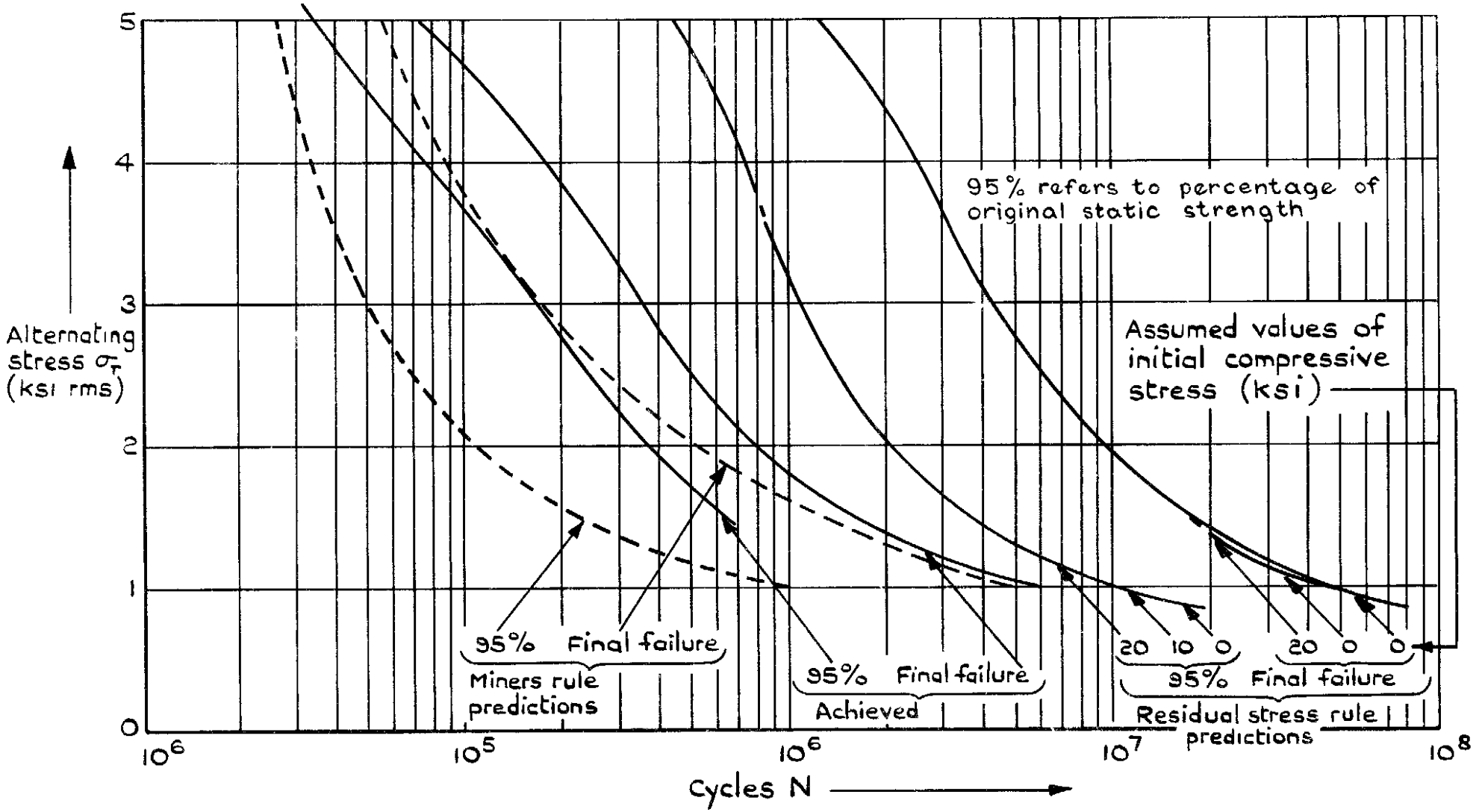

Fig. 35 Performance of cumulative damage rules under stationary random loading at 25 ksi mean stress

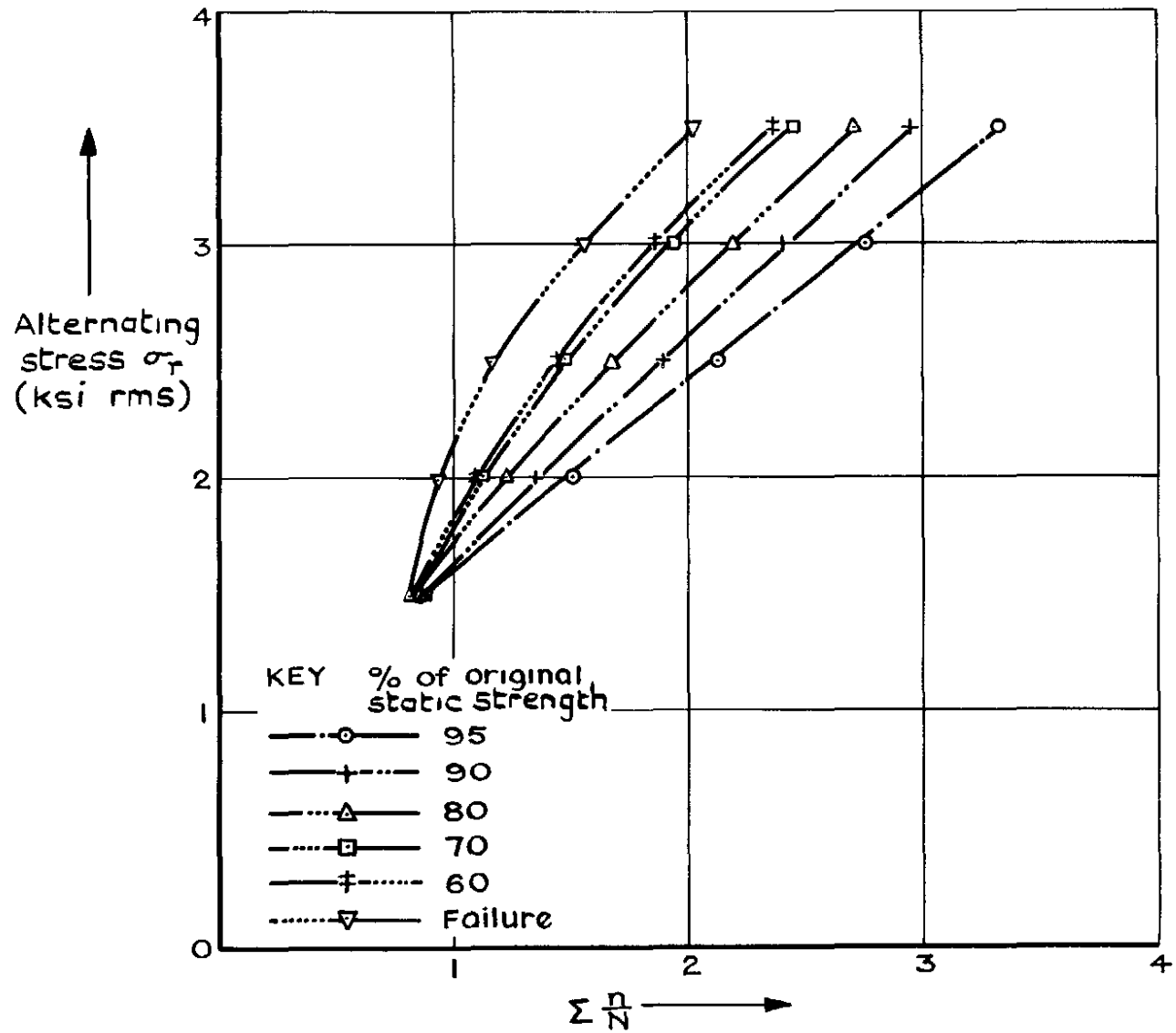

Fig. 36 $\Sigma^n/_N$ values for stationary random loading at 10 ksi mean

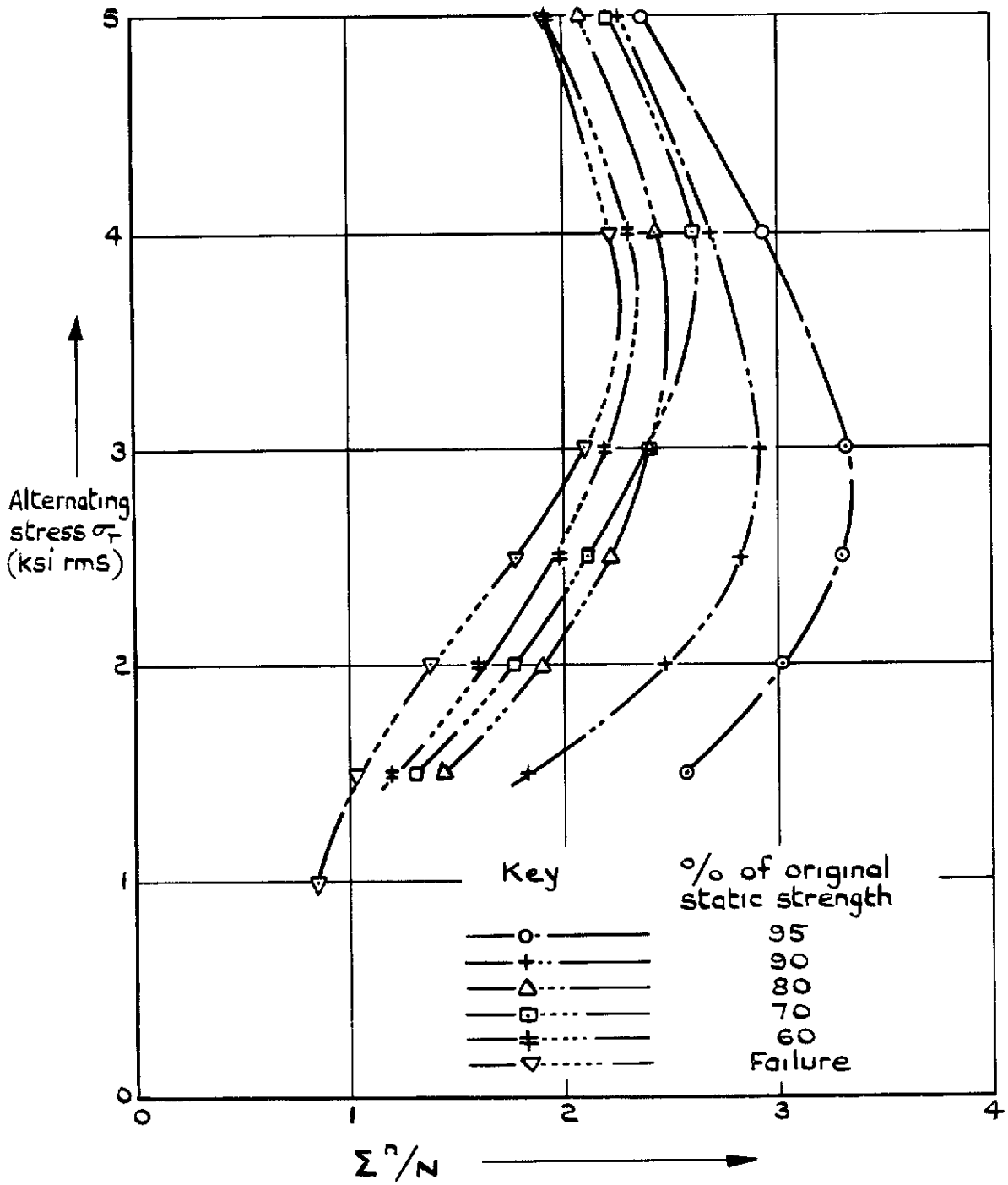

Fig. 37 $\Sigma \frac{n}{N}$ values for stationary random loading at 16 ksi mean

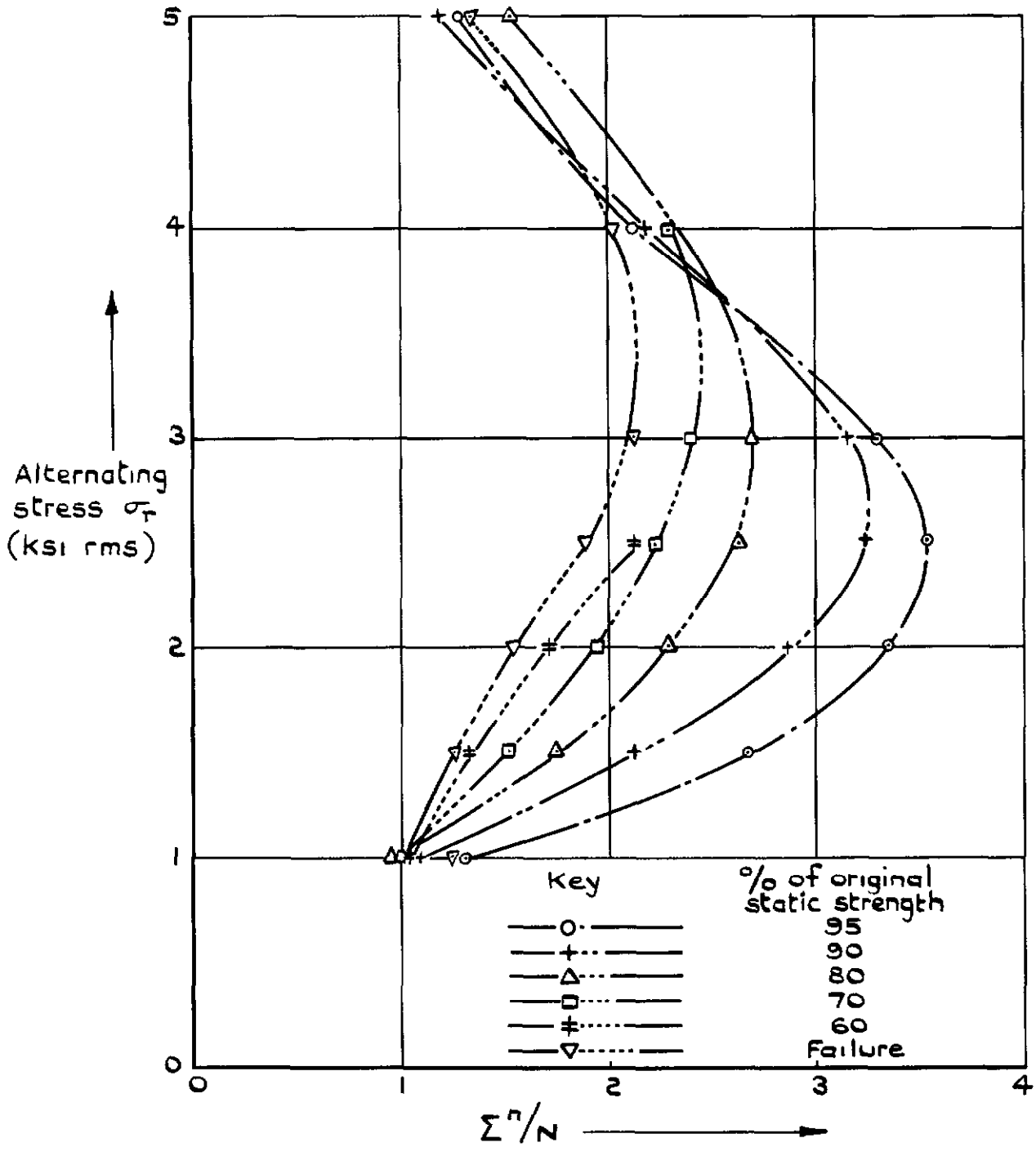

Fig. 38 Σ^n/N values for stationary random loading at 25 ksi mean

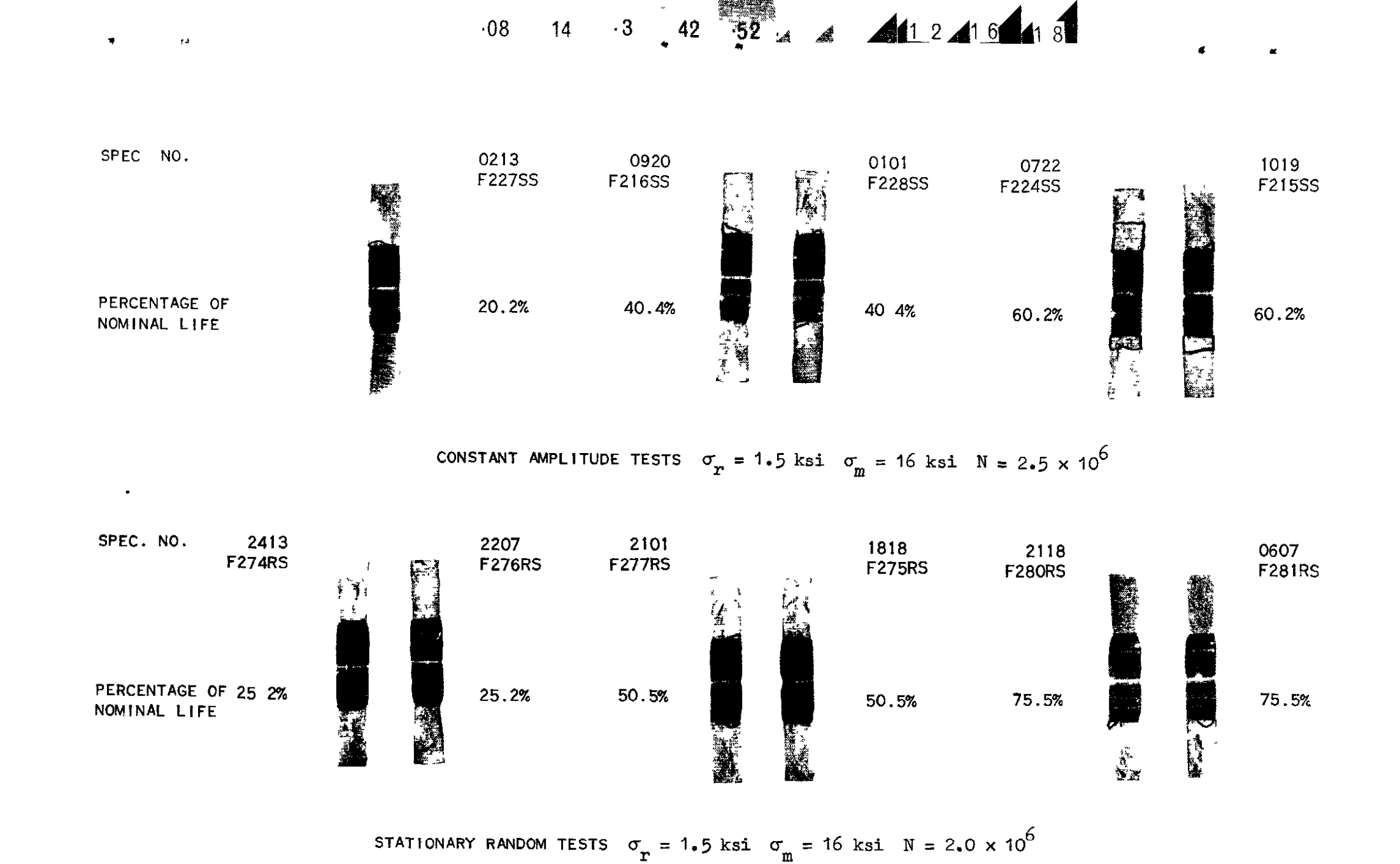

Fig 39. Specimens broken statically after fatigue to stated percentage of nominal life

(cracked areas shown outlined)

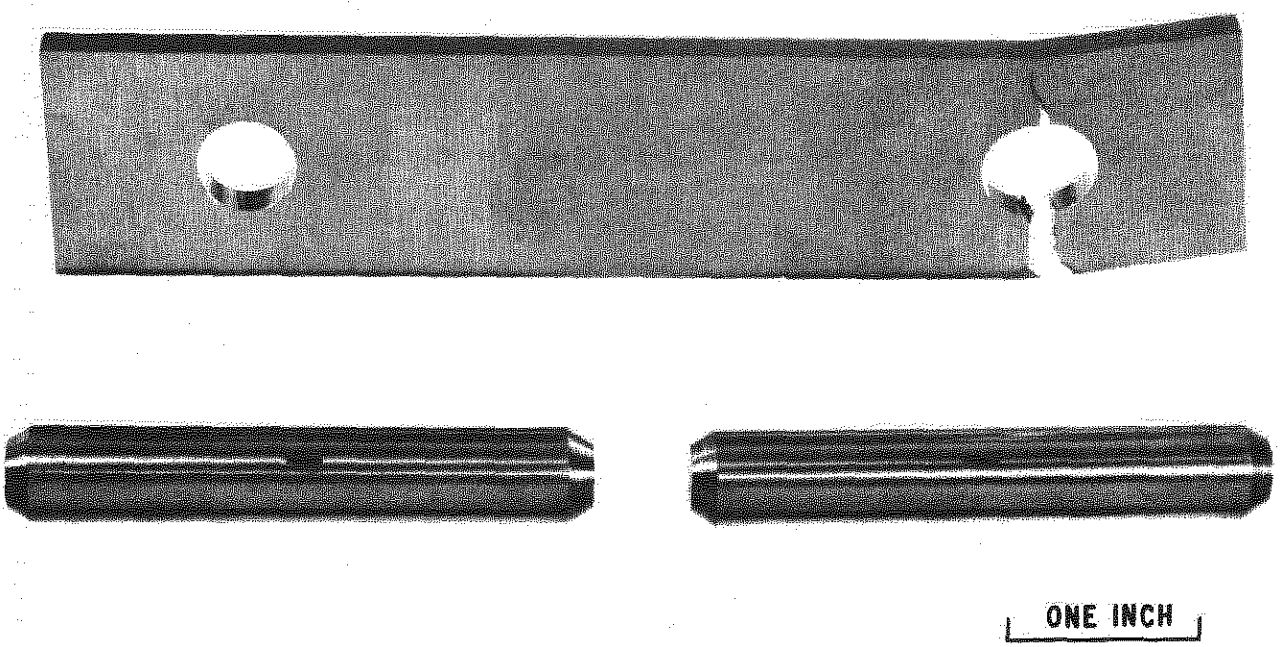

Fig 40. Typical failed specimen showing fatigue failure originating from area of fretting

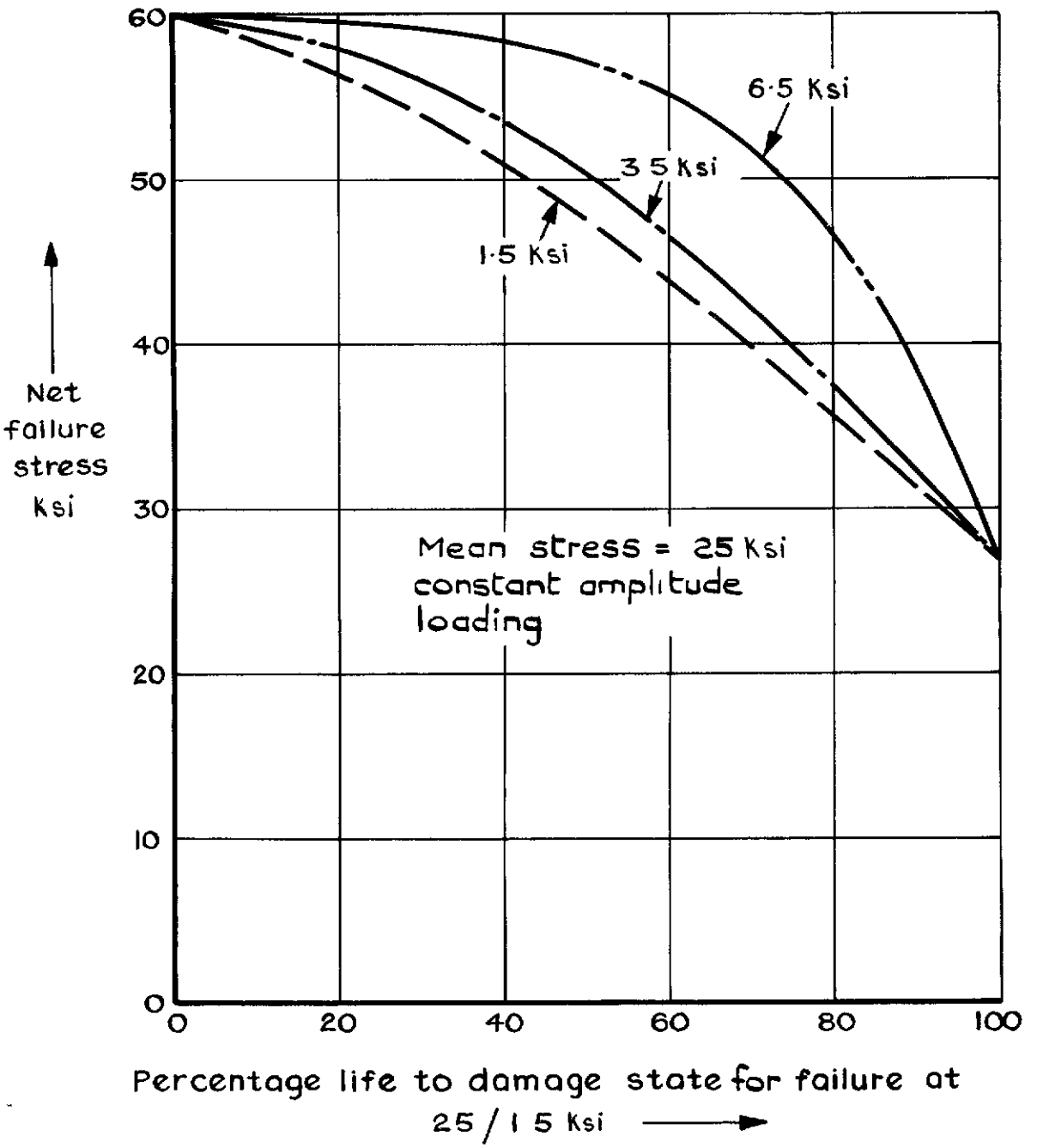

Fig. 41 Static strength against percentage life to a given damage state

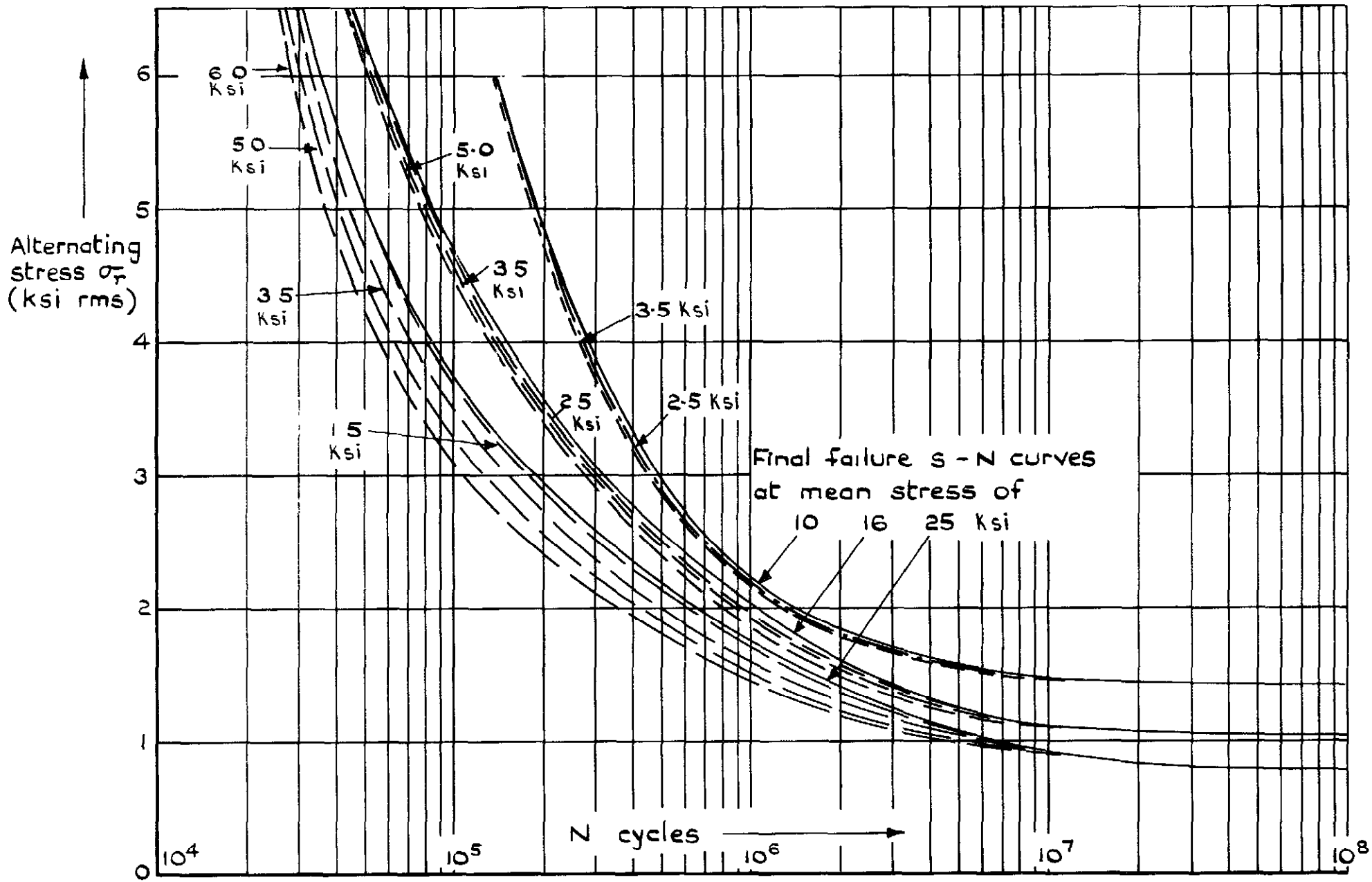

Fig. 42 S – N curves showing calculated curves for damage states corresponding to failure at stated random stresses

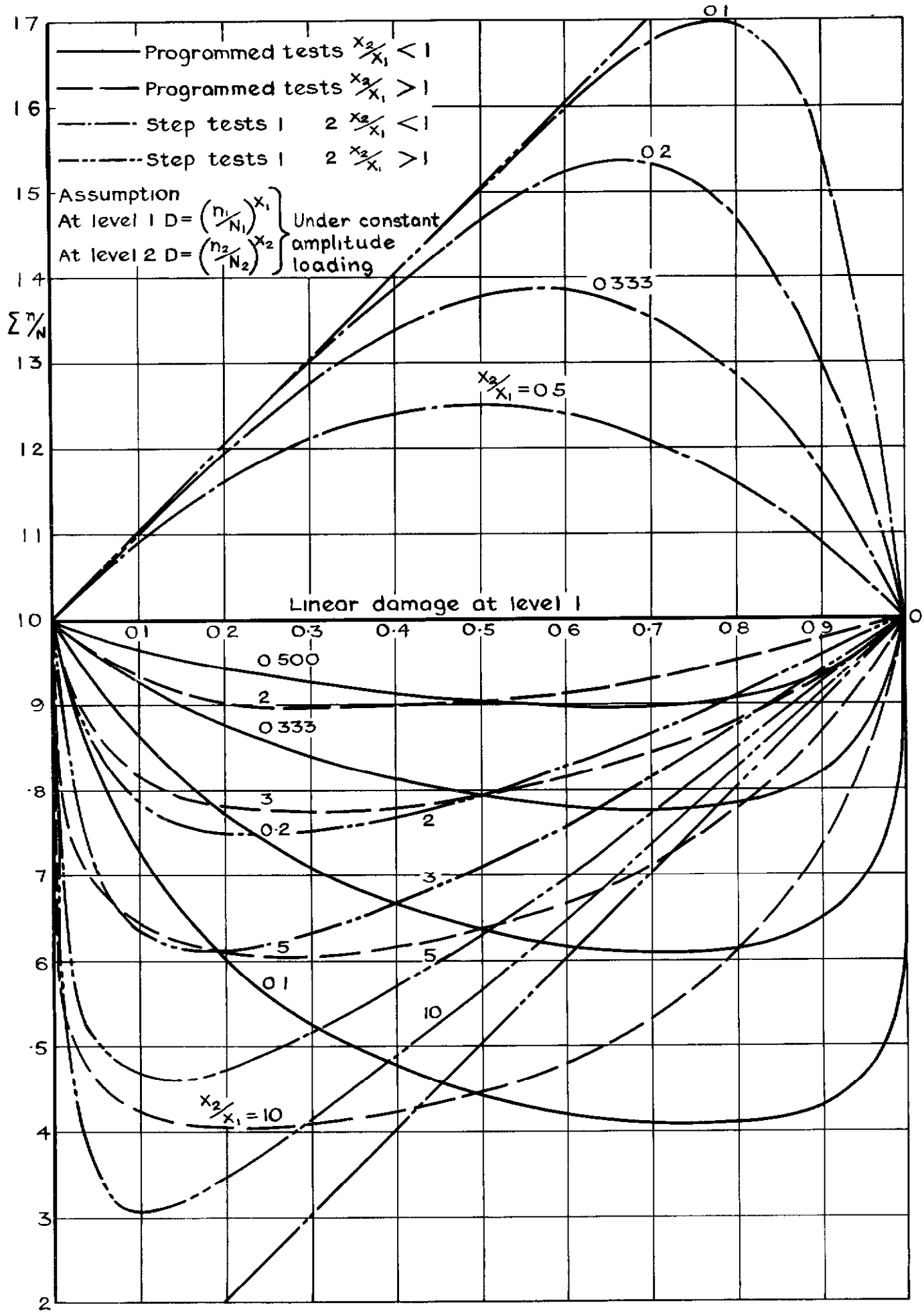

Fig 43 Expected two level programmed and step test results

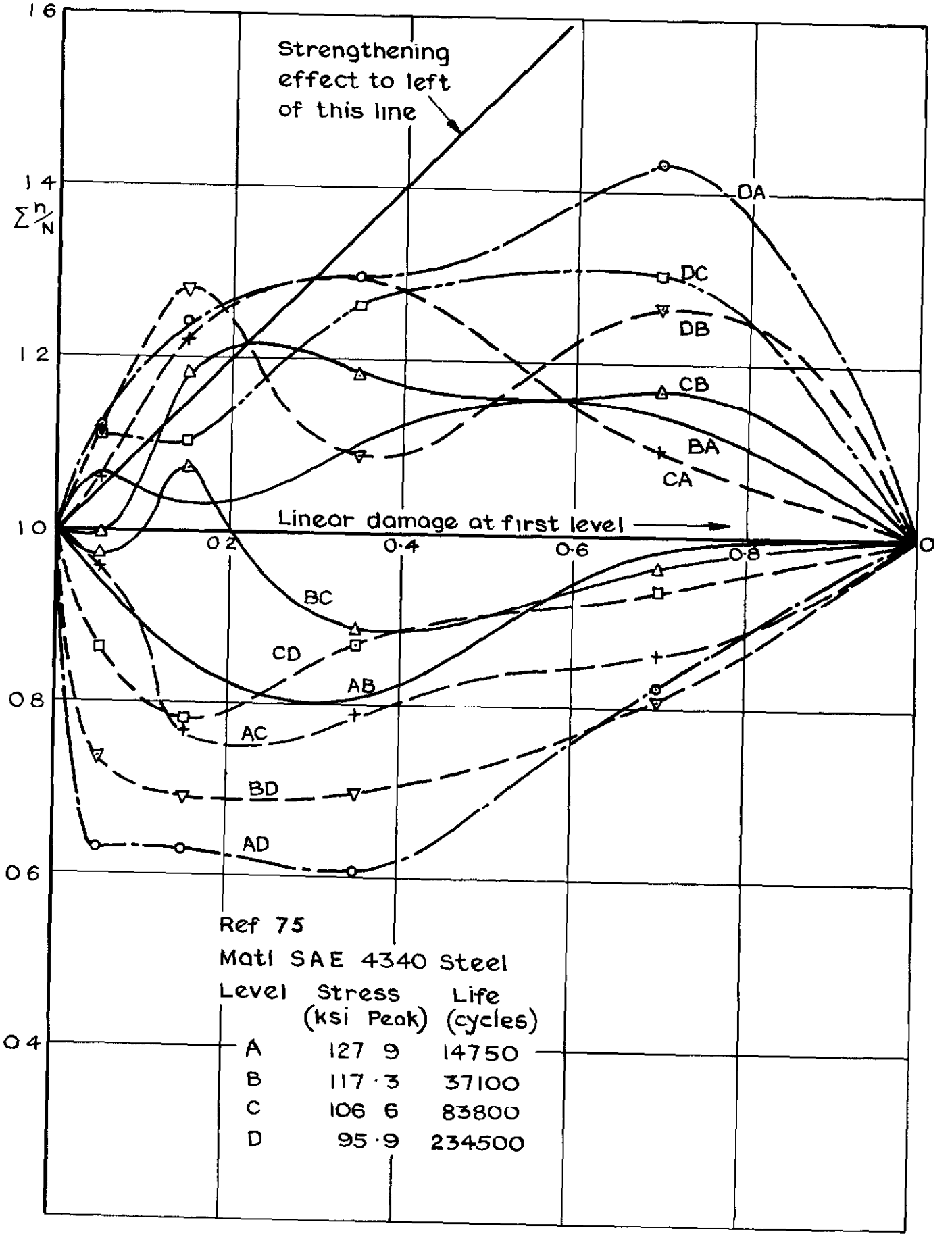

Fig. 44 Results of step tests

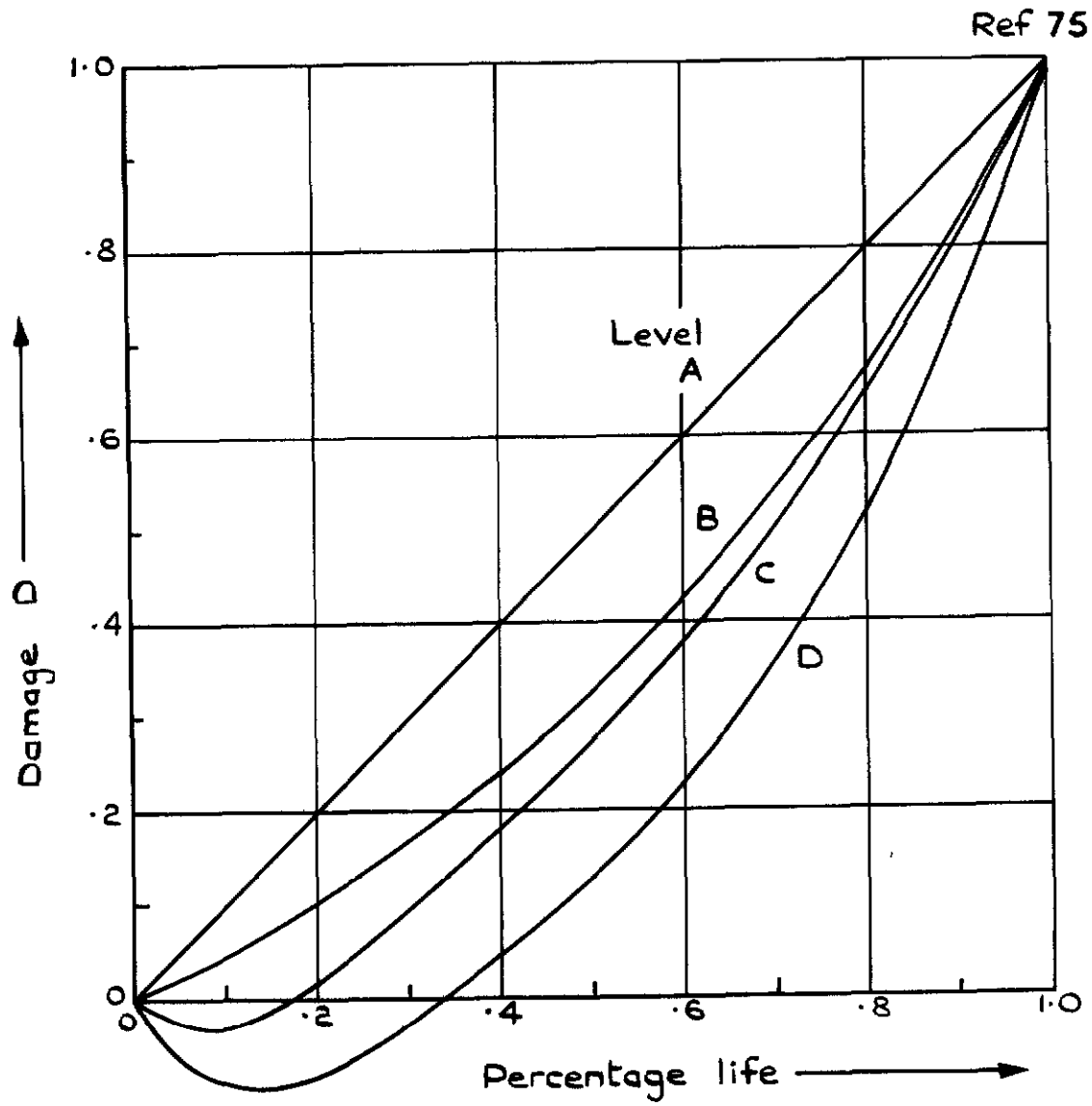

Fig.45 Variation of damage with percentage life (from step tests)

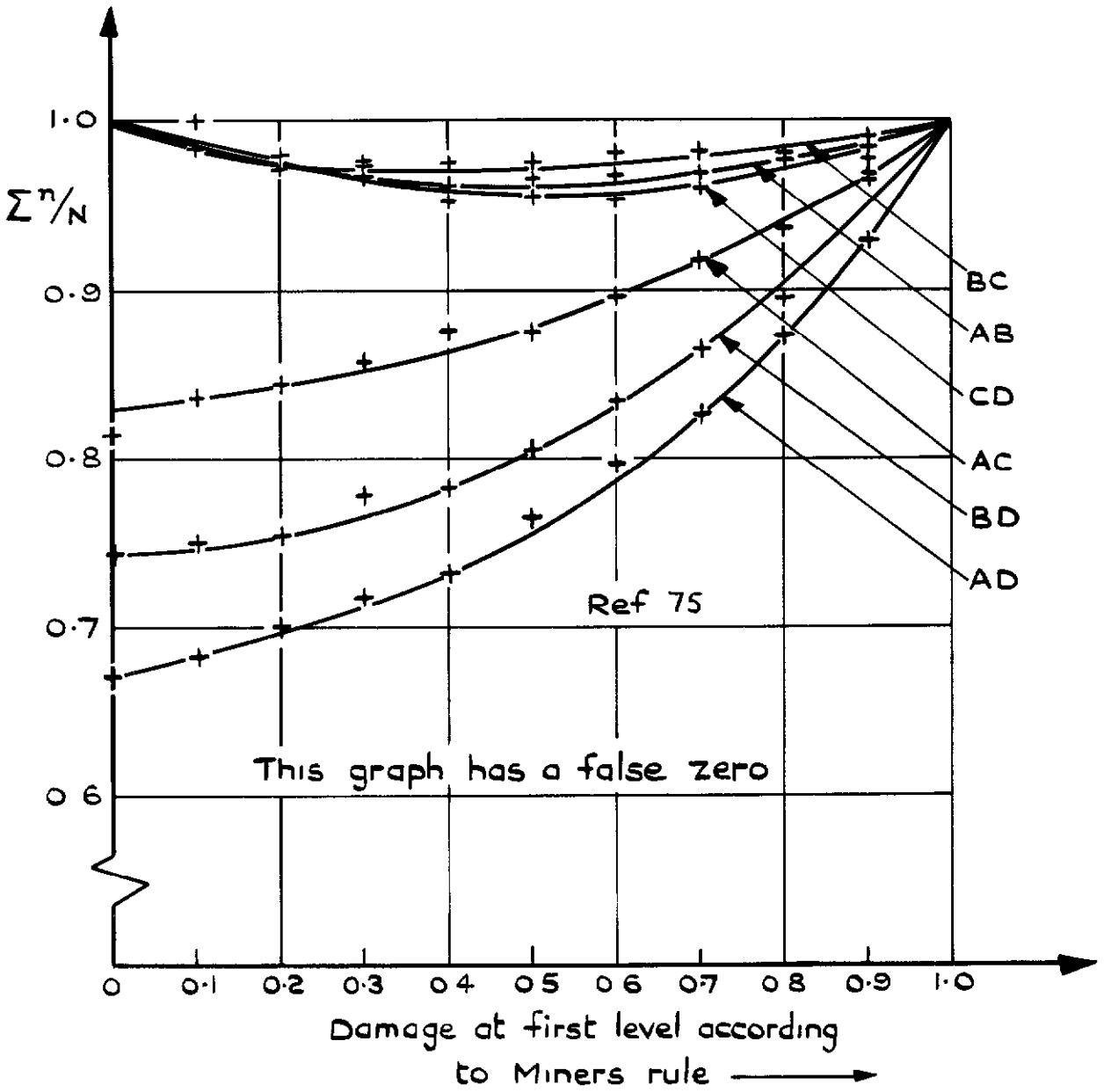

Fig.46 Calculated Σ^n/N values on the basis of relative damage rates

Ref 94

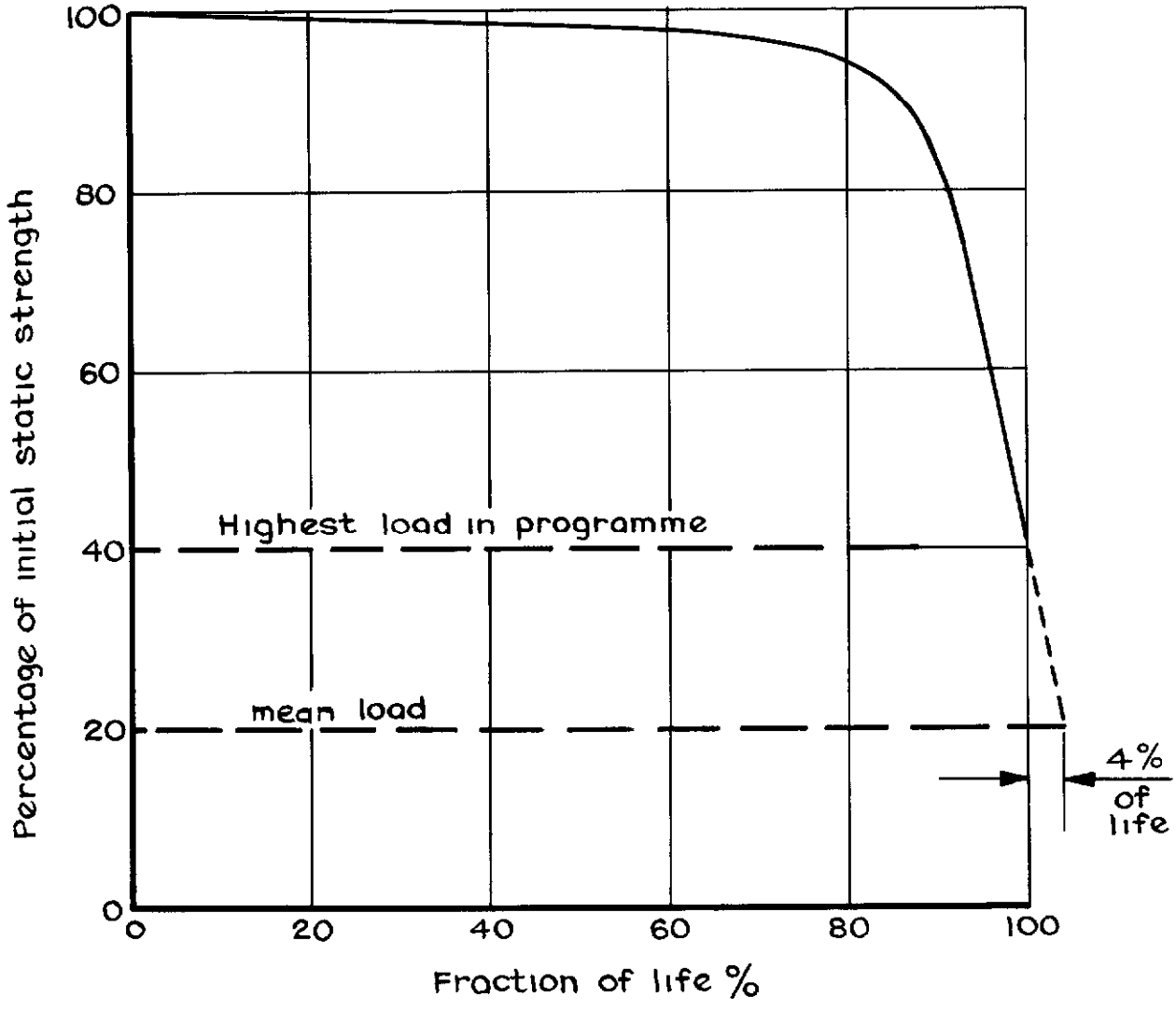

Fig.47 Residual static strength of bolted joint

Printed in England for Her Majesty's Stationery Office by the Royal Aircraft Establishment, Farnborough Dd 502109 K.4

DETACHABLE ABSTRACT CARD

A.R.C. C.P. No.1185
November 1969

Edwards, P. R.

539.431 :
539.319 :
669.715 :
621.886.4

CUMULATIVE DAMAGE IN FATIGUE WITH PARTICULAR REFERENCE TO THE EFFECTS OF RESIDUAL STRESSES

In this Report factors affecting the accuracy of Miner's Rule are discussed. An investigation is also described of the cumulative damage behaviour of DTD 5014 aluminium alloy lug specimens using random loading. It is concluded that the deviations from Miner's Rule observed in the investigation can be ascribed mainly to the action of residual stresses associated with yielding at the point of fatigue initiation. An attempt is made to quantify this effect.

A.R.C. C.P. No.1185
November 1969

Edwards, P. R.

539.431
539.319
669.715
621.886.4

CUMULATIVE DAMAGE IN FATIGUE WITH PARTICULAR REFERENCE TO THE EFFECTS OF RESIDUAL STRESSES

In this Report factors affecting the accuracy of Miner's Rule are discussed. An investigation is also described of the cumulative damage behaviour of DTD 5014 aluminium alloy lug specimens using random loading It is concluded that the deviations from Miner's Rule observed in the investigation can be ascribed mainly to the action of residual stresses associated with yielding at the point of fatigue initiation. An attempt is made to quantify this effect.

A.R.C. C.P. No.1185
November 1969

Edwards, P. R.

539.431
539.319
669.715
621.886.4

CUMULATIVE DAMAGE IN FATIGUE WITH PARTICULAR REFERENCE TO THE EFFECTS OF RESIDUAL STRESSES

In this Report factors affecting the accuracy of Miner's Rule are discussed. An investigation is also described of the cumulative damage behaviour of DTD 5014 aluminium alloy lug specimens using random loading. It is concluded that the deviations from Miner's Rule observed in the investigation can be ascribed mainly to the action of residual stresses associated with yielding at the point of fatigue initiation. An attempt is made to quantify this effect.

Published by
HER MAJESTY'S STATIONERY OFFICE

To be purchased from
49 High Holborn, London WC1 V 6HB
13a Castle Street, Edinburgh EH2 3AR
109 St Mary Street, Cardiff CF1 1JW
Brazennose Street, Manchester M60 8AS
50 Fairfax Street, Bristol BS1 3DE
258 Broad Street, Birmingham B1 2HE
80 Chichester Street, Belfast BT1 4JY
or through booksellers

C.P. No. 1185

SBN 11 470453 8